The Thesis Committee for Kelsey Tull Stilson
certifies that this is the approved version of the following thesis:

A Critical Analysis of Skull Osteology in Australian Agamidae with Implications for the Fossil Record

Committee:

_____
Christopher J. Bell, Supervisor

_____
Julia Clarke

_____
Jessica Maisano

_____
Travis LaDuc

A Critical Analysis of Skull Osteology in Australian Agamidae with Implications for the Fossil Record

by

Kelsey Tull Stilson, B.S.

Thesis

Presented to the Faculty of the Graduate School

of The University of Texas at Austin

in Partial Fulfillment

of the Requirements

for the Degree of

Master of Science in Geological Sciences

The University of Texas at Austin

May 2016

Acknowledgements

I would like to thank the Jackson School of Geosciences, especially the paleontology faculty, for their support and guidance. I am particularly indebted to Dr. Christopher J. Bell, whose intolerance for laziness has pushed me to new heights. Thank you also to Dr. Clarke, Dr. LaDuc, and Dr. Maisano for helping to guide me through the different aspects of this thesis. I would also like to thank everyone out at the Non-vertebrate Paleontology Laboratory, especially Dr. Ann Molineux, for two fantastic summers of work. Thank you as well to my collaborator, Dr. Jim Mead. The translation of Brůna (1996) by Gary Kocurek and Kadlec Jaroslav was also very helpful. Thank you also to Robert Burroughs, James Proffitt, Alicia Power, Josh Lively, Will Gelnaw, Kenneth Bader, Zach Morris, and Felicia Kulp for keeping me sane.

A Critical Analysis of Skull Osteology in Australian Agamidae with Implications for the Fossil Record

Kelsey Tull Stilson, M.S.Geo.Sci.

The University of Texas at Austin, 2016

Supervisor: Christopher J. Bell

The Australian agamid radiation was long noted for homogeneity of morphological characters and remains one of the most poorly studied major clades of squamates. Anatomical studies of the various lineages of endemic Australian agamids lag far behind genetic studies and would greatly enhance our knowledge of the current status and evolution of this complicated and dynamic clade. Australian agamids are an ideal group with which to test hypotheses of squamate speciation, diversity, and disparity because of their relatively recent diversification into Australia, about 30 Million Years Ago and geographical constraints. The two chapters of this thesis address two aspects of my research. In Chapter 1, I compile and evaluate morphological characters previously suggested to be useful for identifying Agamidae. I evaluate these characters for intraspecific variation, ontogenetic influence, and sexual dimorphism, for which sample sizes approached 20: *Ctenophorus caudicinctus, Ctenophorus isolepis,* and *Ctenophorus reticulatus*. Within the invariant characters, six were invariant only in *Ctenophorus caudincinctus,* five were invariant only for *Ctenophorus isolepis,* and two were invariant only in

Ctenophorus reticulatus. Morphological characters that varied within taxa (thus, excluding all invariant morphological characters) were statistically tested for covariance with ontogeny (using skull length as a proxy) and sexual dimorphism. Sixteen of the 60 characters measured varied for at least one taxon with ontogeny and nine varied with sex.

In Chapter 2, I use X-ray computed tomography (CT) of two specimens to describe the skull of the Australian agamid *Cryptagama aurita*, a species known only from only four alcohol-preserved specimens. *Cryptagama aurita* appears to share a great number of skull characters with other desert-dwelling Australian agamids.

I conclude that the information currently available for Australian Agamidae is inadequate to interpret the fossil record of Australian Agamidae. Any identifications and phylogenetic analyses are likely to be inaccurate because most of the characters proposed by previous authors are not demonstrably apomorphic. Ontogenetic age is an important source of variation for the three species of *Ctenophorous* I examined. Morphological variation of extant taxa must be understood in order to compare extant and extinct species to study the recent radiation of Australian Agamidae.

Table of Contents

Chapter 1: Patterns of Variation in the Cranial Osteology of Three Species of the Endemic Australian Genus *Ctenophorus* (Squamata: Agamidae) with Implications for Morphological Analyses made with Limited Sample Sizes

INTRODUCTION

There are over 350 extant lizard species currently recognized in the squamate clade Agamidae (Heying 2003). Species of the clade are present on Africa, Europe Asia, and Australian continents, as well as across insular southeast Asia from the Malay Archipelago to New Guinea (Witten 1993). Agamidae show an astonishing lability of form and function that often is dependent on environment (Estes at al. 1988, Honda et al. 2000, Stuart-Foxx and Owens 2003, Townsend et al. 2004, Melville et al. 2006, Wagner et al. 2011, Smith et al. 2011, Östman and Stuart-Foxx 2011, Pyron et al. 2013). Sexual dimorphism, ontogenetic variation, and other sources of phenotypic plasticity in the skeletal system remain largely unexplored for the group, and agamids remain one of the most poorly known of the major clades of lizards in terms of skeletal morphology. The most detailed studies of the skeletal anatomyof the group as a whole remain the pioneering work by Siebenrock (1895), and Moody's (1980) unpublished Masters thesis. The compilation of morphological characteristics of Agamidae by Siebenrock (1895) included a list of 50 skeletal characters, 33 of which were from the cranium. He reviewed 32 species, and focused on diagnostic morphological characters at both the genus and species levels. Subsequent reviews and observations of osteological characters of Agamidae were made periodically through the decades by various authors (e.g. Camp 1923, Waite 1929, El-Toubi 1945, El-Toubi 1947, Jollie 1960, Badham 1976, Greer 1989a, Cogger 1992, Smirina and

Ananjeva 2007, Evans 2008), but all of them relied heavily on Siebenrock's study as a foundation. The last systematic analysis of skeletal morphology of Agamidae was completed by Scott Moody as a Master's thesis (Moody 1980), but was never formally published. Seventy cranial characters were identified and evaluated by Moody (1980) and his study included many of Siebenrock's original specimens. A total of 861 specimens representing 120 species were observed by Moody for osteological data, and a subset of 317 specimens representing 45 genera was used to frame a hypothesis of relationships among them (Moody 1980). In both the general and specific study, this meant that an average of seven individuals were observed for each taxon. However, individual variation was not recorded in Moody's (1980) thesis, only, presumably, the character state that occurred most often. Also, the analysis was polarized by a hypothetical outgroup ancestor, instead of an actual outgroup species. His analysis necessarily conformed to limited computing power available at that time, and his results were ambiguous.

Subsequent work on osteology of agamids was completed as part of broader systematic analyses of Squamata (Estes et al. 1988, Gauthier et al. 1988, Greer 1989a, Caldwell 1999; Hocknull 2002, Conrad 2008, Herrel and De Vree 2009, Smith 2011, Gauthier et al. 2012) or as shorter papers on particular species (e.g., Harris 1963, Cooper and Poole 1973, Hocknull 2000, Smirina and Ananjeva 2007, Moazen et al. 2008, Bell et al. 2009, Fathinia et al. 2011, Banzato et al. 2012, Porro et al. 2014), but a general synthesis still is lacking. In part, the relative paucity of modern data probably results from the fact that the group received little attention from Estes et al. (1980) in a work that laid the foundation for most hypotheses of realationships of squamates. The scant coverage in that work was a reflection of the uncertain phylogenetic position of the group within Iguania, itself a reflection of a general lack of systematically informative anatomical data.

A close relationship of Agamidae, Chameleonidae, and Iguanidae was recognized by Camp (1923), who aggregated the families into a suprafamilial group, Iguania. Iguanians with acrodont tooth implantation – agamids and chamaeleonids – were united in Acrodonta by Estes et al. (1988), and were reconstructed as the sister taxon to Iguanidae (sensu lato). Phylogenetic relationships and nomenclature of the group are still being explored, but molecular studies over the last 15 years helped both to clarify relationships within the group and to establish its monophyly within Iguania (e.g., Macey et al. 2000, Honda et al. 2000, Schulte et al. 2003, Townsend et al. 2004, Hugall and Lee 2004, Hugall et al. 2008, Collar et al. 2010, Wiens et al. 2012, Pyron et al. 2013). Molecular phylogenies of Agamidae coarsely follow geographic distribution, with endemic continent-level radiations (Honda et al. 2000).

Australian Agamidae

The last major review of the Australian Agamidae recognized 78 species, distributed within 14 genera (Wilson and Swan 2013). Traditional classifications recognized several monotypic genera (e.g., *Moloch*, *Chelosania*, and *Chlamydosaurus*) as well as several speciose groups (e.g., *Diporiphora*, *Ctenophorus* and *Amphibolurus*). Recent molecular phylogenies challenged the monophyly of many traditionally recognized genera, which were based primarily on soft-tissue characters, and a number of taxonomic rearrangements have been proposed in recent years (Melville et al. 2001, Doughty et al. 2007, Hugall et al. 2008, Smith et al. 2011, Rabosky et al. 2011, Chen et al. 2012, McLean et al. 2013, Cogger 2014, Doughty et al. 2014, Melville et al. 2014, Edwards et al. 2015).

The diversity and increaslingly obvious cryptic variation of endemic Australian agamids is hypothesized to be a result of a relatively recent radiation. Agamids are thought to have reached Australia around 30 Ma, probably from the Philippine Islands (Molnar 1991, Hugall et

al. 2008). Divergences within Australian Agamidae occurred after colonization onto Australia, although this is still under study (Schulte et al. 2003, Hugall and Lee 2004, Hugall et a. 2008).

Australian agamids are characterized by the early divergence of a relatively small number of specialized taxa compared to the huge diversity of desert specialists. Early divergences include the terrestrial *Moloch horridus*, the semi-arboreal *Chelosania brunnea*, and several aquatic taxa within the genus *Hypsilurus* as well as a *Physignathus leseureii*. Within the remaining Australian agamids the *Ctenophorus* clade is thought to have diverged around 21 Ma (Hugall et al. 2008) and perhaps diversified between 19 Ma (Hugall and Lee 2004, Byrne et al. 2008, Hugall et al. 2008) and 11-12 MA (Melville et al. 2001). Phylogenies constructed from mitochondrial DNA (Melville et al. 2001, Schulte et al. 2003, Hugall et al. 2008, Collar et al. 2010, Smith et al. 2011, Rabosky et al. 2011, McLean et al. 2013) reveal great lability of habitat-associated traits and a number of cryptic species complexes, which were not obvious from the data derived from nuclear DNA (Hugall et al. 2008, Levy et al. 2012). This is consistent with the hypothesis that Australian Agamidae diversified quickly and fairly recently, only giving time for the faster-evolving mitochondrial DNA to differentiate, and implying a high degree of phenotypic plasticity.

Most known Australian agamids are diurnal heliotherms and are the most visually oriented of all Australian lizards (Greer 1989a). Agamids are thought to preferentially utilize sight over the chemosensory systems that are ubiquitous among squamates, because of their ambush predatory behavior and diverse coloration (Wilson 2012).

Ctenophorus, as currently recognized, is the most speciose group of Australian agamids (Greer 1989a, Melville et al. 2001, Doughty et al. 2007), with 28 currently recognized species (Wilson and Swan 2013). The species are spread throughout the arid regions of Australia, with the highest density in Western Australia (Cogger 2014, Uetz 2016). Species of *Ctenophorus* are

known for their bright coloration, active lifestyle, and sexual dimorphism (Greer 1989a). Males generally display greater variation between species than do females (Melville et al. 2001). However, color often varies with age, season, and temperature of the lizard (Greer 1989a). Body shape and choice of retreat (burrows, no burrows, and rocks) covaries in *Ctenophorus*, with the notable exception of *Ctenophorus caudicinctus*, which was categorized as a generalist by Thompson and Withers (2005).

The three species considered here are *Ctenophorus caudicinctus* (Günther 1875), *Ctenophorus isolepis* (Fischer 1881), and *Ctenophorus reticulatus* (Gray 1845). All are ground-dwelling lizards that exhibit bipedal running behavior (Greer 1989a, Clemente et al. 2008). These three species were chosen because they are ubiquitous, closely related, and have similar ecologies, reducing the number of obvious variables influencing the system.

Ctenophorus caudicinctus ranges across the Pilbara and Kimberley region of Western Australia, across much of the Northern Territory and into western Queensland (Cogger 2014, Uetz 2016). *Ctenophorus caudicinctus* is a diurnal, saxicolous lizard found on rocky slopes (Cogger 1992) or hard soil (Greer 1989a). The species is insectivorous (Cogger 1992). The tail is 170-204% snout-vent length (SVL; Witten 1993).

Ctenophorus isolepis is the most widely distributed of the three taxa I examined, found across most of eastern and northern Western Australia, though the central portion of the continent, and into southwestern Queensland (Cogger 2014, Uetz 2016). *Ctenophorus isolepis* is a ground-dwelling lizard closely associated with arid habitats, sand dunes, and grasses of the genus *Triodia* (Witten 1993, Doughty et al. 2007). The tail is 200-250% SVL (Cogger 1992). This taxon may be an annual species (Greer 1989a).

Ctenophorus reticulatus is found from the northern Gascoyne Coast and the Pilbara region of Western Australia across the central part of that state into north-central South Australia

(Cogger 2014, Uetz 2016). These are ground-dwelling, herbivorous lizards that hide under logs and in stony soils (Cogger 2000, Greer 1989a). The tail is about 150% SVL (Cogger 2000). *Ctenophorus reticulatus* traditionally was considered to be a subspecies of *Ctenophorus nuchalis* (Storr 1966, Greer 1989a, Witten 1993) but genetic data support a sister relationship (Melville et al. 2001).

The fossil record of Australian Agamidae is sparse and mostly unpublished (Molnar 1991). However, little currently can be understood regarding the fossil record because the variation within and between extant Australian Agamidae also remains unexplored. Relatively little is published about the osteology of the Australian agamids (e.g., Greer 1987, Greer 1989a, Greer 1989a, Witten 1993, Bell et al. 2009, Banzato et al 2012). The most serious limitation to the development of a rigorous understanding of the skeletal morphology of the group is a simple lack of osteological preparations in museum collections (Bell and Mead 2014). The recent development of an adequate collection at WAM provides an opportunity to begin exploration of patterns of variation.

As a first step, I set out to answer three questions. First, how many previously published morphological characters are invariant for each species? Second, which states exhibiting no variation are shared among species and which are unique to a given species? Third, when morphological characters vary within a species, do the character states change (i.e., correlate) with ontogeny or sex of the individuals? There certainly are other factors that influencemorphological expression, climate in a given year, which could influence size and degree of development in a species. But they are beyond the scope of the study, which is primarily focused on factors that could be directly evaluated from available skeletal specimens.

MATERIALS AND METHODS

All specimens I examined were collected as part of an ongoing effort to build and develop a skeletal collection at WAM that comprises skeletal specimens with associated tissue samples that are available for subsequent or concurrent molecular analysis. Eighteen to twenty osteological preparations of each of the three species of *Ctenophorus* were available for study. *Ctenophorus caudicinctus* is represented by 18 individuals, and both *Ctenophorus reticulatus* and *Ctenophorus isolepis* are represented by 20 individuals (Tables 1.1-1.2). All individual specimens were collected in Western Australia (Figure 1.1) between 2005 and 2008, and all are registered in the collection of the WAM.

For convenience, morphological data are recorded in a taxon-character matrix, and although the phylogenetic utility of characters is discussed, phylogenetic informativeness is not directly tested in this study.

Morphological characters were selected from previously published studies that included Australian Agamidae and also the unpublished Masters thesis by Moody (1980). The thesis is included because it is the primary source for the data collected and is referenced many times within the literature (e.g., Borsuk-Białynicka and Moody 1984, Estes et al. 1988, Gauthier et al. 1988, Greer 1989a, Melville et al. 2001, Evans et al. 2002, Hocknull 2002, Stuart-Fox and Owens 2003, Hugall and Lee 2004, Ord and Stuart-Fox 2006, Lee 2005, Ananjeva et al. 2007, Hugall et al. 2008, Bell et al. 2009, Ananjeva et al. 2011, Smith et al. 2011, Wagner et al. 2011, Gauthier et al. 2012, Blain et al. 2013). Characters from different sources were combined if they described the same character. A total of 53 morphological characters survived the initial vetting process. I added 13 novel characters as well for an initial total of 66 morphological characters. After scoring, eight morphological characters were removed because the given character on the

observed skulls was not as easily categorized as originally anticipated (see Results). Anatomical terminology follows Evans (2008).

All skulls were examined under a Zeiss microscope. Scores for each morphological character were recorded one at a time for all three species before the next morphological character was considered. Using only three taxa creates a tractable study because it limits the number of ways morphological characters can be shared within and between species. This system can be visualized using Venn diagrams, in which each circle represents one species. Shared characters can be placed in the appropriate overlapping portion of the circle, while unique characters can be placed in the nonoverlapping portion.

Two types of data were recorded for this study. Continuous data were collected from four measurements of the skull of each individual in dorsal view (Figure 1.2) and categorical data were collected from the 60 morphological characters. All measurements were recorded in Microsoft Excel. If the skull was not complete, measurements that could not be recorded were recorded as 'NA.' The skull of each individual was photographed using a Canon EOS 5D Mark 2 camera with a Canon Macro Lens EF 100 mm 1:2.8 USM. Digital photos of each skull were taken in dorsal view. The mandible of each individual was photographed in labial and lingual view. All images were taken using the program Helicon Remote 2.4.4W and stacked in Helicon Focus version 5.3. Details of each skull were taken with the Zeiss microscope using the program Zen version 8. All skull measurements (Tables 1.3-1.4) were made from the dorsal view of each individual using the program ImageJ 1.49 (Rasband 1997-2014).

All morphologic states were described *a priori*. The first question of this study was whether or not previously proposed characters for Australian Agamidae are invariant within species. Invariant is defined as 100% of the individuals of that species showing expression of only one morphologic state. NA scores were not counted. Using discreet data, invariant

morphologic states are easily identified within each species. This same method was used to identify invariant characters between species.

To test if variation in morphological characters correlated with ontogeny and sexual dimorphism, I used the Pearson product-moment correlation coefficient (CC). The CC was calculated in Excel within each species for ontogeny vs. morphological character and sex vs. morphological character (Tables 1.5-1.6). This metric compares two distributions with an equal number of samples and measures how close the variables are to a perfect linear relationship. The metric scores from 1, a perfect positive linear relationship, to -1, a perfect negative relationship. A zero indicates there is no relationship between the two distributions. Any distribution set with 100% invariant morphologic states will give back an error message, making invariant morphologic states easily identified as well. Any CC ≥ 0.5 or ≤ -0.5 was considered significant (Zar 2010) because this meant that there was at least a moderate amount correlation between a morphological character and ontogeny or sex. The test is purposefully weak to capture any signal that might be in the data in this first-pass study.

Sex of the individual was coded as 1 for female and 2 for male. Missing data were labeled as 'NA.' Skull length was used as a proxy for ontogenetic age and was measured in dorsal view from the anteriormost tip of the skull to the posteriormost tip of the postparietal process of the parietal (Fig. 1.2). For relatively smaller Australian agamid skulls the posteriormost portion of the skull is often the occipital condyle, while for relatively larger agamids the posteriormost portion of the postparietal process of the parietal is the posteriormost portion of the skull. However, these two sets of measurements did not differ significantly (Supplementary File 1) so one was chosen arbitrarily.

The common test of categorical variables is the Chi-Square Test (Zar 2010), but that test fails if one or more character states have a frequency of zero (which often occurs in

morphological character data); the test also requires an ideal distribution to compare against the collected data. The one-sided independent samples T-test also does not work because the data are already effectively binned, decreasing the degrees of freedom. Sampling could have been increased by using a bootstrap method (Zar 2010), but this would not have added any additional information pertaining to the questions I am asking in this study (e.g. character distribution and variance in each species).

Abbreviations

Institutional abbreviations include NT R, Museum and Art Gallery of the Northern Territory, Darwin, Northern Territory, Australia; WAM R, Western Australian Museum, Perth, Western Australia, Australia; TMM, Texas Memorial Museum, The University of Texas at Austin, Austin, Texas; VPL, Vertebrate Paleontology Lab, The University of Texas at Austin, Austin, Texas; The University of Texas at Austin, Austin, Texas; JIM, James I. Mead Collection, East Tenesee State University, Tenesee. A list of anatomical abbreviations used in the figures is provided in the Glossary.

Descriptions of Morphological Characters

Descriptions are supplemented by visualizations of each character (Appendix A). Citations are provided for characters or non-explicit description of characters derived from previous sources. Novel characters are marked with an asterisk

1. In palatal view, the maxillae contact each other posterior to the premaxilla and anterior to the vomers; 0 = the maxillae do not contact, Fig. A1; 1 = the maxillae contact, Fig. A2 (modified from Moody 1980, character 40; Estes et al. 1988, Agamidae character 3).
2. *Contact of the internarial process of the premaxilla with the frontal; 0 = the internarial process of the premaxilla does not contact the frontal, Fig. A3; 1 = the internarial process of the premaxilla contacts the frontal, Fig. A4.

3. Number of pleurodont teeth in the premaxilla; Fig. A5 (Moody 1980, character 69).

4. Contact of the facial process of the maxilla and the nasal; 0 = the facial process of the maxilla does not contact the nasal, Fig. A6; 1 = the facial process of the maxilla contacts the nasal, Fig. A7 (Moody 1980, character 41).

5. Diastema between the lateralmost premaxillary tooth position and the premaxilla-maxilla suture; 0 = absent, Fig. A8; 1 = present, Fig. A9 (Hocknull 2002).

6. *Distinct midline diastema between the premaxillary tooth positions; 0 = absent, Fig. A10; 1 = present, Fig. A11.

7. Total number of pleurodont tooth postitions on the five tooth-bearing skeletal elements (azygous premaxilla, paired maxillae, and paired dentaries); Fig. A12 (Moody 1980, character 67).

8. From palatal view, the labial margin of the premaxilla and maxilla; 0 = form a continuous arc, Fig. A13; 1 = the premaxilla is flat, Fig. A14; 2 = the premaxilla interrupts a continuous arc; Fig. A15 (modified from Moody 1980, character 39).

9. Fenestra formed by the nasals and frontals; 0 = absent, Fig. A16; 1 = present, Fig. A17, (Siebenrock 1895, El-Toubi 1945, 1947).

10. *In dorsal view, the position of the pineal foramen relative to a straight line formed between the lateral margins of the frontoparietal suture; 0 = the pineal foramen is anterior, Fig. A18; 1 = the pineal foramen is in line, Fig. A19; 2 = the pineal foramen is posterior, Fig. A20.

11. In palatal view, contact of the vomer with the contralateral element; 0 = contact along less than half their length, Fig. A21; 1 = contact at least half, but less than the entire length, Fig. A22; 2 = contact along their entire length, Fig. A23 (modified from Siebenrock 1895, Jollie 1960).

12. *In palatal view, the connection of the palatine with the contralateral element; 0 = no contact or contact along less than half the entire length, Fig. A24; 1 = contact along half or more than half the entire length, Fig. A25; 2 = contact along the entire length, Fig. A26.

13. In palatal view, anterior contact of the pterygoid with the contralateral element; 0 = do not contact each other anteriorly, Fig. A27; 1 = contact each other anteriorly, Fig. A28 (modified from Siebenrock 1895, character 26).

14. Distal portion of the pterygoid displays a distinct hooked ventral flange anterior to the pterygoid-quadrate articulation; 0 = flange is absent, Fig. A29; 1 = flange is present, Fig. A30 (modified from Moody 1980, character 47).

15. *Distal contact of the pterygoid with the quadrate; 0 = narrow, Fig. A31; 1 = broad, Fig. A32.

16. Size of the lacrimal duct relative to the infraorbital foramen; 0 = small, similar in size or not much larger than the infraorbital foramen, Fig. A33; 1 = large, significantly larger than the infraorbital foramen, Fig. A34 (Moody 1980, character 35).

17. In lateral view of the skull, the alignment of the most distal portion of the descending coronoid process of the ectopterygoid compared to the postorbital margin of the orbit; 0 = coronoid process projects anterior to the postorbital margin of the orbit, Fig. A35; 1 = coronoid process projects posterior to the postorbital margin of the orbit, Fig. A36 (Moody 1980, character 48).

18. In anterior view of the skull, the contribution of the ectopterygoid to the pterygoid-ectopterygoid vertical flange; 0 = pterygoid forms the majority of the process, Fig. A37; 1 = pterygoid and ectopterygoid contribute equally, Fig. A38; 2 = ectopterygoid forms the majority of the process, Fig. A39 (modified from Moody 1980, character 51).

19. In posterior view of the skull, the contribution of the ectopterygoid to the pterygoid-ectopterygoid vertical flange; 0 = pterygoid forms the majority of the process, Fig. A40; 1 = pterygoid and he ectopterygoid contribute equally, Fig. A41; 2 = ectopterygoid forms the majority of the process, Fig. A42 (modified from Moody 1980, character 51).

20. Dorsal process of the medial head of the ectopterygoid that overlaps the dorsolateral surface of the pterygoid; 0 = short, Fig. A43; 1 = completely overlaps the pterygoid surface to the midline, Fig. A44 (Moody 1980, character 52).

21. *Foot of the epipterygoid; 0 = articulates only with the pterygoid, Fig. A45; 1 = articulates with both the pterygoid and the basipterygoid process of the sphenoid, Fig. A46.

22. Dorsal epipterygoid contact; 0 = epipterygoid has a bony dorsal tip which closely approaches the ventral process of the parietal, Fig. A47; 1 = epipterygoid short and does not closely approach the ventral process of the parietal, Fig. A48 (Moody 1980, character 26).

23. Epipterygoid in lateral view; 0 = contacts the parietal or anterodorsal process of the prootic, Fig. A49; 1 = contacts the exterior of the anterior bulge of the semi-circular canal of the prootic or anteroventral surface of the prootic or does not contact the parietal or prootic, Fig. A50; (Moody 1980, character 27).

24. Lateral cranial wall of parietal; 0 = possesses a sharp downward process with which the epipterygoid has a ligamentous contact, Fig. A51; 1 = lateral wall is straight or with only a slightly rounded process, Fig. A52 (Moody 1980, character 15).

25. In lateral view, the postparietal process of the parietal in the transverse plane; 0 = horizontal or slightly curved projection ventrally, Fig. A53; 1 = obvious downward projection, Fig. A54 (Moody 1980, character 14).

26. In posterodorsal view of the skull, the posterior semicircular canals of the braincase; 0 = are not apparent, Fig. A55; 1 = are apparent only on the supraoccipital, Fig. A56; 2 = are apparent on both the supraoccipital and otooccipital, Fig. A57 (Moody 1980, character 8).

27. Supratemporal; 0 = absent, Fig. A58; 1 = present, Fig. A59 (Moody 1980, character 17).

28. Temporal arch portion of the jugal in lateral view; 0 = area of contact with squamosal approximately equal to that of the postorbital, Fig. A60; 1 = the jugal has a larger contact area with the squamosal than the postorbital, allowing only a small narrow process of the postorbital to contact the squamosal, Fig. A61; 2 = the jugal contact with the squamosal excludes any postorbital contact with the squamosal, Fig. A62 (Moody 1980, character 28; Gauthier et al., 2012, character 154(2)).

29. Orbital portion of the jugal in lateral view; 0 = majority of the infraorbital region formed by a broad jugal, Fig. A63; 1 = maxilla and jugal contribute approximately equally, Fig. A64 (Moody 1980, character 29).

30. Jugal contribution to the infraorbital canal; 0 = absent, Fig. A65; 1 = present, Fig. 66 (Moody 1980, character 30).

31. Quadrate notch that accommodates the squamosal articulation; 0 = absent, Fig. A67; 1 = present, Fig. A68 (Moody 1980, character 23).

32. Transverse angle of the basal tubera of the basioccipital, one arm measured relative to the other; 0 = approximately perpendicular, 90-110 degrees, Fig. A69; 1 = obtuse angle, 111-140 degrees, Fig. A70 (Moody 1980, character 2).

33. From a sagittal plane, the basal tubera of the basioccipital; 0 = project perpendicularly downward, Fig. A71; 1 = project in a posterior angle, Fig. A72 (Moody 1980, character 3).

34. In lateral view the fenestra ovalis, when compared to the lateral aperture of the recessus scalae tympani (modified from 'fenestra cochlea' of Moody 1980, character 5); 0 = fenestra ovalis is obviously smaller than the lateral aperture of the recessus scalae tympani, Fig. A73; 1 = fenestra ovalis is approximately equal in size to the lateral aperture of the recessus scalae tympani, Fig. A74; 2 = fenestra ovalis is larger than the lateral aperture of the recessus scalae tympani, Fig. A75 (Moody, 1980, character 5).

35. The angle of the paroccipital (opsithotic) process of the otooccipital, when viewed in a lateral transverse plane; 0 = angle obviously above horizontal, Fig. A76; 1 = projects approximately horizontally, Fig. A77; 2 = angle obviously below horizontal, Fig. A78 (modified from Moody 1980, character 4).

36. Size of the recess containing the foramen ovale and lateral aperture of the recessus scalae tympani (tympanic-occipital recess of Moody, 1980, character 6); 0 = recess large, including an excavation of the basioccipital process, Fig. A79; 1 = recess large, omits an excavation of the basioccipital process, Fig. A80; 2 = absent, Fig. A81 (Moody 1980, character 6).

37. Sphenoccipital foramen; 0 = absent, Fig. A82; 1 = present, Fig. A83 (Siebenrock 1895; Moody, 1980, character 11; Borsuk-Białynicka and Moody 1984, character 1; Gauthier et al. 2012, character 304(1)).

38. Anterodorsal (alar) process of the prootic; 0 = little or no prootic between the anterior semicircular canal bulge and the ventral process of the parietal with which it makes contact, Fig. A84; 1 = anterodorsal process of the prootic distinct between the anterior semicircular canal bulge and the ventral process of the parietal, Fig. A85 (Moody 1980, character 9).

39. Supratrigeminal process of the prootic; 0 = absent, Fig. A86; 1 = tiny, Fig. A87; 2 = strongly projecting, Fig. A88 (Moody 1980, character 10).

40. Contribution of the parasphenoid portion of the sphenoid bone to the basal tubercle of the basioccipital; 0 = parasphenoid contributes to the process of the basal tubercle, Fig. A89; 1 = suture between the parasphenoid and basioccipital lies immediately anterior to the process, Fig. A90; 2 = suture far anterior to the processes, Fig. A91 (Moody 1980, character 12).

41. Shape of the prefrontal margin of the orbit; 0 = round, follows the shape of the orbit, Fig. A92; 1 = knobbed or with a sharp process, Fig. A93 (modified from Moody 1980, character 32).

42. Lacrimal; 0 = absent, Fig. A94; 1 = present, Fig. A95 (modified from Moody 1980, character 33).

43. Postfrontal; 0 = absent, Fig. A96; 1 = present, Fig. A97 (Estes et al. 1988, character 1).

44. Anterodorsal process of the postorbital; 0 = lacking or only slightly rounded, Fig. A98; 1 = distinct knob or boss, Fig. A99 (modified from Moody 1980, character 21).

45. Dorsal process of the squamosal extending along the medial wall of the upper temporal fenestra; 0 = absent, Fig. A100; 1 = present, Fig. A101 (Moody 1980, character 22).

46. Tympanic conch of the quadrate; 0 = anteriorly concave, broadly arching lateral margin with a thickened edge, Fig. A102; 1 = anteriorly concave conch present, but lateral margin straight and without a thickened edge, Fig. A103; 2 = conch rudimentary, only a small flat flange or absent, Fig. A104 (Moody 1980, character 24).

47. Mandibular articulating head of the quadrate; 0 = medial condyle substantially larger than the lateral, Fig. A105; 1 = condyles approximately equal in size, Fig. A106 (Moody 1980, character 25).

48. Meckelian groove; 0 = remains on medial surface of dentary at the symphysis, Fig. A107; 1 = rotates to the ventral edge, Fig. A108 (Moody 1980, character 57).

49. Coronoid has a small labial process that overlaps the dentary; 0 = absent, Fig. A109; 1 = present, Fig. A110 (Moody 1980, character 59; see also Estes et al. 1988, character 5; Gauthier et al. 1988, character 46).

50. Posterior medial process of the coronoid; 0 = short, not reaching the ventral edge of the mandible, Fig. A111; 1 = long, completely overlapping the prearticular and reaching the ventral edge of the mandible, Fig. A112; 2 = absent, Fig. 113 (modified from Moody 1980, character 61).

51. Prearticular; 0 = absent, Fig. A114; 1 = present, Fig. A115 (modified from Gauthier et al. 2012, character 401).

52. Angular foramen (posterior mylohyoid foramen) location; 0 = on the ventral edge of the angular, Fig. A116; 1 = on the medial surface of the angular, Fig. A117 (Moody 1980, character 65).

53. Splenial; 0 = absent, Fig. A118; 1 = present, Fig. A119 (Moody 1980, character 66; Estes et al. 1988, character 2).

54. *Mandibular fossa; 0 = absent, Fig. A120; 1 = present, Fig. A121.

55. *Diastema present between last posterior acrodont tooth postition and coronoid process. Diastema must not be the result of a tooth still forming and must be greater than the anteroposterior width of the most posterior acrodont tooth; 0 = absent, Fig. A122; 1 = present, Fig. A123.

56. *Lingual portion of the surangular pierced by the foramen for the maxillary division of cranial nerve V (SUas; e.g., anterior mylohyoid foramen of Oelrich 1956); 0 = absent, Fig. A124; 1 = present, Fig. A125.

57. *From a labial view of the dentary, anterior supra-angular foramen; 0 = not visible, Fig. A126, 1 = present, Fig. A127.

58. *From a labial view of the dentary, posterior supra-angular foramen; 0 = not visible, Fig. A128; 1 = present, Fig. A129.

59. *Chorda tympani foramen in the mandibular fossa; 0 = not visible, Fig. A130; 1 = present, Fig. A131.

60. *Number of mental foramina on right dentary; Fig. A132.

Discarded Morphological Characters

61. Septomaxilla; 0 = absent, Fig. A133; 1 = present, Fig. A134.

62. Number of lateral maxillary foramina; Fig. A135.

63. In palatal view, maxilla-palatine suture, as measured by a straight line from the most anterior to the most posterior visible contact points; 0 = parallel to maxillary tooth row, Fig. A136; 1 = acutely angled anteromedially, Fig. A137 (Moody 1980, character 42).

64. Scleral ossicle number; 0 = 12, Fig. A138; 1 = 11, Fig. A139 (Moody, 1980 character 56; Estes et al. 1988, character 8).

65. Postorbital and postfrontal; 0 = both bones present, Fig. A142; 1 = fusion of postorbital and postfrontal or loss of one bone, Fig. A143.

66. Posterior medial process of the coronoid; 0 = strongly ridged, Fig. A144 ; 1 = weakly ridged or flat, Fig. A145 (Moody 1980, character 61).

Data Access

Original data collection files, analyses files, and figures of each character can be found in the appendices and online at Morphobank.org http://morphobank.org/permalink/?P1262 (O'Leary et al. 2012).

RESULTS

Sixty morphological characters were retained for the analysis portion of this study and eight were not used. The maxilla-palatine suture (number 63) and the posterior medial process of the coronoid (number 66) were discarded because the morphological character displayed too subtle a gradient to classify as discrete states. The septomaxilla (number 61), number of maxillary foramina (number 62), scleral ossicle number (number 64), and postorbital-postfrontal fusion (character 65) were too difficult to observe in available specimens.

Each of the three species had at least one unique morphological character quantitatively unique to that species (Figure 1.3). Invariant characters are those that were always scored as the same state for all specimens of a given species, regardless of sex or ontogenetic age. Thirty-nine of the 60 morphological characters are invariant for at least one of the three taxa. Within this group of invarient characters I recognize three categories. The first includes characters that were unique to a single species. The second category includes characters scored as the same state for two of the three species. The third category includes those characters that were scored as the same state for all three species. Invariant characters for *Ctenophorus caudicinctus* are 5(1), 8(0), 28(1), 35(1), 51(0), and 59(1). Invariant characters for *Ctenophorus isolepis* are 10(2), 11(1), 17(0), 24(1), and 58(1). The invariant characters for *Ctenophorus reticulatus* are 1(1) and 50(1). Among the second category of characters, *Ctenophorus reticulatus* and *Ctenophorus isolepis* were both invariant for characters 2(0) and 31(1). *Ctenophorus reticulatus* and *Ctenophorus caudicinctus* were both invariant for character 25(1). *Ctenophorus caudicinctus* and *Ctenophorus isolepis* were invariant for characters 13(0), 15(1), 19(0), 38(1), 47(0), 53(1), and 56(0). Morphologically invariant characters shared by all three taxa are 4(1), 9(1), 16(1), 21(0), 22(1), 23(1), 26(2), 27(1), 37(1), 41(1), 42(0), 43(0), 48(1), 49(0), 57(1), and 54(1).

Morphological characters that varied within taxa (thus, excluding all invariant morphological characters) were statistically tested for covariance with ontogeny (using skull length as a proxy) and sexual dimorphism. Sixteen of the 60 characters measured varied with ontogeny for at least one taxon and nine varied with sex for at least one taxon. These measurements can also be divided into the three categories: those that are unique characters for a single given taxon; those that are the same for two taxa; and those shared between all taxa. For only *Ctenophorus caudicinctus*, characters 33, 45, and 50 were positively correlated with ontogeny, while characters 32 and 46 negatively correlated with ontogeny. For only *Ctenophorus caudicinctus*, characters 17,18, 33, 39, 50, and 52 positively with sex and zero characters varied negatively. For only *Ctenophorus isolepis*, no characters varied with ontogeny or sex. For only *Ctenophorus reticulatus*, characters 10, 15, and 38 varied positively with ontogeny, while character 35 varied negatively with ontogeny. For sexual dimorphism, characters 7, 36, and 55 varied positively.

Characters that varied with ontogeny or sexual dimorphism in the same direction (e.g., positive or negative) for groups of species were also measured. For *Ctenophorus caudicinctus* and *Ctenophorus reticulatus* characters 7, 17 and 55 varied positively, while 40 varied negatively. *For Ctenophorus caudicinctus and Ctenophorus isolepis*, character 52 varied with ontogeny. For *Ctenophorus isolepis* and *Ctenophorus reticulatus*, no characters varied in the same direction with ontogeny (but note that there is a negative correlation for character 6). For all three taxa, character 39 varied positively with ontogeny. No shared characters varied with sexual dimorphism.

DISCUSSION

These data have important implications for understanding patterns of morphological variation among extant Australian agamids, and for interpretations of the fossil record of the

group. Morphological characters examined here were not originally identified as being useful for distinguishing species of *Ctenophorus*, nor for distinguishing *Ctenophorus* from other endemic Australian agamids. Nonetheless they show interesting patterns of variation among the three species of *Ctenophorus* I studied. Each of the species had at least one invariant character that was invariant for just that species among the three. If a morphological character continues to be invariant for just a single species, even as more species of *Ctenophorus* are evaluated and scored, such invariant characters would be important diagnostic characters for the identification of particular species, and would be optimized as autapomorphies in a phylogenetic analysis of the group. If the character and state can be assessed for isolated skeletal elements, those characters would be particularly important for making reliable identifications of specimens preserved in the fossil record.

Of the characters unique to *Ctenophorus reticulatus*, 5(1), 35(1), and 59(1) all could be readily identified in isolated skeletal elements, and so could be useful for interpreting fossils. Characters 8(0), 35(1), and 59(1) are likely to be interpretable only from articulated or partially articulated skulls; their applicability to the interpretation of fossils would thus be dependent upon preservation and the degree to which disarticulation happened during fossilization. Of the characters unique to *Ctenophorus isolepis*, 24(1) and 58(1) could be readily identified on isolated skeletal elements, while characters 10(2), 11(1), and 17(0) are likely to be interpretable only from articulated or partially articulated skulls. The characters unique to *Ctenophorus isolepis*, 1(1) and 50(1), are likely to be interpretable only from articulated or partially articulated skulls.

The second category of characters includes states that were invariant, but are shared by two among the three species. In a phylogenetic character analysis, those characters are potential synapomorphies that might yield evidence of relationship. Determination of synapomorphic

status would be dependent upon a phylogenetic analysis and the resolution of any character conflict that might be present within the data set.

The third category of characters includes those that were invariant, but were scored the same way in all three species. Those are clearly characters that are diagnostic at some deeper phylogenetic level (e.g., diagnostic of all *Ctenophorus*, or of larger species groups, or of the endemic Australian clade as a whole).

The sobering reality here is that my analysis included adequate sample sizes for only three species of *Ctenophorus*. No fewer than 25 additional species of *Ctenophorus* must be evaluated and assessed before any reasonably confident statement can be made about the distribution of character states among species of the group.

CONCLUSION

The elucidation of patterns of morphological variation in the skeleton of Australian endemic agamids remains an important goal. A relatively rich but largely untapped fossil record for the group is available for study. Efforts to interpret that fossil record reliably must be grounded in a solid understanding of the skeletal system of the group, with special attention paid to the intraspecific differences in skeletal morphology that result from differences in ontogenetic age and from sexual dimorphism. Such data are lacking for almost all clades of extant squamates, and existing holdings of skeletal specimens in museum collections are, for the most part, wholly inadequate for addressing this problem (Bell and Mead 2014). A reliable interpretation of the fossil record must await a more refined understanding of the morphological patterns exhibited in the extant biota.

The importance of understanding interspecific and intraspecific patterns of skeletal variation is, thus, acute. Agamids remain one of the most poorly understood clades of squamates. No modern morphological database or matrix exists for the Australian endemics, nor for

Agamidae as a whole. Efforts to gather, collate, and analyze such data sets must be initiated. The only attempts at summaries of the morphological patterns in the skull as a whole are those of Siebenrock (1895) and Moody (1980). Detailed study of the maxilla and dentary of the Australian agamids was presented by Hocknull (2005) with the specific aim of building a framework from which fossils could be identified. Hocknull's data provide a crucial first step in shaping a list of morphological characters by which the Australian endemics may be evaluated and identified. Here I provide an addition to, not evaluation of, his seminal work. My goal was to explore the patterns of variation of other previously published characters and to assess whether larger sample sizes were important for recording variant phenotypes. Some of those morphological characters show some promise for taxon discrimination even among closely related species within a speciose clade. Adequate sample sizes do not yet exist to test the broader utility of those characters for taxon discrimination. In my expanded data set (Appendix B, Tables A2.1-A2.5), there are eight other taxa within the *Ctenophorus* clade, albeit at smaller sample sizes. When I compared all of the characters proposed to be unique to either *Ctenophorus caudicinctus*, *Ctenophorus reticulatus*, or *Ctenophorus isolepis* to this expanded data set, all appeared to share their 'unique' characters with at least one other species. This suggests that characters require rigorous evaluation, both within and between taxa, to confirm morphological states before phylogenetic analyses can be made.

Alternative approaches also can be brought to bear on the problem. For example, morphometric analysis of skull shape will certainly yield interesting insights into ontogenetic transformations of the skull, and might reveal subtle differences between the sexes that are not readily discernible from discrete character data alone. However, as evidenced by my dataset, most morphological characters will not be invariantly scored for most taxa. Efforts to quantify and evaluate patterns of variation, and to explore differences in the tendency of particular

lineages to express variation, will be important avenues of future work on the group. In all cases, more expansive collections will be required to gather the relevant data.

My data confirm that published morphological characters of the skull in agamids do appear to vary in systematically informative ways, even when applied in contexts for which they were not originally conceptualized. But those data are simultaneously promising and sobering. They hold out the promise that morphological characters of the skull may indeed permit species-level discrimination, even among speciose clades. But they also suggest that unambiguously diagnostic characters will likely remain elusive, and they emphasize the importance of relatively large sample sizes for documenting patterns of variation within agamids. The ability to resolve fine-scale taxonomic categories from isolated skeletal elements preserved in the fossil record may be limited in speciose clades. The occurrence of diagnostic characters in the several monotypic genera of Australian endemic agamids remains largely untested, but at least some diagnostic characters do occur in the iconic thorny devil, *Moloch horridus* (Bell et al., 2009).

Ultimately, the integration of detailed morphological data, from the fossil record and from the extant biota, with molecular data will provide a holistic perspective on the evolution of this interesting clade of lizards. The molecular data are increasingly more robust and are helping to shape new questions regarding biogeographic patterns, and the timing of divergence among the various lineages (e.g, Melville et al. 2001, Hugall and Lee 2004, Byrne et al. 2008, Hugall et al. 2008, Doughty et al. 2014, Melville et al. 2014, Edwards et al. 2015). The fossil record can and will yield relevant data in both of those areas, but those data will be meaningful only if the fossil record is interpreted with care, and in the context of a robust understanding of the skeletal morphology of the extant species.

Tables and Figures for Chapter 1

Table 1.1. Data available on the three species in this study. All specimens are hosued in the Western Australian Museum recent collection (WAM R). SVL = Snout-vent Length. Tl Length = Tail Length. NA = information not available. mm = millimeters. g = grams.

Institution Number (WAM R)	Genus	Species	SVL (mm)	T1 Length (mm)	Mass (g)	Sex	date day/mo/yr
162820	*Ctenophorus*	*caudicinctus*	NA	NA	NA	NA	NA
162819	*Ctenophorus*	*caudicinctus*	NA	NA	NA	NA	NA
167625	*Ctenophorus*	*caudicinctus*	38	109	2.05	F	05/06/05
167626	*Ctenophorus*	*caudicinctus*	35	NA	1.6	M	05/06/05
167673	*Ctenophorus*	*caudicinctus*	36	115	1.8	F	09/06/05
167679	*Ctenophorus*	*caudicinctus*	32	95	1.55	F	11/06/05
162822	*Ctenophorus*	*caudicinctus*	NA	NA	NA	NA	29/05/06
167676	*Ctenophorus*	*caudicinctus*	39	119	1.95	F	11/06/05
111747	*Ctenophorus*	*caudicinctus*	NA	NA	NA	NA	02/10/05
162887	*Ctenophorus*	*caudicinctus*	46	151	4.45	F	11/06/06
167665	*Ctenophorus*	*caudicinctus*	62	148	8.6	NA	08/06/05
167670	*Ctenophorus*	*caudicinctus*	62	191	9.5	F	09/06/05
167667	*Ctenophorus*	*caudicinctus*	64	206	11	M	09/06/05
167672	*Ctenophorus*	*caudicinctus*	67	222	11.25	M	09/06/05
167632	*Ctenophorus*	*caudicinctus*	72	217	16	M	05/06/05
165036	*Ctenophorus*	*caudicinctus*	NA	NA	NA	NA	03/05/05
93130	*Ctenophorus*	*caudicinctus*	NA	NA	NA	NA	NA
167652	*Ctenophorus*	*caudicinctus*	79	235	19.5	M	08/06/05
162898	*Ctenophorus*	*isolepis isolepis*	35	107	1.8	M	09/06/06
149693	*Ctenophorus*	*isolepis gularis*	43	81	2.7	F	27/09/08
149279	*Ctenophorus*	*isolepis gularis*	43	93	2.7	F	29/09/08
149444	*Ctenophorus*	*isolepis gularis*	46	99	3.3	M	24/09/08
162896	*Ctenophorus*	*isolepis*	40	125	2.15g	NA	09/06/06
149574	*Ctenophorus*	*isolepis gularis*	46	55 (tip missing)	3.5	M	27/09/08
149689	*Ctenophorus*	*isolepis gularis*	48	102	3.55	F	29/09/08
149710	*Ctenophorus*	*isolepis gularis*	46	96	3.3	F	27/09/08
162895	*Ctenophorus*	*isolepis*	46	150	3.2	M	09/06/06
149094	*Ctenophorus*	*isolepis gularis*	50	102	4.3	M	27/09/08

Table 1.2. Data available on the three species in this study (continued). All specimens are housed in the Western Australian Museum recent collection (WAM R). NA = information not available.

Institution Number (WAM R)	Genus	Species	SVL (mm)	Tl Length (mm)	Mass (g)	Sex	date day/mo/yr
149943	*Ctenophorus*	*isolepis gularis*	48	101	3.6	M	29/09/08
149179	*Ctenophorus*	*isolepis gularis*	51	115	5.2	M	29/09/08
149677	*Ctenophorus*	*isolepis gularis*	50	111	4.15	M	29/09/08
149917	*Ctenophorus*	*isolepis gularis*	49	99	3.9	F	27/09/08
162894	*Ctenophorus*	*isolepis*	51	171	4.6	F	09/06/06
149161	*Ctenophorus*	*isolepis gularis*	52	122	6.3	M	27/09/08
111736	*Ctenophorus*	*isolepis*	NA	NA	NA	NA	01/10/05
111894	*Ctenophorus*	*isolepis gularis*	NA	NA	NA	M	NA
111903	*Ctenophorus*	*isolepis isolepis*	NA	NA	NA	M	NA
156956	*Ctenophorus*	*isolepis isolepis*	NA	NA	NA	NA	11/10/05
162795	*Ctenophorus*	*reticulatus*	NA	NA	NA	NA	NA
162744	*Ctenophorus*	*reticulatus*	NA	NA	NA	NA	NA
162821	*Ctenophorus*	*reticulatus*	NA	NA	NA	NA	29/05/06
162759	*Ctenophorus*	*reticulatus*	NA	NA	NA	NA	22/05/06
162779	*Ctenophorus*	*reticulatus*	NA	NA	NA	NA	NA
162856	*Ctenophorus*	*reticulatus*	NA	NA	NA	NA	NA
162881	*Ctenophorus*	*reticulatus*	NA	NA	NA	NA	NA
167575	*Ctenophorus*	*reticulatus*	72	163	13.5	NA	02/06/05
167589	*Ctenophorus*	*reticulatus*	61	140	10	F	04/06/05
167590	*Ctenophorus*	*reticulatus*	75	181	16.5	F	04/06/05
167591	*Ctenophorus*	*reticulatus*	73	163	14	F	04/06/05
156678	*Ctenophorus*	*reticulatus*	77	192	17.8	M	25/05/05
167503	*Ctenophorus*	*reticulatus*	80	~186	20.5	F	25/05/05
167551	*Ctenophorus*	*reticulatus*	80	201	21	M	29/05/05
162855	*Ctenophorus*	*reticulatus*	NA	NA	NA	F	31/05/06
167514	*Ctenophorus*	*reticulatus*	95	243	29	M	27/05/05
167563	*Ctenophorus*	*reticulatus*	94	258	37	M	02/06/05
167567	*Ctenophorus*	*reticulatus*	98	264	40	M	02/06/05
162760	*Ctenophorus*	*reticulatus*	NA	NA	NA	NA	23/05/06
162878	*Ctenophorus*	*reticulatus*	NA	NA	NA	NA	02/06/06

Table 1.3. Skull measurements (mm) for all taxa. All specimens are housed in the Western Australian Museum recent collection (WAM R).

Institution Number (WAM R)	Genus	Species	Occipital Skull Length (mm)	Parietal Skull Length (mm)	Maximum Skull Width (mm)	Preorbital Boss Width (mm)
162820	*Ctenophorus*	*caudicinctus*	9	9	8	3
162819	*Ctenophorus*	*caudicinctus*	10	9.5	8	4
167625	*Ctenophorus*	*caudicinctus*	10	10	8	5
167673	*Ctenophorus*	*caudicinctus*	10	10	8	5
167676	*Ctenophorus*	*caudicinctus*	10	10	9	5
167679	*Ctenophorus*	*caudicinctus*	10	10	8	4
167626	*Ctenophorus*	*caudicinctus*	10	10	8	5
162822	*Ctenophorus*	*caudicinctus*	10	10	9	5
162887	*Ctenophorus*	*caudicinctus*	13	13	10	5
167665	*Ctenophorus*	*caudicinctus*	15	16	12	7
167670	*Ctenophorus*	*caudicinctus*	15	16	12	7
167667	*Ctenophorus*	*caudicinctus*	16	16	13	7
167672	*Ctenophorus*	*caudicinctus*	17	18	12	8
167632	*Ctenophorus*	*caudicinctus*	18	19	14	8
111747	*Ctenophorus*	*caudicinctus*	18	19	6	8
165036	*Ctenophorus*	*caudicinctus*	19	20	16	8
93130	*Ctenophorus*	*caudicinctus*	19	20	16	8
167652	*Ctenophorus*	*caudicinctus*	20	21	17	9
162898	*Ctenophorus*	*isolepis*	10	9	8	4
149279	*Ctenophorus*	*isolepis*	11	10	9	5
162896	*Ctenophorus*	*isolepis*	11	11	9	4
149693	*Ctenophorus*	*isolepis*	11	11	8	5
149444	*Ctenophorus*	*isolepis*	11	11	9	5
149574	*Ctenophorus*	*isolepis*	12	11	9	4
149689	*Ctenophorus*	*isolepis*	12	12	9	5
149710	*Ctenophorus*	*isolepis*	12	12	9	4
149094	*Ctenophorus*	*isolepis*	12	12	10	5
149943	*Ctenophorus*	*isolepis*	12	12	10	5
162895	*Ctenophorus*	*isolepis*	12	12	9	5
149917	*Ctenophorus*	*isolepis*	13	12	10	5
149179	*Ctenophorus*	*isolepis*	13	12	10	5
162894	*Ctenophorus*	*isolepis*	13	13	10	5
149677	*Ctenophorus*	*isolepis*	13	13	10	5
149161	*Ctenophorus*	*isolepis*	15	14	11	6
111894	*Ctenophorus*	*isolepis*	15	15	12	6
111736	*Ctenophorus*	*isolepis*	15	15	12	6
111903	*Ctenophorus*	*isolepis*	16	16	12	?

Table 1.4. Skull measurements (mm) for all taxa (continued). All specimens are housed in the Western Australian Museum recent collection (WAM R). Measurements of elements that appeared to be broken were excluded from further analyses.

Institution Number (WAM R)	Genus	Species	Occipital Skull Length (mm)	Parietal Skull Length (mm)	Maximum Skull Width (mm)	Preorbital Boss Width (mm)
156956	*Ctenophorus*	*isolepis*	16	17	12	6
162795	*Ctenophorus*	*reticulatus*	8	8	6	0.3 (broken?)
162821	*Ctenophorus*	*reticulatus*	9	0	8	4
162744	*Ctenophorus*	*reticulatus*	9	9	8	0.4 (broken?)
162759	*Ctenophorus*	*reticulatus*	10	10	9	5
162779	*Ctenophorus*	*reticulatus*	10	10	9	5
162856	*Ctenophorus*	*reticulatus*	12	12	11	5
162881	*Ctenophorus*	*reticulatus*	13	13	11	6
167589	*Ctenophorus*	*reticulatus*	15	15	13	8
167590	*Ctenophorus*	*reticulatus*	15	15	14	8
167575	*Ctenophorus*	*reticulatus*	15	15	13	8
167591	*Ctenophorus*	*reticulatus*	15	16	14	8
156678	*Ctenophorus*	*reticulatus*	16	16	15	9
167503	*Ctenophorus*	*reticulatus*	16	17	15	18
167551	*Ctenophorus*	*reticulatus*	17	18	16	9
162855	*Ctenophorus*	*reticulatus*	18	18	17	8
167514	*Ctenophorus*	*reticulatus*	18	20	17	9
167563	*Ctenophorus*	*reticulatus*	19	20	17	9
167567	*Ctenophorus*	*reticulatus*	20	22	19	10
162760	*Ctenophorus*	*reticulatus*	20	22	21	9
162878	*Ctenophorus*	*reticulatus*	21	22	22	0

Table 1.5. Invariant Morphological Characters and Correlation Coefficients (CC) for all taxa. Invariant Morphological Characters are defined as 100% of the individuals within a given species showing expression of only one morphological state. Invariant Characters are recorded as 'None (invariant state score)'. The invariant state is indicated to allow comparison between taxa. CCs were calculated in Excel and compare two sets of data with an equal number of variables to a perfect linear relationship. Any CC ≥ 0.5 or ≤ -0.5 was considered significant (bolded). CC for size and sex were calculated separately. Parietal skull length (mm) was used for size. Both invariance and CC can be shown in one table, because the test for correlation does not work when all the variables for one set of data are the same (that is, invariant). MC = morphological character.

Agamidae	***Ctenophorus caudicinctus***		***Ctenophorus isolepis***		***Ctenophorus reticulatus***	
MC	**Size (n = 18)**	**Sex (n = 11)**	**Size (n = 20)**	**Sex (n = 17)**	**Size (n = 20)**	**Sex (n = 10)**
1	0.345669381	0.430331483	-0.43931066	-0.018993429	None (1)	---
2	0.265024561	0.346410162	None (0)	---	None (0)	---
3	-0.290406746	-0.313527223	-0.319550098	0.137532786	-0.359834666	0
4	None (1)	---	None (1)	---	None (1)	---
5	None (1)	---	0.169882397	-0.269679945	-0.236956873	0
6	-0.020333493	0.043033148	**0.52614488**	---	**-0.522440798**	0.333333333
7	**0.717278701**	0.237112943	0.45995938	0.142436933	**0.730515502**	**0.820782682**
8	None (0)	---	0.063705899	-0.018993429	0.081850743	-0.2
9	None (0)	---	None (0)	---	None (0)	---
10	0.292921883	---	None (2)	---	**0.695637267**	---
11	-0.092224056	0.149071198	None (1)	---	-0.209256739	-0.21821789
12	-0.210294882	-0.202547873	0.254823596	-0.112366644	0.084381801	0.156173762
13	None (0)	---	None (0)	---	0.238736461	0.333333333
14	0.087152086	---	0.293840483	-0.117697977	0.331794469	---
15	None (1)	---	None (1)	---	**0.520314054**	---
16	None (1)	---	None (1)	---	None (1)	---
17	**0.871692405**	**0.828078671**	None (0)	---	**0.754171098**	0.35
18	0.027111324	**0.559016994**	-0.101929438	0.117697977	-0.24132736	0
19	None (0)	---	None (0)	---	0.234898088	0.333333333
20	0.254942644	0.069006556	-0.121578783	-0.034815531	0.174295773	0.333333333
21	None (0)	---	None (0)	---	None (0)	---
22	None (1)	---	None (1)	---	None (1)	---
23	None (1)	---	None (1)	---	None (1)	---
24	-0.37661385	-0.346410162	None (1)	---	-0.470196718	-0.21821789
25	None (1)	---	0.058460542	-0.184637236	None (1)	---
26	None (2)	---	None (2)	---	None (2)	---
27	None (1)	---	None (1)	---	None (1)	---
28	None (1)	---	0.169882397	-0.112366644	0.294090552	0.333333333
29	-0.420094317	-0.346410162	-0.058460542	0.184637236	-0.309172119	0.333333333

Table 1.6. Invariant Morphological Characters and Correlation Coefficients (CC) for all taxa (continued). MC = Morphological Character.

MC	**Size (n = 18)**	**Sex (n = 11)**	**Size (n = 20)**	**Sex (n = 17)**	**Size (n = 20)**	**Sex (n = 10)**
30	0.320819206	---	0.321141965	-0.341881729	None (0)	---
31	-0.209229917	-0.346410162	None (1)	---	None (1)	---
32	**-0.797919687**	-0.260874597	-0.129660759	0.184637236	-0.070067457	-2.26623E-17
33	**0.647304859**	**0.645497224**	0.057949839	0.034815531	0.352281938	0.05976143
34	-0.156980891	-0.149071198	-0.323669437	-0.170697185	-0.221846604	0
35	None (1)	---	0.084941199	-0.269679945	**-0.68125101**	-0.40824829
36	-0.468131205	-0.346410162	0.058460542	-0.184637236	-0.024879993	**0.5**
37	None (1)	---	None (1)	---	None (1)	---
38	None (1)	---	None (1)	---	**0.540170947**	---
39	**0.732102944**	**0.5**	**0.692045665**	0.21821789	**0.812755579**	0.2
40	**-0.689985913**	-0.448542614	-0.250107491	0.066666667	**-0.658221233**	-0.333333333
41	None (1)	---	None (1)	---	None (1)	---
42	None (0)	---	None (0)	---	None (0)	---
43	None (0)	---	None (0)	---	None (0)	---
44	0.072094861	0.1	-0.332939555	-0.03030303	0.259194018	0.21821789
45	**0.553344333**	0.430331483	0.169882397	0.184637236	0.259756536	-0.333333333
46	**-0.649144972**	0.043033148	-0.333642405	-0.333711906	-0.158788539	0.21821789
47	None (0)	---	None (0)	---	-0.280255845	---
48	None (1)	---	None (1)	---	None (1)	---
49	None (0)	---	None (0)	---	None (0)	---
50	**0.732005748**	**0.559016994**	-0.026712771	0.206583561	None (1)	---
51	None (0)	---	0.281718085	-0.382518426	-0.157013777	---
52	**0.563867139**	**0.6**	**0.520156487**	-0.063564173	0.374691733	-0.21821789
53	None (1)	---	None (1)	---	-0.349577844	-0.333333333
54	None (1)	---	None (1)	---	None (1)	---
55	**0.871692405**	0.448542614	None (1)	---	**0.735650663**	**0.6**
56	None (0)	---	None (0)	---	0.349577844	0.333333333
57	None (1)	---	None (1)	---	None (1)	---
58	0.353525546	---	None (1)	---	0.384054307	---
59	None (1)	---	0.058460542	-0.184637236	0.355866781	---
60	0.336533699	0.346410162	-0.416125189	-0.177639282	0.003879701	0.333333333

Figure 1.1. Map of collected specimens in Western Australia. Latitude and longitude were collected concurrent with specimen capture. Indicators of collection location may overlap. The map was created using the DigitalGlobe feature of Google Maps (Data SIO, NOAA, U.S. Navy, NGA, GEBCO; Image Landsat; Imagery Date: April 9 2013).

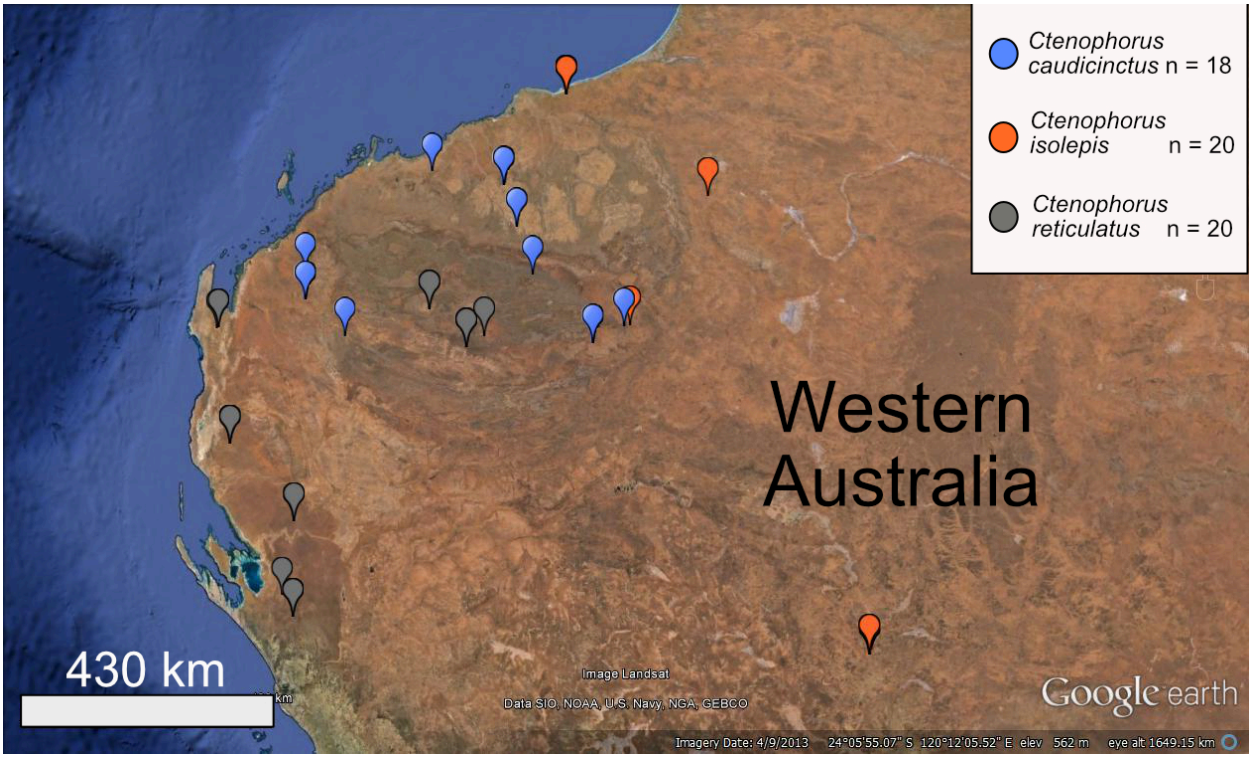

Figure 1.2. Example of skull measurements used in this study for all three taxa. The skull shown is WAM 167665. All measurements were taken in dorsal view using the program ImageJ 1.49 software (2014). Measurement labels correlate with Tables 1.3-1.4.

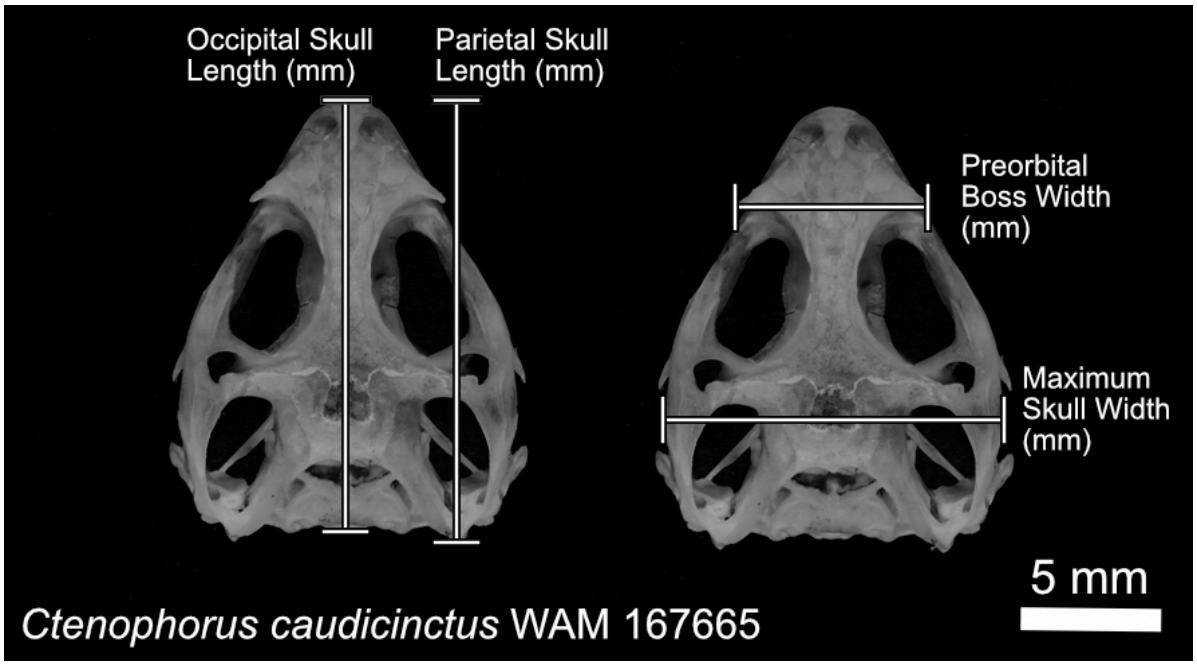

Figure 1.3. Venn Diagrams of shared and unique Invariant Morphological Characters, as well as significant CC for Sexual Dimorphism and Ontogenetic Variation per Species. Invariant traits do not have CC's, so the category that included all taxa, Sexual Dimorphism, was used to tabulate shared and unique Invariant Morphological Characters.

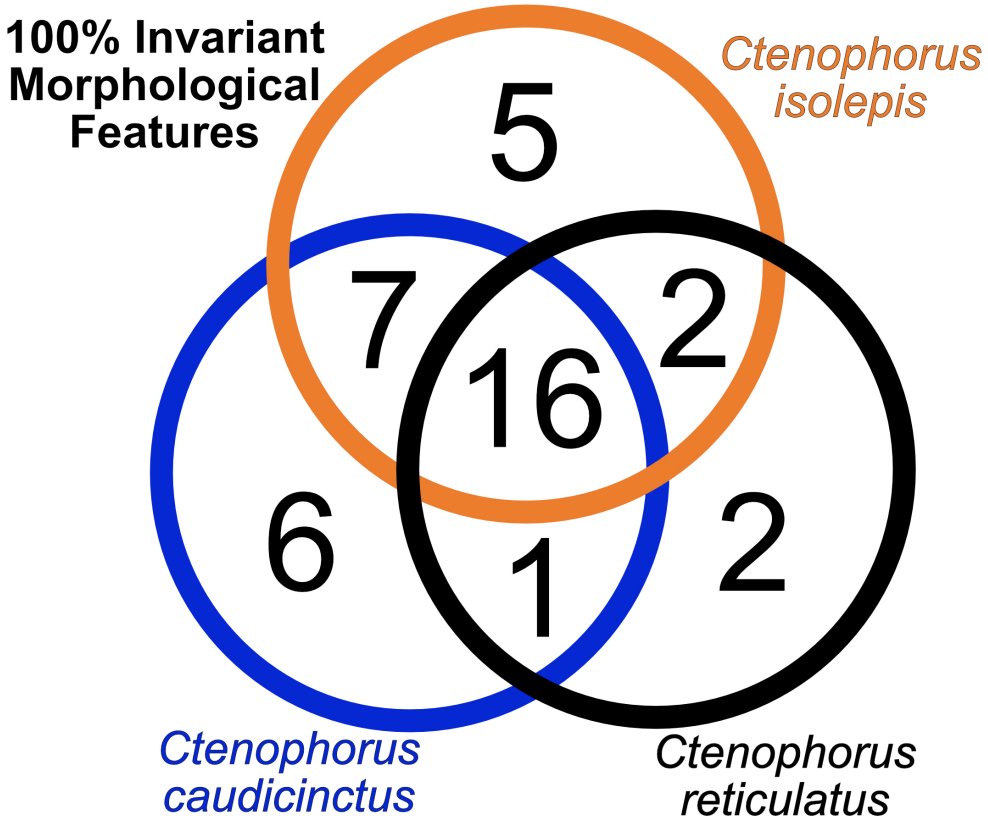

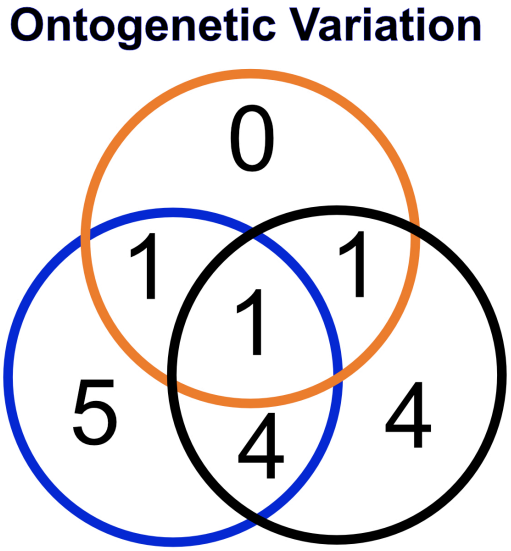

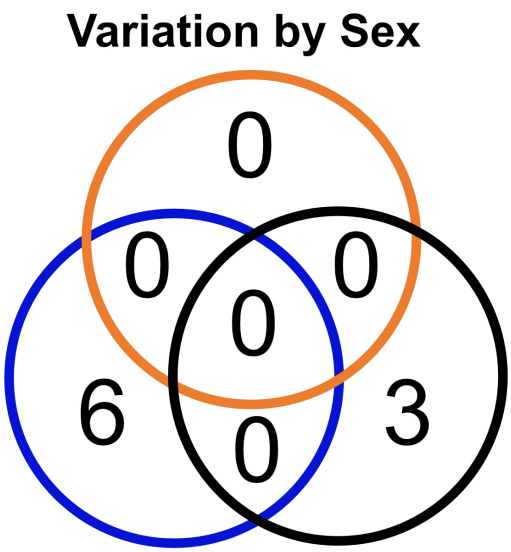

Chapter 2: The Cranial Osteology of *Cryptagama aurita*

INTRODUCTION

Cryptagama aurita is a species of agamid lizard from Northwestern Australia that is currently known from only four specimens. The holotype (WAM R66296) is a male caught in the east Kimberly of Western Australia by M.C. Ellis on 4 September 1979 among small tussocks of *Triodia* on a stony hillside 27 km south-southeast of Halls Creek (Storr 1981). Two juvenile specimens (paratypes, WAM R64051 and R64052) were collected by A.A. Burbidge et al. on 22 April 1979 in bulldozed *Triodia* on a lateritic plain 0.4 km west of World Creek Meteorite Crater (Storr 1981). The second paratype (WAM R64052) is one of the two individuals used in this study. The other individual used in this study, and the most recent specimen to be collected, is a Museum and Art Gallery of the Northern Territory (MAGNT) individual (NT R12804), collected on Buchanan Highway, 15 km west of Wave Hill Police Station (Atlas of Living Australia). A fifth specimen of *Cryptagama aurita* was photographed in the King Leopold Ranges, Western Australia, by I. Dudgeon, but was not collected or tissued; a photo of the individual was published by Wilson (2012; p. 96). All existing museum specimens are formalin-fixed and preserved in alcohol; no tissues are available. Genetic information and skeletal data are lacking, and the species has not been included in any published phylogenetic analysis.

Despite the paucity of data, *Cryptagama aurita* appears in numerous field guides and publications (Cogger 1983, 1992, 1996, 2000, 2014; Witten 1993; Brůna 1996; Manthey and Schuster 1996; Wilson 2012; Vitt and Caldwell 2013). *Cryptagama aurita* was initially classified within the genus *Tympanocryptis* (Storr 1981). The taxon was later placed in the genus *Amphibolurus auritus* (Cogger et al. 1983) and then transferred to a new genus *Cryptagama* (Witten 1984). *Cryptagama aurita* is a terrestrial agamid found in areas with thick shrubbery and

boulders (Storr 1981). The lizards are brown to red, with a lighter belly and dark brown specks. The tail is red-brown, with grey-brown irregular bands, and is shorter than the snout-vent length (Storr 1981). The scales on the head are smooth or weakly rugose. The scales on the neck, back, flanks, tail, and legs are very small, densely intermixed with slightly to much larger keeled scales (not large relative to other agamids), which are randomly distributed. Confusingly, Storr (1981) reported the lengths of the holotype and paratypes together. He reported a snout-vent length (SVL) of 29-46 mm. The lengths of appendages were reported as a percentage of SVL, with the foreleg 41-42%, hind leg 61-63%, and tail 69-77%. The number of upper labials is 16-20 and the lamellae under the fourth toe number 15-18. There are 5/6 (presumed left/right, but this is not specified in Storr 1981) femoral pores in the holotype, 2/2 in the larger of the paratypes, and 0/0 in the smaller paratype. Preanal pores number 3/3 in the holotype and 0/0 in the paratypes. The SVL of NT R12804 is 53 mm, making it the larger of the two specimens I studied.

The taxonomic history of *Cryptagama aurita* is typical of Australian Agamidae and highlights the range of variation within and between clades that makes classification difficult. Here I review the similarities and differences in the various clades in which *Cryptagama aurita* has been placed.

Cryptagama aurita was first classified as *Tympanocryptis* because of the similarity in round body shape and size (Storr 1981). However, there are a number of gross anatomical characters in *Cryptagama aurita* that diverge from the genus *Tympanocryptis*. For example, *Tympanocryptis cephalus* has no visible tympanum, a reduced phalangeal formula and pores that are longer anteroposteriorly than they are mediolaterally between the scales and labials (Witten 1984). *Cryptagama aurita* has a visible tympanum and a full phalangeal formula, and does not have pores that are longer anteroposteriorly than they are mediolaterally between the scales and labials (Witten 1984). *Cryptagama aurita* has a prominent, denticulate, scalloped fringe on the

upper lip (Witten 1984). The mid-body scale count is below 100 for all *Tympanocryptis*, but for *Cryptagama aurita* the count is 140-164 (Witten 1984). Witten also mentioned that the holotype is female and does not have a canthus rostralis, directly contradicting Storr's (1981) description of a male with a swollen canthus rostralis. Witten does not give the holotype specimen number, but mentions both the paratype numbers. One possibility is that Witten described one of the paratypes instead of the holotype and that *Cryptagama aurita* has sexually dimorphic characters.

Cryptagama aurita also shares many characters with *Moloch horridus*. The limbs and tail are short, with the tail shorter than the SVL, scalation is heterogeneous, and the whole body is dorsoventrally compressed (Storr 1981, Manthey and Schuster 1996, Hocknull 2000, Bell et al. 2009). The femoral pores are widely spaced on the ventral surface of the thigh, with each pore penetrating the posterior margin or middle of a scale (Witten 1984). Large tubercles are scattered across the dorsal surface and tail, similar to the spines of *Moloch* (Hocknull 2000, Bell et al. 2009) and they share a similarly high scale count as well (along with *Pogona barbata* and *Ctenophorus ornatus*; Witten 1982, 1984).

Cryptagama aurita could also be reclassified as a species within the genus *Ctenophorus*. Two of the species that Storr (1981) suggested are most closely related to *Cryptagama aurita* have since been moved from *Tympanocryptis* to *Ctenophorus*: *Ctenophorus ornatus* and *Ctenophorus scutulatus* (Cogger 2000). Most *Ctenophorus* have femoral pores that penetrate the posterior margin of the scale (Witten 1984).

Details about *Cryptagama aurita* not available in previous sources were provided by Manthey and Schuster (1996), although the authors did not mention any novel sources of data or whether they looked at any specimens. For instance, they mentioned that males have conspicuous hemipenis pouches and describe the hunting habits of *Cryptagama aurita*. They also

outline the terrarium conditions for *Cryptagama aurita*, which, given that no members of the species are known to have been captured live, seems to be, at best, an educated guess.

Synonyms

Tympanocryptis aurita — Storr 1981, Cogger 1983

Amphibolurus auritus — Cogger et al. 1983

Cryptagama aurita — Witten 1984; Cogger 1992, 1996, 2000, 2014; Brůna 1996; Witten 1993; Manthey and Schuster 1996; Cogger 2000; Wilson and Swan 2013.

MATERIALS AND METHODS

I used high-resolution X-ray computed tomography (HRXCT) scans of two specimens of *Cryptagama aurita*, NT R12804 (Figs. 2.1 – 2.5) and WAM R64052 (Figs. 2.6, 2.7). The entire bodies of both specimens were scanned at the High-Resolution X-ray CT Facility (UTCT), Jackson School of Geosciences, The University of Texas at Austin, and 3D renderings as well as stills are available through the UT Digital Morphology website (www.DigiMorph.org). The raw files are available from UTCT.

The head of a whole preserved specimen of *Cryptagama aurita* (NT R12804, Western Australia Museum) was extracted from the body scan. The skull measures 7.6 mm in length and 6.7 mm at its widest point. The specimen was scanned using a FeinFocus microfocal X-ray source operating at 210 kV and 0.15 mA with no X-ray prefilter employed. An empty container wedge was used. Slice thickness corresponded to one line in a CCD image intensifier imaging system, with a source-to-object distance of 38.5 mm. For each slice, 2000 views were taken with 4 samples per view. The field of image reconstruction was 10 mm, and an image reconstruction offset of 7200 was used with a reconstruction scale of 6300. The dataset consists of 872 HRXCT slices taken along the transverse axis of the skull from the tip of the snout to the occiput. Each slice image was gathered at 1024 X 1024 pixel resolution, resulting in an in-plane resolution of

9.8 μm per pixel. Each slice represents a thickness of 13 μm, with a 13 μm interslice spacing. The dataset was rendered in three dimensions by J. Maisano using VGStudio MAX 2.0 (Volume Graphics, Heidelberg, Germany).

The head of a second whole preserved specimen of *Cryptagama aurita* (WAM R64052, Western Australia Museum) was also extracted from the body scan. The skull measures 4.7 mm in length and 4.1 mm at its widest point. The specimen was scanned using a FeinFocus microfocal X-ray source operating at 190 kV and 0.14 mA with no X-ray prefilter employed. An empty container wedge was used. Slice thickness corresponded to one line in a CCD image intensifier imaging system, with a source-to-object distance of 43 mm. For each slice, 1200 views were taken with four samples per view. The field of image reconstruction was 12.5 mm, and an image reconstruction offset of 7300 was used with a reconstruction scale of 6100. The dataset consists of 1941 HRXCT slices taken along the transverse axis of the skull from the tip of the snout to the occiput. Each slice image was gathered at 1024 X 1024 pixels resolution, resulting in an in-plane resolution of 9.8 μm per pixel. Each slice represents a thickness of 13 μm, with 13 μm interslice spacing. The dataset was rendered in three dimensions by J. Maisano using VGStudio MAX 2.0 (Volume Graphics, Heidelberg, Germany).

To compare the relative size of *Cryptagama aurita* with as many other Australian Agamidae as possible, 115 skulls from nine genera were measured by the author. The skull of each individual was photographed using a Canon EOS 5D Mark 2 camera with a Canon Macro Lens EF 100 mm 1:2.8 USM. Digital photos of each skull were photographed in dorsal, ventral, and left lateral view (Supplementary Info 1).

Data Access

Original data collection files, analyses files, photo documentation of all specimens, and additional examples of characters can be found in the appendices and online at Morphobank.org http://morphobank.org/permalink/?P1262 (O'Leary et al. 2012).

Abbreviations

Institutional abbreviations include NT R, Museum and Art Gallery of the Northern Territory, Darwin, Northern Territory, Australia; WAM R, Western Australian Museum, Perth, Western Australia, Australia; TMM, Texas Memorial Museum, The University of Texas at Austin, Austin, Texas; VPL, Vertebrate Paleontology Lab, The University of Texas at Austin, Austin, Texas; The University of Texas at Austin, Austin, Texas; JIM, James I. Mead Collection, East Tennesee State University, Johnson City, Tennesee. A list of anatomical abbreviations used in the figures is provided in the Glossary.

ANATOMICAL DESCRIPTION

The Skull

General Description

The skull forms a rounded triangle in dorsal view and fits within the size distribution (using maximum length and width of skull) of smaller Australian Agamidae using a comparative data set collected by the author. Given the limited sample number I found it difficult to age the individuals, but their small size suggests they are fairly young. The majority of the osteological contacts of the skull in both specimens appear to be articulating and unfused or only lightly fused. Sutures between bones are readily visible. Gaps between bones with complicated sutures are attributed to shrinkage from preservation. Gaps between bones with simple or hinge-like articulations may be an indicator of cranial kinesis (Evans 2008).

Premaxilla (PM)

In both individuals, the fused premaxilla is a midline element that forms the anterior snout and medial portion of the external naris of *Cryptagama aurita* (Fig. 2.3B, D). The nasal process (PMnp) extends posterodorsally and the vomerine process (PMvp) posteriorly. The premaxilla contacts the nasals dorsally, the maxilla laterally, and the vomer posteriorly. The premaxilla is pierced by small foramina (Figs. 2.1D, 2.6D) that presumably transmitted branches of the medial ethmoidal foramen (Oelrich 1956). There are four fully formed pleurodont premaxillary teeth on the larger individual, two on each side of the midline (NT R12804; Fig. 2.1C), and three premaxillary teeth on the smaller individual (WAM R64052; Fig. 2.6C), with a medial tooth fully formed and two lateral teeth still emerging from the premaxilla.

The nasal process of the premaxilla is rounded posterodorsally and forms a tapering wedge that separates the anterior portion of the paired nasals (Figs. 2.1D, 2.6D). The nasal process covers the medial portion of the external naris (Fig. 2.5B). The premaxilla flares out ventrolaterally, forming a slanted flat contact with the anteromedial premaxillary process of the maxillae (Figs. 2.1D, 2.6D). In WAM R64052 this contact is interrupted on the left side, likely by a branch of the medial ethmoidal foramen (Fig. 2.6 D).

Within the external naris, the nasal process is relatively flat and probably serves as an attachment point for the cartilaginous nasal septum (Oelrich 1956). The posteroventral vomeronasal processes of the premaxilla underly the maxillae (Fig. 2.5C). In most agamids (except for *Moloch horridus*) the premaxilla, when viewed ventrally, is separated from the vomer by medial extensions of the maxilla (Evans 2008), forming a continuous arc of the maxillae. The maxillae in *Cryptagama aurita* are separated medially by the ossified septum of the premaxilla (Figs. 2.1C, 2.6C). The premaxilla and maxillae together ventrally form a continuous arc that posteriorly contacts the anterior portion of the vomer. The premaxilla does not protrude

anteriorly beyond the maxillae. There is an incisive process (Oelrich 1956), i.e., an extra extension of bone or boss, directly behind the premaxillary teeth on the premaxillae of both individuals (Figs. 2.1C, 2.6C).

Maxilla (MX)

The maxilla is a paired, anterolateral bone that has three distinct processes (Fig. 2.1A): the anteromedial premaxillary process (MXpp); a dorsally directed facial process (MXfp) (Fig. 2.5A); and a posterior orbital process. The maxilla contacts the premaxilla and vomer anteromedially, the palatine medially, the nasal and prefrontal dorsally, the jugal posterodorsally and the ectopterygoid posteromedially (Fig. 2.1A, C). A distinct lateral maxillary ridge (MXlr) runs horizontally from above the most anterior acrodont tooth to the midpoint of the maxilla-jugal suture (Fig. 2.3A). Above the lateral maxillary ridge, the maxilla is angled dorsomedially and below it the maxilla is angled ventromedially.

The anteromedial premaxillary process contacts the premaxilla, vomer, and septomaxilla. The maxilla curves inward toward the premaxilla and forms a shelf (MXs) at the external naris. The articulation with the premaxilla is vertical, but curve inward slightly, so the dorsal edge of the anteromedial premaxillary process comes to a point medially (Fig. 2.5B). The maxilla lightly contacts the contralateral element on the inner surface of the rostrum where they overly the premaxilla. The contact is ventral to the naris and abuts the vomers posteriorly (Fig. 2.4B).

The maxilla is penetrated by the superior alveolar foramen (MXsaf) at the curve between the anteromedial premaxillary process and the facial process, at the external naris (Figs. 2.3C, 2.5A). The superior alveolar foramen transmits the ethmoidal nerve (part of the ophthalmic division of the trigeminal nerve, V1), as it does in other iguanians (Oelrich 1956, Harris 1963, Evans 2008) and it opens into the superior alveolar nerve canal that can be traced along the anteromedial surface of the maxilla (Bell et al. 2010). Several maxillary labial foramina are

present on the lateral side of the maxilla, above the maxillary ridge (Figs. 2.1A, 2.6A), and most likely also transmit branches of the ophthalmic division of V1 (Evans 2008, Bell et al. 2010).

The facial process contacts the nasals anteromedially, sloping to form the curve of the snout (Fig. 2.5A). There is a small nobby process medially which is overlapped by the lateral extension of the nasal (Figs. 2.1D, 2.6D). The facial process forms a tapering, overlapping contact with the prefrontals and forms the anterior margin of the lacrimal fenestra (lf; Figs. 2.1A, 2.6A).

The maxilla contacts the palatine along the medial maxillary shelf (Fig. 2.4A). The medial shelf is deeply notched dorsally, probably for the maxillary artery and superior alveolar nerve, which are enclosed by the maxilla anteriorly. The palatine forms a bridge over the canal. The canal emerges posteriorly, forming a ventrally concave elongate notch on the medial surface of the maxilla (Fig. 2.4B). The medial articular process of the palatine bridge is much more robust than the lateral process (Fig. 2.4A).

The posterior orbital process of the maxilla forms a horizontal contact with the jugal laterally and the ectopterygoid medially. This horizontal contact between the maxilla and jugal is relatively flat anteriorly, but posteriorly the tapering maxilla is weakly notched by the jugal (Fig. 2.4 A, B). The majority of the maxilla-ectopterygoid contact is on the medial surface of the maxilla and abuts the contact of the maxilla with the jugal (Fig. 2.3D).

Nasal (NA)

The nasal is a paired, thin, concave, rectangular bone located anteriorly on the dorsal surface of the skull (Figs. 2.1A, 2.6A). The nasal roofs at least the anteriormost portion of the vomeronasal chamber (vc; nasal capsule of Bellairs 1970, nasal cavity of Harris 1963; Fig. 2.5C), which houses two membranous nasal sacs (one on each side, separated by a cartilaginous nasal septum) and Jacobson's organ (Bellairs 1970).

The nasal bifurcates anteriorly. The medial process of the nasal slots into the nasal process of the premaxilla and the lateral process of the nasal articulates with a facet on the facial process of the maxilla (Figs. 2.1D, 2.6D). The anterior portion of each nasal is dorsally convex and widens laterally, forming an arch-like dorsal margin of the external naris. In the dorsoventral plane the nasal thickens medially and abuts the contralateral element, except for the anteriormost portion, which is separated from the contralateral element by the premaxilla (Fig. 2.3A). The lateral edge of the nasal anteriorly overlaps the maxilla at an angle that widens anterolaterally. The lateral edge of the nasal medially abuts the prefrontal along a relatively straight anteroposterior margin (Figs. 2.1D, 2.6D). The posteriormost third of the nasal forms a squat triangle. The medial edges of the triangle overlap the anterior shelf of the frontal and the lateral edge of the triangle abuts the medial edge of the prefrontal (Figs. 2.1B, 2.6B). In the smaller individual (WAM R64052) the articulation of the nasal with the frontal and prefrontal is wider and more rounded (Fig. 2.6B).

Septomaxilla (SX)

In *Cryptagama aurita* the septomaxilla is paired, only partly ossified, and forms part of the cartilaginous network separating the various sensory organs of the inner skull (Jollie 1960, Bellairs 1970: 139). The septomaxilla arches dorsally over Jacobson's organ in the vomeronasal chamber, forming a dorsally concave, inverted triangle that widens posterolaterally (Figs. 2.3A, 2.5C). The lateral edge of the septomaxilla is obliquely notched for what may be a nerve or blood vessel. The septomaxilla weakly contacts the anterodorsal portion of the vomer, separating the external naris from the vomeronasal chamber.

Prefrontal (PF)

The prefrontal is a paired bone that forms the anterior portion of the orbit and the posterior margin of the lacrimal fenestra. The prefrontal articulates with the facial process of the

maxilla anteriorly, the frontal dorsomedially, and the palatine ventromedially (Figs. 2.1A, 2.6A). The dorsolateral portion of the prefrontal extends into a slightly rugose triangular boss that is roughly perpendicular to the horizontal plane (Figs. 2.1B, 2.6B).

The prefrontal is overlapped anteriorly by the facial process of the maxilla and medially articulates with the nasal (Fig. 2.5A) and frontal along the frontal process (Fig. 2.5A, B). The prefrontal and facial process of the maxilla both taper where the prefrontal is overlapped. The prefrontal-maxilla articulation is perpendicular to the abutting articulation of the nasals with the prefrontal, making the prefrontal appear in dorsal view to have a squared corner anteromedially (Figs. 2.1D, 2.6D). The medial portion of the prefrontal articulation with the nasal is parallel to the midline and abuts the lateral edge of the nasal (Fig. 2.3B). As the articulation progresses posteriorly, toward the frontal, the prefrontal wraps around the nasal, forming a deep grove into which the nasal fits. This tongue-and-groove articulation continues with the lateral groove of the prefrontal wrapping around the lateral frontal (Fig. 2.3C). Posteriorly, the tongue-and-groove articulation reverses: the medial edge of the prefrontal begins to be wrapped ventrally by the frontal, so by the posteriormost extension of the articulation both the prefontal and the frontal are grooved by the other bone (Fig. 2.5B).

The lateral surface of the prefrontal tapers posteromedially and forms a convex surface as part of the anterior orbit (Figs. 2.3C, 2.5A). This convex surface has three or four small foramina, which are perhaps an indication of the ophthalmicus profundus nerve (from the geniculate ganglion) or the palatine nerve (Harris 1963).

Ventrally, the prefrontal extends ventromedially, dividing the lacrimal foramen (lf) and the orbit into two separate cavities (Fig. 2.1A, 2.6A). The ventral prefrontal palatine process (PFplp) forms a tongue-and-groove articulation with the maxillary process of the palatine (Fig.

2.5B). The contact is angled in a dorsomedial direction. The ventral prefrontal extends to form most of the anterior wall of the orbit and the posterior wall of the lacrimal foramen.

Lacrimal (LA)

Cryptagama aurita does not have a lacrimal. This bone may be completely lost or fused with another bone. Among Australian Agamidae, only *Physignathus*, *Hypsilurus*, and *Chelosania* are known to exhibit a lacrimal (Witten 1993).

Frontal (FR)

The frontal is a prominent bone that forms the central portion of the dorsal skull roof. The frontal is shaped like an inverted capital T, with the crossbar of the T oriented posteriorly (Fig. 2.1B, 2.6B). The frontal articulates with the nasals anteriorly, the prefrontals anterolaterally, the postorbitals posterolaterally, and the parietal posteriorly. In the larger individual (NT R12804) the anterior and posterior articulations appear to be tight (with the exception of the parietal fontanelle; Fig. 2.1B), but there are gaps (presumably unossified regions) between both the anterior and posterior articulations in the smaller individual (WAM R64052; Fig. 2.6B).

The frontal is notched anteriorly, with roughly triangular facets to accommodate the overlying nasals. Both nasals and the frontal are tapered where they contact, forming, in dorsal view, a W-shaped articulation centered at the midlength of the prefrontals (Fig. 2.1B, 2.6B). The dorsal surface is lightly rugose. The frontal forms a tongue-and-groove articulation with the prefrontal anterolaterally (Fig. 2.3C). The frontal is thickest dorsoventrally at the margins of this articulation and thinnest at the midline.

The frontal covers part of the cerebral hemispheres, the olfactory tract, and olfactory bulbs (Harris 1963). Portions of the olfactory tract can be seen as a ventral trough on the underside of the frontal, where the thick frontal portion of the prefrontal-frontal articulation extends ventrally, forming an arch over the anterior-posterior axis (Fig. 2.3C). The arch

continues as the prefrontals end in a tapered point, and the lightly concave lateral surfaces of the frontal forms the dorsal edge of the orbits (Fig. 2.5A). The ventral arch of the frontal narrows posteriorly and flattens out into a sheet that is thickest on the lateral edges.

The frontal widens at the posteromedial margin of the orbits. The bone extends laterally with a ventromedial inflection where it contacts the postorbital bone (Fig. 2.3D). Only the posterolateral tip of the frontal contacts the postorbital (Fig. 2.1B, 2.6B). The frontal abuts the parietal posteriorly (Fig. 2.5A). The contact terminates medially, where the frontal forms the anterior margin of the parietal fontanelle (Fig. 2.5C). The bone along the margin of the parietal fontanelle is irregular. In the larger individual (NT R12804) this margin accounts for about one-fifth of the posterior edge of the frontal (Fig. 2.1B), whereas in the smaller individual (WAM R64052) it accounts for about one-third (Fig. 2.6B).

Parietal (PA)

The parietal is a roughly X-shaped bone, with the anterior portions of the 'X' flattened mediolaterally (Fig. 2.1B, 2.6B). The parietal articulates anteriorly with the frontal, anterolaterally with the postorbital, and posterolaterally with the supratemporal and squamosal. There are two bilateral processes of the parietal, the anterior parietal processes (PAap; Oelrich 1956) and the postparietal processes (PApp; Estes 1988, Bell et al. 2009; sometimes called 'supratemporal processes' *sensu* Oelrich 1956, implying a fusion of the postparietal process and the supratemporal ; Fig. 2.1B, 2.6B). The parietal is slightly convex dorsally. The dorsomedial portion of the parietal is deeply notched by the parietal fontanelle (PApf; Bell et al. 2009; pineal foramen of Oelrich 1956, and Evans 2008; parietal foramen of Jollie 1960; Fig. 2.5C).

The lateral and posterior margins of the parietal fontanelle are irregular and formed by the parietal; thus, the parietal fontanelle forms posterior to the frontoparietal articulation (Fig.

2.1B, 2.6B). The fontanelle opens onto the dorsal surface of the cerebrum and presumably the pineal complex (Harris 1963).

The anterior edge of the parietal exhibits two types of articulations. Between the parietal fontanelle and the anterior parietal process the parietal is wedge-shaped and abuts the frontal (Fig. 2.5B). The frontoparietal articulation extends laterally, with a frontal 'tongue' extending ventrally (Fig. 2.5A). Laterally, the articulating processes of both the parietal and the frontal are overlapped by the postorbital. The dorsal surface of the postorbital forms a shelf for both the frontal and parietal (Figs. 2.1B, 2.6B).

The dorsal and lateral surfaces of the parietal are separated by a prominent ridge that becomes the posterior portion of the postparietal process (Fig. 2.1B, 2.6B). The ridge is dorsally concave in lateral view (Figs. 2.1A, 2.6A), perhaps to increase the surface area for adductor muscle attachment (Bell et al. 2010). The entire postparietal process slopes ventrally to articulate posteriorly with the supratemporal, squamosal, and quadrate (Figs. 2.1B, 2.6B).

Posteriorly, the dorsal surface overhangs the supraoccipital, creating two weak fossettes for the bilateral processes of the taenia marginales of the supraoccipital (Evans 2008). A deeper fossa for the processus ascendens is visible on the ventral surface of the posterior parietal (Figs. 2.1E, 2.6E).

Vomer (VO)

The vomer is a paired bone that is tabular anteriorly and triangular posteriorly. The vomer articulates with the premaxilla and maxilla anteriorly, the prefrontal laterally, and the palatine posteriorly (Figs. 2.1C, 2.6C). The vomer forms the medial side of the fenestra vomeronasalis (fv; choana of Jollie 1960, Harris 1963, Bellairs 1970, Estes 1988; Fig. 2.4A, B). The ventral surface of the vomer forms part of the palate, and the dorsal surface forms the bony floor of the internal naris (Fig. 2.5C). The vomers are fused anteriorly, a trait that can be

ontogenetic (Estes 1988). The larger individual (NT R12804) exhibits greater fusion of the vomers (Fig. 2.1C) than the smaller individual (WAM R64052; Fig. 2.6C). The unfused posterior portions of the vomers contribute to the margins of the interpterygoid vacuity (iv; Fig. 2.4A).

The tabular anterior end of the vomer abuts the contact between the maxilla and premaxilla. A medial process runs on the dorsal surface of the vomer and forms part of the nasal septum (Jollie 1960; Fig. 2.3A).

The posterior two-thirds of the vomer forms an obtuse triangle, with the obtuse vertex facing laterally (Figs. 2.1C, 2.6C). Each vomer is dorsally concave (Fig. 2.3A, B). The posterior vomer palatine process (VOpp) tapers medially and is overlain by the palatine (Fig. 2.5C).

Palatine (PL)

The palatine is a paired, dorsally concave bone that forms the posterior portion of the vomeronasal chamber and fenestra vomeronasalis, as well as the central portion of the palate (Fig. 2.5C). The vomerine process (PLvp) of the palatine extends anteriorly to articulate with the vomer. The maxillary process (PLmp) extends anterolaterally to articulate with the maxilla and dorsolaterally with the prefrontal. The pterygoid process (PLpp) extends posteriorly to articulate with the pterygoids (Fig. 2.4A). The interpterygoid vacuity (Fig. 2.4A) extends anteriorly to separate the palatines medially.

The vomerine process of the palatine articulates medially with the posteriormost portion of the vomer and laterally forms the medial portion of the fenestra vomeronasalis (Fig. 2.4A). The medial portion of the palatine forms a truncated, tapering articulation over the vomer. A small tongue of bone dorsomedially extends over the contact, but does not contact the contralateral bone in either individual (Fig. 2.5A). The lateral vomerine process forms a dorsoventrally flat cone that extends towards maxilla, but does not articulate with it. The lateral vomerine process forms the posterior portion of the fenestra vomeronasalis (Fig. 2.4A). The

ventral vomerine process forms the dorsally concave internal choanal groove (PFicg; Fig.2.5C)). The internal choanal groove is ventrally contiguous with the fenestra vomeronasalis.

The maxillary process articulates anterolaterally with the maxillary shelf of the maxilla, dorsolaterally with the prefrontal, and posterolateral surface of the maxillary process forms the anterior edge of suborbital fenestra (sof; Fig. 2.4A). The anterior portion of the maxillary contact forms a bridge over the superior alveolar nerve canal (infraorbital cana of Jollie 1960 and Harris 1963), which emerges from the medial maxillary shelf (Fig. 2.3C). The medial articulation of this bridge of the maxillary process is much more robust than the lateral process. The maxillary process tightly articulates with the palatine process of the prefrontal, overlapping the medial edge of the prefrontal posteriorly (Figs. 2.4A, 2.5C).

Posteriorly, the pterygoid process of the palatine is relatively flat and forms an irregular contact with the pterygoid. The pterygoid extends medially along the contact and the palatine extends laterally, creating a laterally slanted contact (Fig. 2.4A). The palatine-pterygoid articulation in the smaller specimen (WAM R64052) is thin and incompletely ossified. The lateral edges of the contact in WAM R64052 have circular vacancies, possibly indicating the passage of a nerve or vessel.

Pterygoid (PT)

The pterygoid is a paired, trifurcate bone that the posterior portion of the palate and exhibits a joint-like connection with the braincase (Figs. 2.1C, 2.6C). There are three main processes of the pterygoid; the palatine process (PTpp; Figs. 2.4A, B, 2.5), the ectopterygoid process (PTecp; Figs. 2.1C, 2.6C), and the quadrate process (PTqp; Figs. 2.3E, 2.4B). The pterygoid articulates anteriorly with the palatine, mediolaterally with the ectopterygoid, dorsally with the epipterygoid, posteromedially with the basipterygoid processes of the sphenoid (SDbp), and posteriorly with the quadrate. The pterygoid is separated from the contralateral element by

the interpterygoid vacuity, which surrounds the partially ossified parasphenoid process (pp; Fig. 2.4B). The pterygoid is edentulous, consistent with other acrodont iguanians (Estes et al. 1988).

The pterygoid is overlapped by the pterygoid process of the palatine at an approximately 45 degree angle in palatial view, forming a posterolaterally tapered contact (Fig. 2.4A). The contact is irregular and only ossified medially. Foramina are present at the site of the contact, although this may be evidence of ossification, not a nerve or vessel.

Posterior to the palatine-pterygoid contact, the pterygoid bends to a more horizontal orientation (Fig. 2.5A). At the point of inflection, the pterygoid bifurcates. The ectopterygoid process of the pterygoid extends laterally to contact the ventromedial ectopterygoid (Fig. 2.3D). The lateral portion of the contact descends ventrally and forms the triangular pterygoid flange (sometimes called the dorsal coronoid process, Evans 2008). The ectopterygoid forms the anterior portion of the pterygoid flange and the pterygoid forms the posterior portion of the pterygoid flange (Figs. 2.1C, 2.6C). When the skull and mandible are articulated, this pterygoid flange slots anterior to the mandibular coronoid process.

Posterodorsally to the pterygoid flange are the medial basipterygoid fossa (PTbf; Fig. 2.5C) and the dorsal fossa columella (PTfc; Fig. 2.4B). The medial basipterygoid fossa forms a shallow, medially concave surface for the basipterygoid process of the sphenoid. The dorsal fossa columella of the pterygoid forms a shallow socket, into which the foot of the epipterygoid articulates (Fig. 2.4B) and forms a synovial joint (Oelrich 1956) with a cartilaginous pad on the articular surface (meniscus pterygoideus; Jollie 1960).

The posterior portion of the pterygoid is formed by the quadrate process, which is approximately half the width of the anterior portion of the pterygoid (Figs. 2.1C, 2.6C). The dorsomedial edge of the quadrate process is continuous from the dorsal fossa columella and terminates anterior to the lateral articulation of the pterygoid with the quadrate (Fig. 2.4A, B).

The entire quadrate process of the pterygoid is straight in the frontal plane, having been sharply angled toward the quadrate by the bend at the ectopterygoid. Posteriorly, a relatively thin ventral flange is present (a 'step' of the pterygoid, Estes et al. 1988) anterior to the quadrate contact. The posterolateral edge of the tapering quadrate process closely approaches the medial quadrate (Fig. 2.3E). In both individuals there is a thin space between the quadrate and pterygoid, which is probably filled with cartilage (Jollie 1960).

Ectopterygoid (EC)

The ectopterygoid is a paired, strut-like bone connecting the lateral wall of the skull with the palate (Figs. 2.1C, 2.6C). The midshaft of the ectopterygoid is rounded. The lateral and medial edges each have two processes that splay out in adverse directions, forming wide articular surfaces. The ectopterygoid articulates laterally with the jugal, ventrolaterally with the maxilla (Fig. 2.3D), and posterolaterally with the postorbital (Fig. 2.4A). The medial portion of the ectopterygoid articulates with the pterygoid. The ectopterygoid forms the posterior edge of the infraorbital foramen (Oelrich 1956; palatal vacuity of Jollie 1970; Fig. 2.4A). The posterior edge of the ectopterygoid forms the coronoid recess (Oelrich 1956), into which slots the coronoid process of the mandible.

The lateral articular process of the ectopterygoid (EClap) widens to articulate with the medial portions the maxilla anteriorly and the jugal posteriorly (Fig. 2.3D). The lateral articular process of the ectopterygoid articulates with the tapering posteromedial process of the maxilla ventrolaterally. Doral and contiguous with this contact is the ectopterygoid-jugal contact, which is angled, roughly parallel with the shape of the orbit (Fig. 2.4A). The posteriormost portion of the lateral articular process tapers and ends before the anteriormost portion of the squamosal.

The medial articular process (ECmap) of the ectopterygoid articulates with the ectopterygoid process of the pterygoid (see above). The medial flange of the medial

ectopterygoid extends along the relatively flat dorsal surface of the palatine anterior to the palatine-epipterygoid articulation, but does not reach the medial edge of the palatine in either individual (Figs. 2.4A, B, 2.5A). The medial portion of the ectopterygoid is pierced by a number of foramina. The ventral flange of the medial ectopterygoid forms the anterior portion of the pterygoid flange (Oelrich 1956).

Epipterygoid (EP)

The epipterygoid is a dorsally tapering, columnar bone that often articulates with the braincase and closely abuts the prootic and lateral edge of the parietal through membranes, ligaments, and muscle (Oelrich 1956), but appears anterior to the prootic in *Cryptagama aurita* (Figs. 2.3D, 2.4, 2.5). Anteroposteriorly, the epipterygoid is slightly sinusoidal in shape, curving to follow the shape of the ascending vertical semicircular canals of the prootic. The ventral process is rounded and articulates with the fossa columella of the pterygoid (Fig. 2.4A), forming the synovial columellar joint (Oelrich 1956). The epipterygoid tapers dorsally and is relatively short in comparison to most agamidae (Moody 1980).

Jugal (JU)

The jugal is a paired bone that forms the posteroventral portion of the orbital margin and supports the lateral palate and postorbital regions of the skull (Figs. 2.1A, 2.6A). The maxillary process of the jugal (JUmp) extends anteriorly, and the postorbital process (JUpop) of the jugal extends posterodorsally (Fig. 2.4A). The jugal articulates with the maxilla ventrally, the ectopterygoid ventromedially, the postorbital dorsomedially, and the squamosal posteroventrally. The maxillary nerve (V) pierces the jugal medially (Oelrich 1956) and appears to branch laterally through multiple jugal maxillary nerve foramina (JUmnf; Figs. 2.3D, 2.4A). The jugal is medially concave, following the shape of the skull, and is smooth laterally. The orbital ridge of the jugal is rounded (Fig. 2.3D).

The ventral portion of the jugal is a broad, flat surface that articulates with the maxilla and tapers anteriorly, not quite reaching the infraorbital foramen of the maxilla (Fig. 2.4A). A small lateral process of the maxilla notches into the anterior portion of the jugal. A three-way contact with the maxilla and ectopterygoid is formed just posterior to the maxillary notch, on the medial edge of the jugal (Fig. 2.3D). The lateral process of the ectopterygoid wedges medially into the maxilla-jugal contact. The maxillary portion of this three-way contact remains horizontal and the jugal-ectopterygoid contact angles dorsomedially. The jugal-ectopterygoid contact surface increases posteriorly as the ectopterygoid begins to wrap around the jugal (Fig. 2.3D, 2.4B). The ventral portion of the jugal, still in contact with the maxilla, becomes undulate, forming an interlocking surface. The maxilla ends posteriorly and is abutted by the lateral ectopterygoid, which thickens and forms a ventral knobby process (Figs 2.1C, 2.6C).

The posterodorsal portion of the jugal articulates with the postorbital. The posteroventral edge of the jugal articulates with the squamosal (Figs 2.1A, 2.6A). The postorbital and squamosal meet posteriorly, wedging out the jugal.

Postorbital (PO)

The postorbital is a paired, ventrally concave bone that forms the posterodorsal portion of the orbit, the anteroventral portion of the supratemporal fossa, and lateral roof of the skull. The postorbital is a triradiate bone, articulating dorsally with the frontal and parietal (Fig. 2.1B, 2.6B), anteroventrally with the ectopterygoid (Fig. 2.4A), ventrally with the jugal, and posteroventrally with the squamosal (Fig. 2.1A, 2.6A). The postorbital represents either a fusion of the postorbital and postfrontal, or the postfrontal has been lost (Evans 2008).

The dorsal portion of the postorbital forms an antero-posteriorly flattened column that arches medially to articulate with the lateral portions of the frontal and parietal, along the frontoparietal suture (Fig. 2.1B, 2.6B). The postorbital is wedged by the two roofing bones in the

frontal plane so that the dorsal articulation forms an irregular rounded shapes. The anterodorsal portion of the postorbital forms a wide, irregular boss.

The ventral portion of the postorbital entends both anteriorly and posteriorly. The ventral jugal process of the postorbital (POjp; Fig. 2.3D) forms a wide, vertical articulation with the dorsomedial jugal and weakly articulates with the posteriormost portion of the lateral ectopterygoid (Fig. 2.1B, 2.6B). The ventral articulation with the jugal continues posteriorly onto the squamosal, preventing the jugal from contributing to the supratemporal fossa. Only the posterior tapering portion of the postorbital articulates with the squamosal (Fig. 2.3E).

Postfrontal

There is no distinct postfrontal in *Cryptagama aurita*. Within Squamata the postfrontal is often lost or fused with the postorbital (Evans 2008).

Scleral Ossicles (SC)

The scleral ossicles are thin sheets of bone within the eye. They articulate with one another to form the scleral ring (sr), a flattened torus of overlapping plates. The overlapping scleral ossicles wedged between a thickened, fibrous surface called the sclera and the clear, protective cornea (Underwood 1970, Bellairs 1970). The scleral count is 1,6;4,9 (Figure 2.8; notation following Lemmrich 1931).

Squamosal (SQ)

The squamosal is a flat, elongate bone that is angled dorsomedially and forms the posterolateral portion of the supratemporal fenestra (Fig. 2.1B, 2.6B). Anteriorly, the squamosal articulates with the jugal and postorbital. Posteriorly, the squamosal articulates with the cephalic condyle (QUcc; Fig. 2.4A) of the quadrate, the postparietal process of the parietal, and the supratemporal (Fig. 2.1E, 2.6E).

The squamosal tapers anteriorly, forming a dorsal sloping edge that articulates with the posterior portion of the jugal and posteroventral portion of the postorbital (Fig 2.3E). The bone follows the shape of the jugal and postorbital processes, angling dorsomedially, and twisting dorsolaterally at the quadrate articulation (Fig. 2.3E). The squamosal arcs over the dorsal portion of the tympanic crest (Oelrich 1956) of the quadrate (Fig. 2.1A, 2.6A). Posterior to the dorsal typmpanic crest, the squamosal forms a saddle-like articulation with the cephalic condyle (Figs. 2.1E, 2.3F, 2.6E). The posterior portion of the squamosal forms a flat, ventromedial articulation with the postparietal process of the parietal and the supratemporal (Fig. 2.1E, 2.3F, 2.6E).

Supratemporal (ST)

The supratemporal forms a continuation of the distalmost portion the postparietal process of the parietal (Figs. 2.1E, 2.6E). The supratemporal articulates medially with the parietal, laterally with the squamosal, and medioventrally with the lateral flange of the quadrate.

The supratemporal is a teardrop-shaped bone that begins to articulate with the postparietal processes ventrolaterally, about halfway between the main body of the parietal and the posterior articulation. The supratemporal thickens posteriorly, eventually forming a cup around the posterior posparietal process and the greater portion of the posterior articulation, blocking the posparietal process from the quadrate (Figs. 2.1E, 2.6E).

The supratemporal may appear to be part of postparietal process of the parietal. The ventromost portion of the postparietal process notches into the anterior supratemporal and the two bones are held together with fibrous cartilage that may become ossified (Oelrich 1956). The medial portion of the dorsal notch of the supratemporal is weakly developed. The lateral portion of the notch is more widespread and almost prevents (NT R12804) the squamosal from articulating with the postparietal process of the parietal (Fig. 2.1E). In the smaller individual

(WAM R64052) the supratemporal does prevent the squamosal-postparietal articulation (Fig. 2.6E).

The posterior portion of the supratemporal is an irregular cuboid shape with a distinct, posteriorly rounded process. In the larger individual (NT R12804) anterolateral supratemporal forms a flat articulation with the squamosal so that both the postparietal process and squamosal are sandwiched between the paroccipital process of the otooccipital and the squamosal (Fig. 2.11E). In the smaller individual only the supratemporal is sandwiched between the paroccipital process of the otooccipital and the squamosal (Fig. 2.6E). In both individuals, the posterior ventral process of the supratemporal is rounded and articulates with the dorsomedial portion of the tympanic crest of the quadrate and the squamosal.

The three bones that form the posterior portion of the suspensorium probably form a joint, but it is very difficult to confirm this without a live individual (Oelrich 1956, Evans 2008). Many agamids show reduced cranial kinesis relative to other squamates (Evans 2008).

Quadrate (QU)

The quadrate is a paired, lopsided, saddle-shaped bone that is the center of motion between the mandible and the cranium (Figs. 2.1A, 2.6A). The quadrate articulates ventromedially with the pterygoid (Fig. 2.4B). The quadrate contributes to joint surfaces dorsally with the squamosal and supratemporal, dorsomedially with the paroccipital process of the otooccipital (Figs. 2.1E, 2.6E), and ventrally with the articular (Fig. 2.4B). The quadrate also forms much of the middle ear and is the primary anterior attachment surface for the tympanic membrane.

The cephalic condyle is a posterodorsally directed smooth convex surface that articulates with the posterior squamosal, supratemporal, and postparietal process of the parietal (Figs. 2.1E,

2.6E). There is a secondary medial condyle that appears to have a thin, unfused epiphyseal plate (Fig. 2.3E, F). The medial condyle also articulates with the supratemporal.

The anteriorly convex tympanic conch (QUtc) and adjacent thickened medial conch (QUmc) forms the majority of the quadrate (Fig. 2.4A). The tympanic conch has a laterally thickened edge called the tympanic crest, which provides attachment for the tympanic membrane. The tympanic crest originates at the cephalic condyle, flattens and undulates anterodorsally for a secondary articulation with the squamosal, then arcs posterovenrally (Figs. 2.1A, 2.6A). The tympanic crest tapers posteriorly to the mandibular condyle (QUmac). There is a small, smooth crest on the posterior concave surface, which is part of the secondary articulation with the squamosal. The medial portion of the quadrate thickens and is relatively straight dosoventrally (Figs. 2.1A, 2.6A).

The mandibular condyle is a spool-shaped, ventrally convex articulation surface that forms the dorsal half of a synovial saddle joint with the articular bone of the mandible. The medial portion of the condyle is larger than the lateral portion (Figs. 2.1C, 2.6C).

The Braincase

The braincase is an oblong spheroid of interlocking bones that houses the posterior portion of the brain. The braincase is compsed of the parietal and supraoccipital dosally (Fig. 2.3E), the prootic and otooccipital laterally (Fig. 2.5C), and is floored by the sphenoid and basioccipital (Fig. 2.4A, B). The anterior portion of the braincase is maintained by cartilaginous and membranous supports, some of which may partially ossify (Harris 1963, Estes et al. 1988). In *Cryptagama aurita* the only apparent ossifications are the orbitosphenoids (OB; Figs. 2.1A, 2.4A, 2.5, 2.6A). The prootic, otooccipital, and supraoccipital contribute portions of the bone surrounding the inner ear. The ossified portion of the braincase is very reduced, to the point where the bone encompassing the semicircular canals are highly visible, which is common for

small iguanids (Estes et al. 1988). The posterior portion of the braincase is dominated by a large foramen magnum (fm; Figs. 2.1E, 2.6E). The braincase contacts the frontal anterodorsally, the pterygoids anterolateraly, the quadrates and suspensorium dorsolaterally, and the cervical vertebrae posteriorly. Cranial kinesis is possible for *Cryptagama aurita* given that the braincase connects to the surrounding skull via joints or cartilaginous contacts.

Extracollumella (EX)

The extracolumella is a small sesamoid or series of sesamoids associated with the extracolumellar ligament of the tympanic membrane (Wever 1978; Fig. 2.3F).

Orbitosphenoid (OB)

The orbitosphenoid is a paired, medially concave bone suspended approximately between the orbits (OB; Figs. 2.1A, 2.4A, 2.5, 2.6A). The orbitosphenoid is suspended by ligamentous or cartilaginous bars and forms part of the structure holding the anteriormost portion of the brain, possibly around the area of the thalamus (Harris 1963, Bellairs 1970). The dorsal and ventral processes of the orbiosphenoid are oriented medially. The lateral process protrudes laterally from the middle of the orbitosphenoid.

Sphenoid (SD)

The sphenoid is a midline bone that forms the floor of the anterior braincase and is a fusion of the parasphenoid and basisphenoid (Evans 2008). The sphenoid articulates with the pterygoid anterolaterally, the prootic laterally, and the basioccipital posteriorly (Figs. 2.1C, 2.6C). The anteriomedial portion of the sphenoid appears contiguous with the parasphenoid rostrum. The pituitary fossa (SDpf; Harris 1963) is anterior to the dorsum sella (SDds), which stretches between the alar processes and separates the pituitary fossa from the relatively flat interior floor of the braincase (Fig. 2.4A, B).

The anteromedial portion of the sphenoid is contiguous with the ossified portion parasphenoid rostrum. The process tapers and probably transitions to cartilage anteriorly (Figs. 2.1C, 2.6C). Posterior to the parasphenoid rostrum, the basipterygoid processes of the sphenoid (SDbp) extend from the anterior sphenoid, roughly 45 degrees in the frontal plane (Figs. 2.4A, B, 2.5C). The processes are columnar and end in a relatively wide, rounded "foot", which articulates with the pterygoid fossa, possibly forming a synovial joint (Jollie 1960). On the anterior edge of the sphenoid, medial to the base of each pterygoid process and lateral to pituitary fossa, is the anterior vidian canal (SDvca; Fig. 2.3A), through which passes the facial branch of the trigeminal nerve (V4) and blood vessels. Medial to the anterior vidian canal and posterior to the parasphenoid rostrum is the cup-shaped pituitary fossa (SDpf; Fig. 2.4). The lateral edges of the pituitary fossa are innervated by the paired internal carotid canals. The internal carotid canal becomes confluent with the vidian canal (vc; Fig. 2.5B) to emerge on the proximolateral edge of the basipterygoid as the posterior vidian canal (SDvcp), lateral to the base of the pterygoid process and anterior to the basipterygoid-prootic contact (Figs. 2.3E, 2.5A).

The majority of the posterior sphenoid abuts the basisoccipital. The medial portion of the sphenoid-basioccipital articulation is anteroventrally slanted so that the sphenoid is more prominent ventrally. The lateral portion of the articulation is dorsoventrally relatively straight (Fig. 2.4B). The sphenoid posteroventrally overlaps the basioccipital with a thin sheet of bone (Figs. 2.1C, 2.5C, 2.6C). These sphenoid extensions spread toward each of the sphenoccipital tubercles of the basioccipital and may be a vestige of the fused parasphenoid portion of the sphenoid (Evans 2008).

Prootic (PR)

The prootic is a paired bone that forms the anterior portions of the braincase and housing for the middle and inner ear. The prootic articulates with the sphenoid anterioventrally, the

basioccipital posteroventrally, the supraoccipital dorsally, and the otooccipital posteriorly. The alar process (PRap) and the superior trabecular process (PRtp) extend anterodorsally (Fig. 2.5C). The crista prootica (PRcp; Fig. 2.4A) extends laterally. The prootic is pierced medially by the acoustic recess (PRacr), the facial foramen (VII), and the perilymphatic foramen (plf; Figs. 2.3F, 2.4B, 2.5B, C). The foramen ovale (fo) is partially formed by the prootic (Fig. 2.3F). The prootic houses approximately half of the anterior vertical semicircular canal (avsc) and the horizontal semicircular canal (hsc; Figs. 2.3F, 2.4A). The prootic also forms the anterior portion of the cavum capsularis (cav; Fig. 2.5A), ventral cochlear cavity (coc; Fig. 2.5A), and vestibule (v; Figs. 2.3F, 2.4A, 2.5A). The anterior ampullar recess (aar) between the anterior vertical semicircular canal and horizontal semicircular canal is completely contained within the prootic and appears to contain a small statolithic mass (Fig. 2.4A).

The anterior portion of the prootic forms anterolateral braincase, the incisura prootica (ip; also called the trigeminal notch, Fig. 2.3D), and anterior semicircular canal. The prootic articulates with the lateral protion of the dorsum sella of the sphenoid, continuing the ridge of bone laterally (Fig. 2.4B). Lateral to the dorsum sella, the anteroverntral prootic forms a dorsally concave recess around the Gasserian (or Trigeminal) ganglion (V), which is the incisura prootica (Harris 1963, Barbarena et al. 1970; Fig. 2.3D). The prootic arcs dorsoposteriorly as it surrounds and closely follows the shape of the anterior vertical semicircular canal (Fig. 2.4A). The alar process projects an articulation dorsally to the parietal, but does not directly articulate (Fig. 2.3E). This articulation may be cartilaginous. The alar process continues posteriorly on the sphenoid. A short ridge of bone, the superior trabecular process (Siebenrock 1895), extends from the prootic just anteroventral to the alar process.

The lateral surface of the prootic is dominated by the lateral bony extension of the crista prootica and the anterior portion of the foramen ovale (Fig. 2.3F). The crista prootica is sigmoid

in shape, extending just lateroposterior to the incisura prootica and traveling in a posterodorsal direction to the foramen ovale. The crista prootica ends in an abutting articulation with the base of the parasphenoid process of the otooccipital (Fig. 2.4A). The posterolateral prootic and anterolateral otooccipital abut to form the foramen ovale (Fig. 2.3F), which is approximately double the radius of the stapedial foot. Ventrolaterally, the prootic articulates with the otooccipital and basioccipital.

The prootic is medially concave to accommodate the brain. The medial surface secondarily follows the contours of the otic capsule and is pierced by the facial foramen and anterior acoustic foramen, as well as the anterior portions of the perilymphatic foramen (Fig. 2.3F). A fenestra formed by the junction between the prootic, otooccipital, and basioccipital is visible from within the braincase (Fig. 2.5C). The acoustic nerve foramen (PRan; Fig. 2.3E, F) is recessed within the acoustic recess (PRacr; Fig. 2.5B, C), which is located dorsomedially on the prootic. The facial foramen (VII) is ventral to the acoustic recess and relatively small and regular in shape (Fig. 2.5B, C). The perilymphatic foramen is posterior to and larger than the facial foramen foramen, although it is irregular in shape (Fig. 2.5B, C).

The ventral portion of the parietal slopes ventromedially from vertical to approximately horizontal to articulate with the sphenoid ventromedially and the basioccipital posterioventrally (Fig. 2.4A, B). The surface is lightly undulate.

Otooccipital (OT)

The otooccipital is a paired element that forms the posterolateral portion of the braincase and the otic capsule. The bone is a fusion of the exoccipital and the opisthotic. The otooccipital articulates with the prootic anteriorly, the supraoccipital dorsally, and the basioccipital ventrally (Fig. 2.5C). The paroccipital process of the otooccipital extends posterolaterally and contacts the quadrate, supratemporal, and parietal (Figs. 2.1E, 2.6E). The otooccipital is pierced medially and

posteriorly by the vagus nerve (X) and the hypoglossal nerve (XII; Fig. 2.4B). The medial aperature of the recessus scalae tympani (OTmarst; Figs. 2.4B, 2.5B, C) and the lateral aperature for the recessus scalae tympani (OTlarst; Fig. 2.5A) are both formed by the otooccipital. The posterior portions of the foramen ovale are formed by the otooccipital (Fig. 2.3F). The majority of the horizontal semicircular canal, cavum capsularis, and cochlear recess are contained within the otooccipital (Fig. 2.4A, 2.5A). The lateral portions of the foramen magnum and occipital condyle (BOoc) are formed by the otooccipital (Figs. 2.1E, 2.6E). The ventral portion of the otooccipital is much thicker than the dorsal portion as it forms a large portion of the base of the braincase and the occipital condyle.

The lateral otooccipital forms the posterior portion of the foramen ovale, all of the recessus scalae tympani, and the paroccipital processes (OTpp; Figs. 2.3F, 2.4A). The otooccipital is laterally overlapped by the crista prootica of the prootic, which overhangs the medially recessed foramen ovale (Fig. 2.3F). Ventral to the foramen ovale is the comparably large lateral aperature for the recessus scalae tympani (Fig. 2.5A). The paroccipital processes of the otooccipital are columnar and extend laterally in the smaller individual (WAM R64052; Fig. 2.6C) and posterolaterally in the larger individual (NT R12804; Fig. 2.1C).

The paroccipital processes of the supraoccipital each contain a portion of the horizontal semicircular canal (Fig 2.3F). A triangular, rounded sheet of bone extends ventrally from the length of the paroccipital process to the base of the lateral otooccipital, forming the posterior portion of the otooccipital recess (Figs. 2.1E, 2.3F, 2.6E). This ridge then extends ventrally to articulate with the sphenoccipital tubercles of the basioccipital.

The otoccipital articulates with the dorsal portion of the prootic. The contact is angled anterodorsally to accommodate the cavity for the posterior vertical semicircular canal (Fig. 2.5A). The housing for the horizontal semicircular canal articulates with the housing for the

posterior vertical semicircular canal primarily within the otooccipital, forming the posterior ampullary recess (par; Fig 2.4A).

Supraoccipital (SO)

The supraoccipital is a midline element that forms the posterior roof of the braincase and contributes to the otic capsule. The element is ventrally concave and articulates with the prootic anterolaterally, otooccipital posterolaterally, and the parietal dorsomedially (Fig. 2.3E). The processus ascendens (SOpa) extends from the supraoccipital posterodorsally (Fig. 2.5C). The supraoccipital contains the dorsal portion of the cavum capsularis, and the bony housings for posterior vertical semicircular canal, the anterior vertical semicircular canal (Fig. 2.5A) and the anterior osseous common crus (SOocc; Fig. 2.5B). The supraoccipital is pierced medially by the endolymphatic duct (SOed; Fig. 2.3F).

The supraoccipital articulates laterally with the prootic and otooccipital. The anterolateral portion of the otoccipital articulates with the prootic, forming the posterior housing for the anterior vertical semicircular canal (Fig. 2.5A). The lateral and lateroposterior otooccipital articulates with supraoccipital, forming the anterior housing for the posterior vertical semicircular canal (Fig. 2.5A). The anterior vertical semicircular canal and posterior vertical semicircular canal cavities merge mediodorsally to form the posterior ampullar recess (Fig. 2.5B) within the supraoccipital. This double arch forms the shape of the external supraoccipital.

The anterior portion of supraoccipital forms an edge that articulates with the parietal. The most prominent point of contact is the processus ascendens of the supraoccipital (Figs. 2.3D, 2.5C). The processus ascendens is a dorsoventrally columnar process extending from the supraoccipital portion of the posterior semicircular canal. The processus ascendens is rounded dorsally and articulates with the posterior medial fossette of the parietal. Two lateral flanges on

either side of the processus ascendens called the taenia marginales likely articulate with the corresponding lateral fossas on the parietal (Figs. 2.1E, 2.6E).

The posterior portion of the supraoccipital forms the dorsal portion of the foramen magnum (Figs. 2.1E, 2.6E). The dorsal portion is roughly arc-shaped and thickens laterally to connect with the lateral fossetts of the otooccipital portion of the foramen magnum.

Basioccipital (BO)

The basioccipital is a midline element that forms the posteroventral braincase and ventral foramen magnum. The tabular bone is roughly pentagonal (Figs. 2.1C, 2.6C). The basioccipital articulates anteriorly with the sphenoid, anterolaterally with the prootic, and ventrolaterally with the otoccipital (Fig. 2.4B).

Anteriorly, the basioccipital abuts the sphenoid (Fig. 2.5C). The basioccipital is overlapped ventrally by two short mediolateral processes of the sphenoid (Figs. 2.1C, 2.6C).

The basioccipital articulates with the prootic anteriolaterally and the otooccipital posteriolaterally. The area where the articulation of the basioccipital transfers from the prootic the otooccipital is not completely fused (Fig. 2.5C).

Posteriorly, the basioccipital articulates with the otooccipital laterally to form the posterior portion of the braincase and medially to form the ventral section of the foramen magnum (Figs. 2.1C, 2.5C, 2.6C). The basioccipital is overlapped posterolaterally by the occipital condyles of the otooccipital. The basioccipital condyle is ventral to the occipital condyles condyles, forming a notch on the ventral foramen magnum (Figs. 2.1E, 2.6E).

The ventral surface of the basioccipital is smooth except for the paired ventrolateral basal tubercles. The basal tubercles are pronounced on the larger individual (NT R12804; Figs. 2.3E, F, 2.6E) and there is an unfused epiphyseal plate capping each process. In the smaller individual

(WAM R64052; Fig. 2.6E) the tubercles are almost nonexistent. The prominence of the basal tubercle may be a function of age.

Stapes (S)

The stapes is a paired, thin columnar bone with a medial footplate that sits in the middle ear. The footplate of the stapes sits within the foramen ovale, but is smaller in diameter than the fenestra and does not articulate directly with the prootic or otooccipital (Fig. 2.3F)). In the larger individual (NT R12804; Figs. 2.3F), the edge of the footplate is equidistant from all edges of the foramen ovale and is approximately the same shape (ovoid). The lateral edge of the stapes, where it would articulate with the tympanic membrane, is rounded (Figs. 2.1C, 2.3F, 2.4A). In the smaller individual (WAM R64052), the footplate is more circular and the columnar portion of the stapes is not fully ossified laterally (Fig. 2.6C).

The Mandible

The mandible is composed of the mandible, coronoid, angular, surangular, articular, and splenial. On the anterodorsal alveolar surface of the mandible, one (WAM R64502; Fig. 2.7A) to two (NT R12804; Fig. 2.2A)) tooth sockets are occupied by pleurodont teeth. Posterior to the pleurodont teeth, a row of acrodont teeth is ankylosed to the dorsal mandible. Ventromedial to the tooth row is the subdental shelf (Dss; Figs. 2.2B, C, D, 2.7B, C, D). The mandible is pierced by multiple mental foramen (mf; Figs. 2.2E, 2.3B, 2.5B, 2.7E), the anterior surangular foramen (SUasf; Figs. 2.2B, 2.7B), posterior surangular foramen (SUpsf; Figs. 2.2A, 2.7A), the chorda tympani foramen of the articular (ATctf; Figs. 2.2C, 2.7C), and the posterior angular foramen (ANpaf; Figs. 2.2B, F, 2.7B, F). The groove/canal containing the Meckelian cartilage is sourrounded by Meckel's canal (Dmc; Figs. 2.3D), and the Meckelian groove (Dmg; Figs. 2.2B,

F, 2.3A, B, C, 2.7B, F). The mandible canal (Dc; Fig. 2.3B, C) forms anterior to Meckel's canal within the dentary.

Meckel's canal is formed by the medial surface of the dentary anteriorly and posteriorly by the angular, splenial, and articular. Meckel's canal is open on the anteroventral and medial portions of mandible as the Meckelian groove. The anterolateral mandible canal merges with the Meckelian groove. The Meckelian groove curves ventrally at the anteriormost portion the mandible. The Meckelian groove transition to the Meckelian canal roughly where the coronoid bone begins anteriorly. The mylohyoid nerve and articular artery are thought to pass through Meckel's canal (Oelrich 1956).

Mandible (D)

The mandible is a paired denticulate bone that articulates the contralateral element anteriorly to form most of the anterior half of the dentary. The mandible is overlapped the angular ventromedially, the splenial medially, the coronoid dorsomedially, and overlaps the surangular posterolaterally (Figs. 2.2, 2.7). The Meckelian groove is located on the anteroventral and medial portions of the mandible. Lateral to the Meckelian groove and encased in the mandible is the mandible canal (Figs2.3A, B, C). The mandible canal likely houses portions of the mandibular nerve and blood vessels (Evans 2008) and anterolaterally pierces the mandible to form three mental foramen, which are visible along the anterolateral surface of the mandible (Figs. 2.2E, 2.3B, 2.5B, 2.7E).

At the posteroventral portion of the Meckelian groove and the Meckelian canal, the mandible is overlapped by the angular (Figs. 2.2B, 2.7B). Thus, only the anterior portion of the Meckelian groove is wholly formed by the mandible. Posteriorly, the mandible contributes only to the dorsal and lateral portions of the Meckelian groove. The articulation of the mandible with

the articular is slanted dorsolaterally and continues to the mandible-surangular contact (Figs. 2.2B, 2.7B).

The mandible is overlapped by the splenial medially, the coronoid dorsomedially, and the surangular posterolaterally (Figs. 2.2A, B, 2.7A, B). The dorsomedial mandible is medially overlapped by the splenial at the transition from the Meckelian groove to the Meckelian canal. Dorsal to the mandible-splenial articulation, the mandible is overlapped by the coronoid mandible lappet and main ventral body of the coronoid (Fig. 2.3D). The mandible-coronoid articulation continues above the splenial and ends just anterior to the anterior surangular foramen (Figs. 2.2B, 2.7B). The mandible overlaps the surangular posterolaterally. The lateroposterior portion of the mandible bifurcates dosoventrally as it tapers. The medial portion of the bifurcation surrounds the anterior surangular foramen (Figs. 2.2A, 2.7A), through which passes a cutaneous branch of the inferior alveolar nerve (sanc), part of the facial nerve (Oelrich 1956).

Coronoid (C)

The coronoid is a roughly triangular bone that extends dorsally from the dorsomedial mandible and is a prominent site of jaw muscle attachment (Oelrich 1956). The coronoid has a rounded dorsal process, a strong bifurcated posterior process and an anteromedial coronoid mandible lapette (Figs. 2.2B, 2.7B). The coronoid articulates with the mandible anteriovenrally, the splenial ventrally, the articular medially, and the surangular posteriorly.

The coronoid process (COcp; Figs. 2.2A, B, C, E, F, 2, 2.7A, B, C, E, F) extends dorsally and is anteriorly convex. When the skull and mandible are articulated, this pterygoid flange slots anteriolaterally to the mandibular coronoid process (Fig. 2.4A, B).

Three processes (‘feet’ of Oelrich 1956) extend ventrally from the coronoid. The coronoid mandible lappet (COdl; Figs. 2.2B, F, 2.7B, F) extends anteriorly along the mandible subdental shelf, notching into the surface of the medial mandible and partially overlapping the

splenial. The posterior process of the coronoid ('lingual process' of Evans 2008) extends along the medial surface of the articular, ventral to the anterior surangular foramen (Figs. 2.2B, 2.7B). A shallow ridge extends from the dorsal coronoid process to the posterior portion of the lingual process. The lateral portion of the posterior process of the coronoid articulates with the surangular and forms the anterior portion of the adductor fossa (af; Figs. 2.3C); (Oelrich 1956, Estes et al. 1988).

Angular (AN)

The angular forms the ventral surface of the mandible and the ventral portion of Meckel's canal from the posterior portion of the mandible to the anterior articular (Figs. 2.2A, B, D, F, 2.7A, B, D, F). The angular tapers anteriorly, beginning as a small process on the ventromedial portion of the mandible and transferring ventrally as Meckel's canal closes. The angular is overlapped within Meckel's canal by the anterior articular and weakly by the splenial (Fig. 2.3D). Both the articular and the angular are visible on the medial side of the mandible. The articular becomes thicker posteriorly as the angular thins. The posterior portion of the angular moves to a ventrolateral position, slotting into the articular (Figs. 2.2D, 2.3E, 2.7D).

The angular is pierced medioventrally by the posterior angular foramen ('posterior mylohyoid foramen' of Oelrich 1956; Figs. 2.2B, F, 2.5A, B, C, 2.5B, F), which transmits the posterior mylohyoid nerve, a small branch of the mandibular division of the trigeminal nerve; (Oelrich 1956).

Surangular (SU)

The surangular forms the roof of the posterior portion of Meckel's canal, the majority of the lateral wall of the adductor fossa (Figs. 2.2B, 2.7B), and the anterolateral portion of dorsal articular facet (ATaf; Figs. 2.2C. 2.7C). The surangular forms the roof of Meckel's canal

between the medial coronoid and lateral mandible (Fig. 2.3C). Posteriorly the bone thickens and forms the lateral wall of the adductor fossa as both the angular and coronoid taper (Fig. 2.3E).

The lateral wall of the surangular is overlapped by the mandible, which bifurcates at the anterior surangular foramen (Figs. 2.2A, 2.7A). According to Oelrich (1956), the surangular is pierced laterally by the anterior and posterior surangular foramen, through which passes a cutaneous branch of the inferior alveolar nerve, part of the facial nerve. I speculate that the majority of the cutaneous branch of the inferior alveolar nerve actually passes through the medial wall of the surangular foramen to the lateral anterior surangular foramen because of the relatively large size of the anterior surangular foramen, and only a minor branch passes through the much smaller posterior surangular foramen.

Articular (AT)

The articular is a roughly conical bone that forms the pivot point and short arm that provides counterforce for the jaw (Oelrich 1956). The articular articulates with the coronoid, surangular, angular, and splenial anteriorly (Figs. 2.2A, B, 2.7A, B). The dorsal articular facet articulates with the quadrate, forming the fulcrum of the lever (Fig. 2.1A, 2.2C, 2.4B, 2.6A 2.7C). The retroarticular process (ATrp; Figs. 2.1A, 2.2A, B, C, D, F, 2.4, 2.5, 2.6A, 2.7A, B, C, D, F,) of the articular forms the short arm of the lever.

The anterior portion of the articular forms much of the posteromedial portion of the mandible. The articular extends anteriorly, lining the medial wall of Meckel's canal the lateral splenial (Fig. 2.3D). Posteriorly, the articular widens to form the dorsally concave ventral and medial surfaces of Meckel's canal. The articular thickens ventrally and medially as Meckel's canal transitions to the adductor fossa (Fig. 2.3E). The posterior portion of the adductor fossa, just anterior to the dorsal articular facet, is also formed by the articular (Figs. 2.2C, 2.7C).

The dorsal articular facet and ventral quadrate form a synovial joint. Just posterior to the articular condyle is the chorda tympani foramen (Figs. 2.2C, 2.7C), through which passes the chorda tympani nerve and the posterior condylar artery (Oelrich 1956). The nerve and artery probably emerge on the posterior surface of the adductor fossa (Oelrich 1956; Fig. 2.2B, 2.7B).

The retroarticular process extends posterior to the articular condyle, tapering to form a sloping conical shape and providing a surface for muscle attachment (Fig. 2.2A, B, 2.7A, B). The tympanic membrane attaches to the lateral portion of the retroarticular process. The angular process extends ventromedially to the articular facet as a raised surface (Fig. 2.2C, 2.7C). The angular process is rounded posteriorly and relatively pointed anteriorly.

Splenial (SP)

The splenial is a relatively flat splint of bone on the medial surface of the mandible. The bone is ventral to the coronoid mandible lappet and dorsal to the angular (Figs. 2.2B, F, 2.5, 2.7B, F). The splenial does not contribute directly to Meckel's canal, but overlays the anterior process of the articular (Fig. 2.3C).

Prearticular

The prearticular is not visible in any of the individuals examined. Within Squamata, the prearticular is often a fusion of the prearticular and articular, or the prearticular has been lost (Evans 2008).

Dentition

General Characters

The premaxillary teeth are located on the medioventral surface of the premaxilla, and are pleurodont, unicuspid, and rounded ventrally (Figs. 2.1A, C, D, 2.6A, C, D). There are four evenly spaced premaxillary teeth in the larger individual (NT R12804; Fig. 2.1D). There are two fully formed teeth and one developing premaxillary teeth in the smaller individual (WAM

R64052; Fig. 2.6D); one fully formed tooth is located along the midline and the other is to the right laterally. A developing tooth is just visible on the left posteroventral surface of the premaxilla.

The maxillary dentition is fully acrodont. The tooth crowns are unicuspid and have a slight medial inflection (Figs 2.1A, C, 2.5C, 2.6A, C). Tooth size increases gradually from mesial to posterior. The lingual surface occludes with the lateral surface of the teeth on the mandible, forming a shearing surface (Fig. 2.3A, B, C). In the larger of the two individuals, NT R12804, there is a diastema between the posteromost and second posteromost tooth on the maxillae. In palatal view the posteromost tooth has a greater anterormedial angle and is noticeably larger (Fig. 2.1C).

The dentition of the mandible is both pleurodont and acrodont. The anterior tooth positions accommodate teeth with pleurodont implantation, but the majority of the teeth are acrodont. There are two anterior pleurodont teeth and 15 acrodont teeth on the left mandible of the larger individual, (NT R12804; Fig. 2.2A, C, E, F). There is a space between the posteriormost acrodont tooth and coronoid process of the larger individual. This space is smaller than the width of one fully developed tooth, so it does not qualify as a diastema as I have defined it (Fig. 2.2A, B). On the smaller individual, (WAM R64052; 2.7A, C, E, F), there is one pleurodont tooth and 11 acrodont teeth on the left mandible. There appears to be a diastema between the posteriormost acrodont tooth and the coronoid process, but closer inspection reveals a tooth bud forming on the medial surface of the 'diastema' (Fig. 2.7A, B, C). All pleurodont tooth sockets on both individual appear to be filled. The anterior acrodont teeth display the characteristic vertical wear pattern indicative of the maxillary teeth laterally overlapping the mandible teeth (Hocknull 2002; Figs. 2.2A, 2.7A).

Hyoid Apparatus

Ceratobrachial I (cb1; Figs.2.1A, B, 2.3E, F, 2.5B, C, 2.6A, B) is a paired, anteroposteriorly elongate collumellar bone. The posterormost third of the bone bends dorsolaterally. The bone is located venteral and posterior to the braincase. The bone exhibits a flat anterior articular surface, presumably to attach to the copula portion of the hyoid apparatus (Jollie 1960), but the copula appears to be mostly unossified. The ceratohyal (ch) and hypohyal (hh) are only partially ossified (Fig 2.4B). The hypohyal is anterior and almost perpendicular ceratobranchial I, the ceratohyal lies lateral and slightly anterior to ceratobranchial 1.

COMPARISONS

My preliminary observations indicate that the majority of characters described in this text are shared the majority of Australian terrestrial and rock-dwelling agamids, including the *Ctenophorus*, *Pogona*, *Diprophora*, and *Tympanocyptis* clades (Collar et al. 2010). These include the overall relative anteroposteriorly squat shape of the skull, lack of articulation between the nasal and maxilla, lack of articulation between the premaxilla and frontal, the shape of the palatine-pterygoid anterior articulation, medial articulation of the vomers, the presence of a supratemporal, and a medially larger articulation surface on the ventral quadrate. For the braincase, *Ctenophorus reticulatus* shares a relatively reduced and unossified braincase, a visible incisura prootica, and the presence of a sphenoccipital foramen. For the mandible, there is a shared fusion or loss of the prearticular, a medially oriented Meckel's groove that anteriorly migrates ventrally, and a dorsally concave dorsal articular facet.

Cryptagama aurita has a number of characters that are only shared with one or a few other known taxa. The coronoid medial portion of the posterior process does not extend to the ventral mandible, a character proposed as shared only with *Moloch horridus* (Bell et al. 2009). Both specimens also share with *Moloch horridus* a reduced nasal that weakly meets the facial

process of the maxilla, weakly developed ventrolateral basal tubercles of the basioccipital, and a flattened quadrate process of the pterygoid. Both specimens of *Cryptagama aurita* also lack of caniniform teeth, a character are also possibly absent in the genus *Chelosania*. However, until it can be confirmed that the larger individual (NT R12804) is an adult, these characters may be the result of observing juveniles, i.e. the characters are ontogenetic.

Novel Character

Cryptagama aurita also shows a character not yet observed in Australian Agamidae. The larger individual exhibits a diastema on the maxilla between the posteromost and second posteromost tooth on each of the maxillae (NT R12084; Fig. 2.1A, C). This character is not seen in any other known Australian Agamidae (Hocknull 2002). The smaller individual does not exhibit this diastema (WAM R64052; Fig. 2.6A, C). These characters are not present in any other endemic Australian agamids, are absent in the proposed outgroups to that clade (e.g., *Physignathus*, *Agama*), and may represent a derived condition within the Australian clade. Futher novel characters may be evident as more agamids are CT scanned for comparison. The majority of characters described in this text are difficult to observe in a skeletal specimen.

CONCLUSION

The comparisons of *Cryptagama aurita* with other extant Australian Agamidae are anchored in the assumption that the anatomical structures observed are constant for the majority of each species. If these characters change over ontogeny within *Cryptagama aurita* and the rest of Australian Agamidae, then the relationships between these taxa is much more complicated and nuanced than originally expected. However, given the paucity of novel characters that even careful anatomical observation yields, the relative change in character states over the ontogenic continuum of a statistically significant number of individuals may be a valuable tool for

understanding present and past phenotypic evolution. This description of *Cryptagama aurita* aims to increase the knowledge of this little-known and disappearing fauna.

FIGURES FOR CHAPTER 2

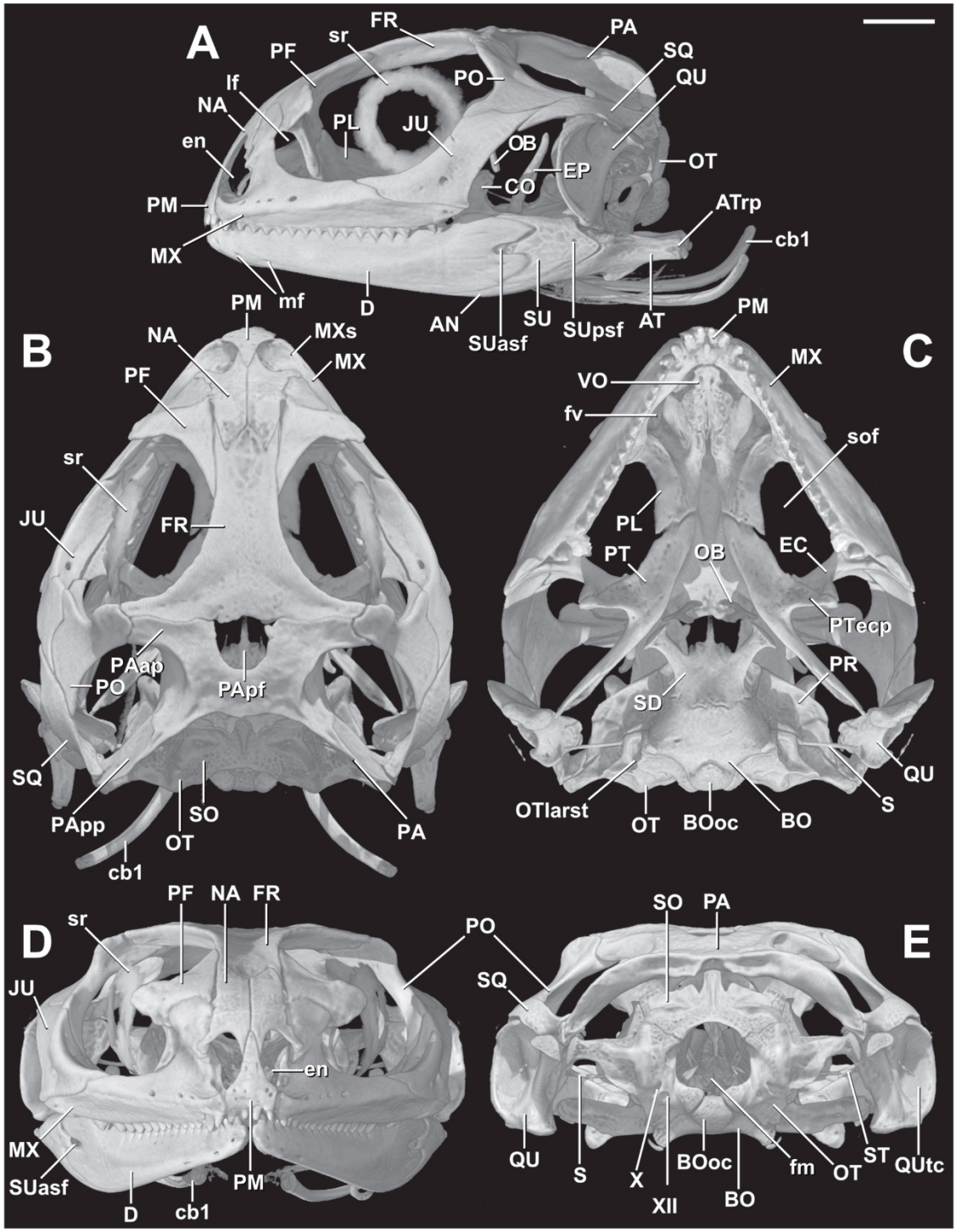

Figure 2.1: Three-dimensional reconstruction of the skull of *Cryptagama aurita* (R12804) based on HRXCT data by J. Maisano. A: Lateral view. B: Dorsal view. C: Ventral view with lower jaw and hyoid digitally removed. D: Anterior view. E: Posterior view with lower jaw and hyoid digitally removed. Scale bar = 2 mm.

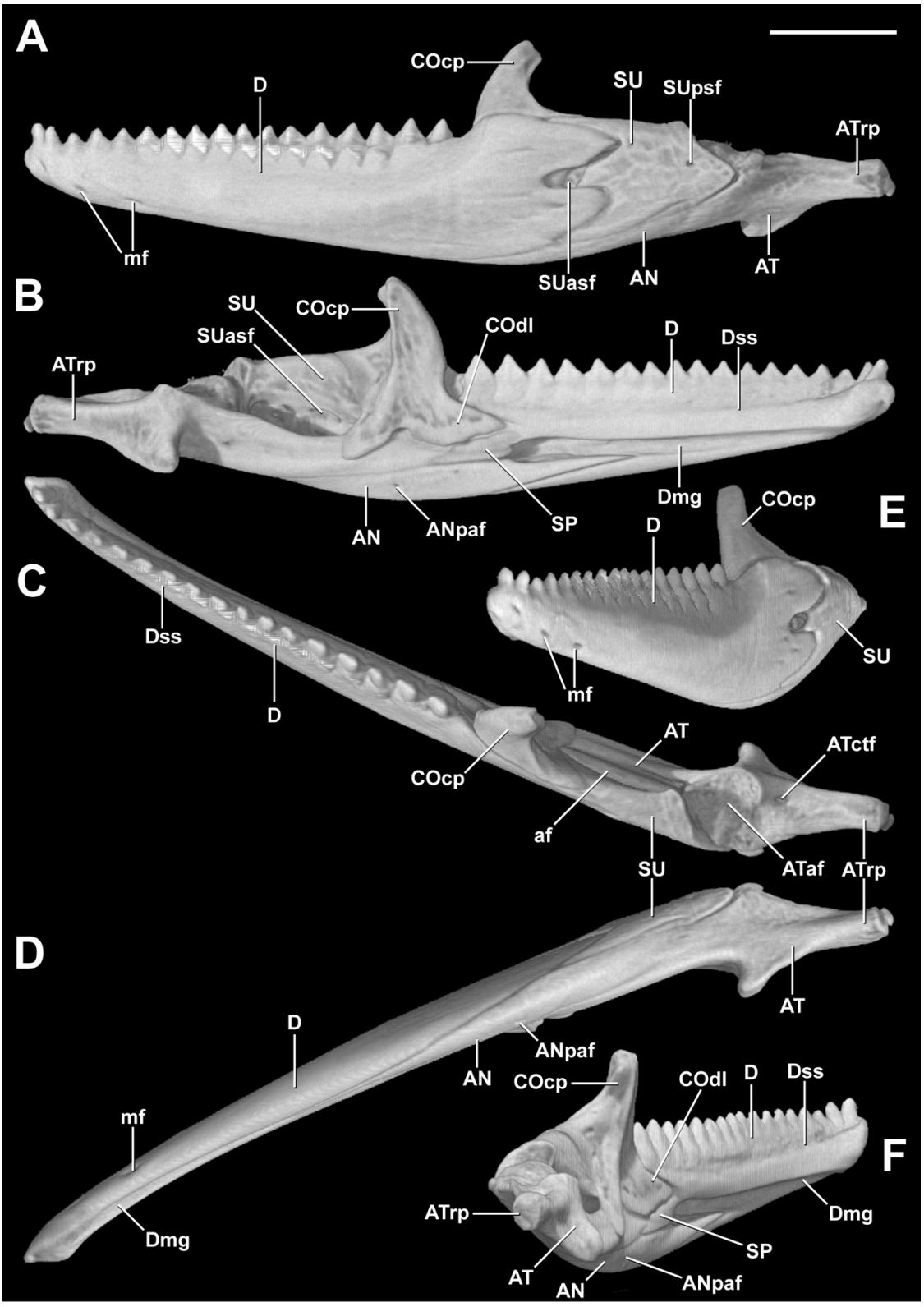

Figure 2.2: Three-dimensional reconstruction of the lower jaw of *Cryptagama aurita* (R12804) based on HRXCT data by J. Maisano. A: Lateral view. B: Medial view. C: Dorsal view. D: Ventral view. E: Anterior view. F: Posterior view. Scale bar = 2 mm.

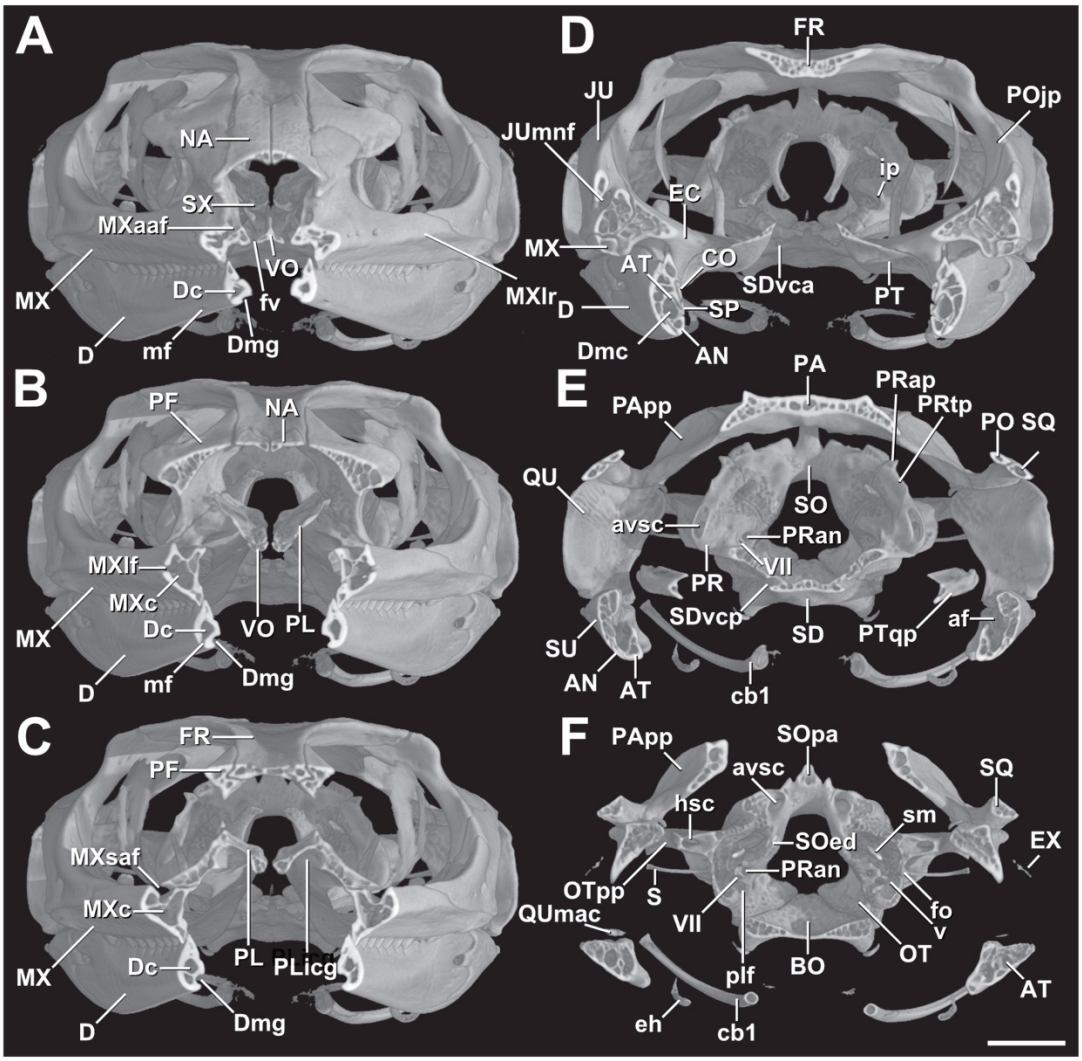

Figure 2.3: Three-dimensional cutaway views along the transverse axis of *Cryptagama aurita* (R12804) based on HRXCT data by J. Maisano. A: ~1.2 mm depth. B: ~2.3 mm depth. C: ~3.0 mm depth. D: ~6.1 mm depth. E: ~9.0 mm depth. F: ~10.3 mm depth. Scale bar = 2 mm.

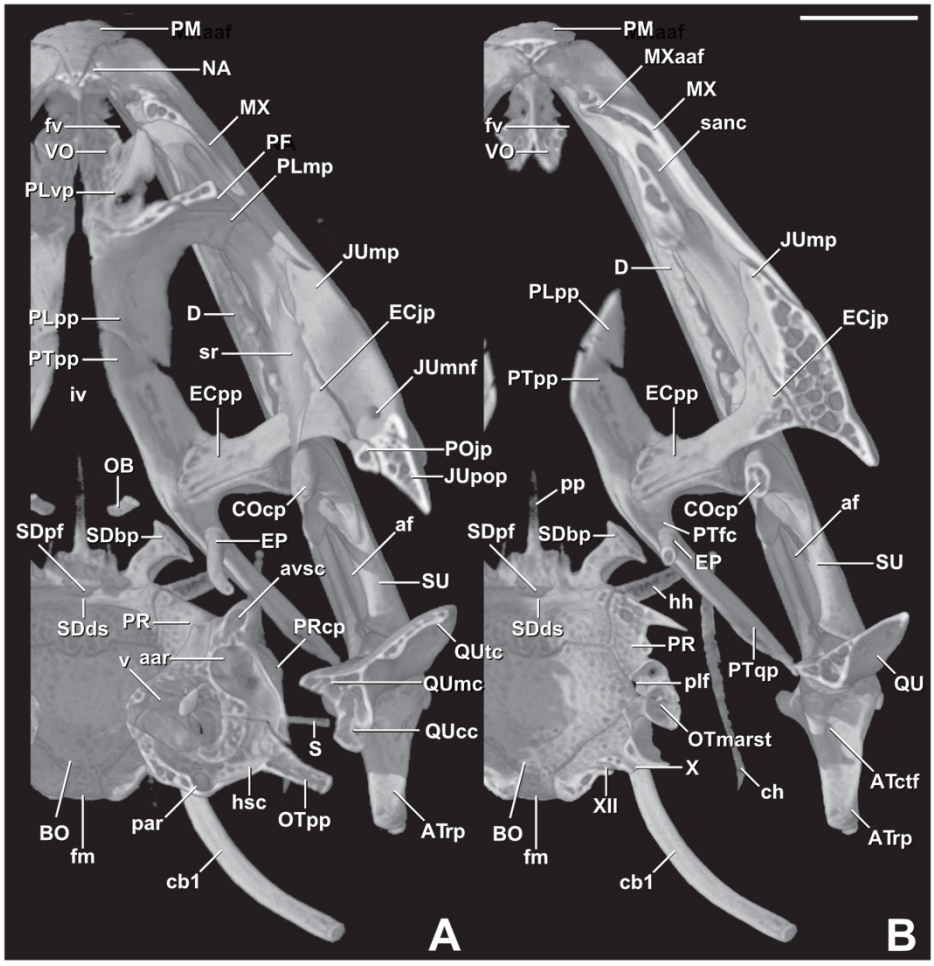

Figure 2.4: Three-dimensional cutaway views along the frontal axis of *Cryptagama aurita* (R12804) based on HRXCT data by J. Maisano. A: ~3.4 mm depth. B: ~4.6 mm depth. Scale bar = 2 mm.

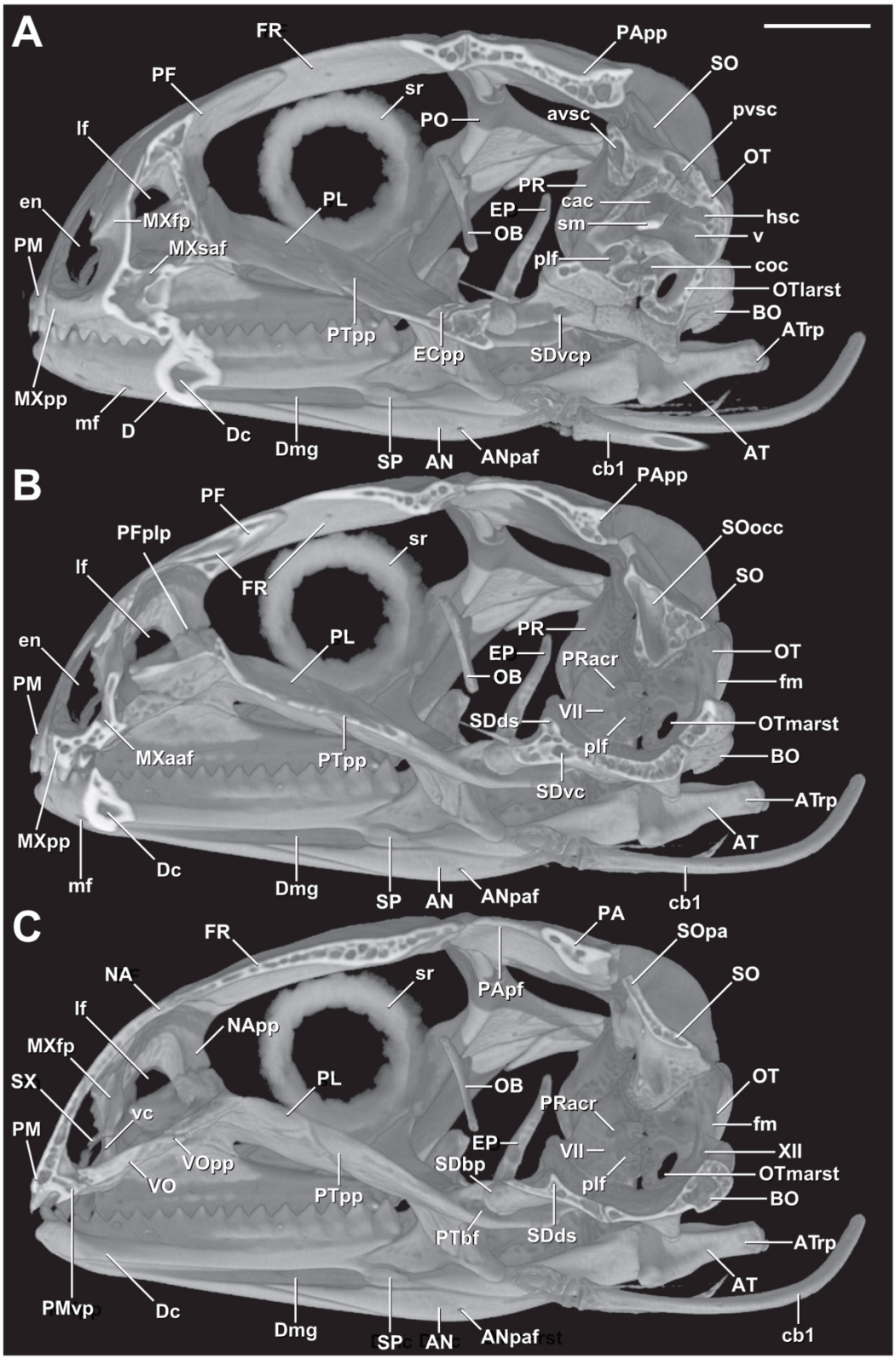

Figure 2.5: Three-dimensional cutaway views along the sagittal axis of *Cryptagama aurita* (R12804) based on HRXCT data by J. Maisano. A: ~4.3 mm depth. B: ~5.2 mm depth. C: ~6.1 mm depth. Scale bar = 2 mm.

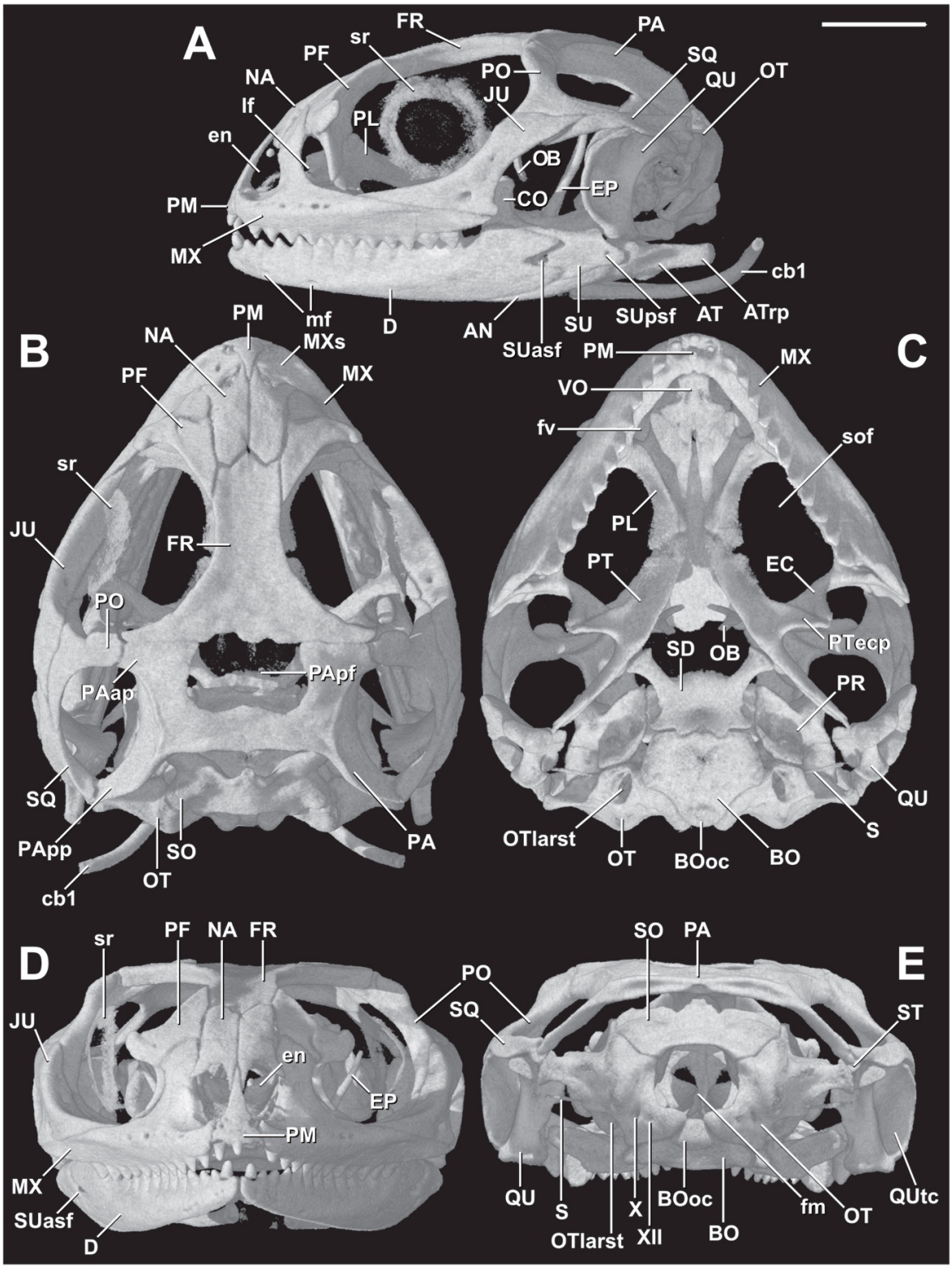

Figure 2.6: Three-dimensional reconstruction of the skull of *Cryptagama aurita* (WAM R64052) based on HRXCT data by J. Maisano. A: Lateral view. B: Dorsal view. C: Ventral view with lower jaw, hyoid and vertebrae digitally removed. D: Anterior view. E: Posterior view with lower jaw, hyoid and vertebrae digitally removed. Scale bar = 2 mm.

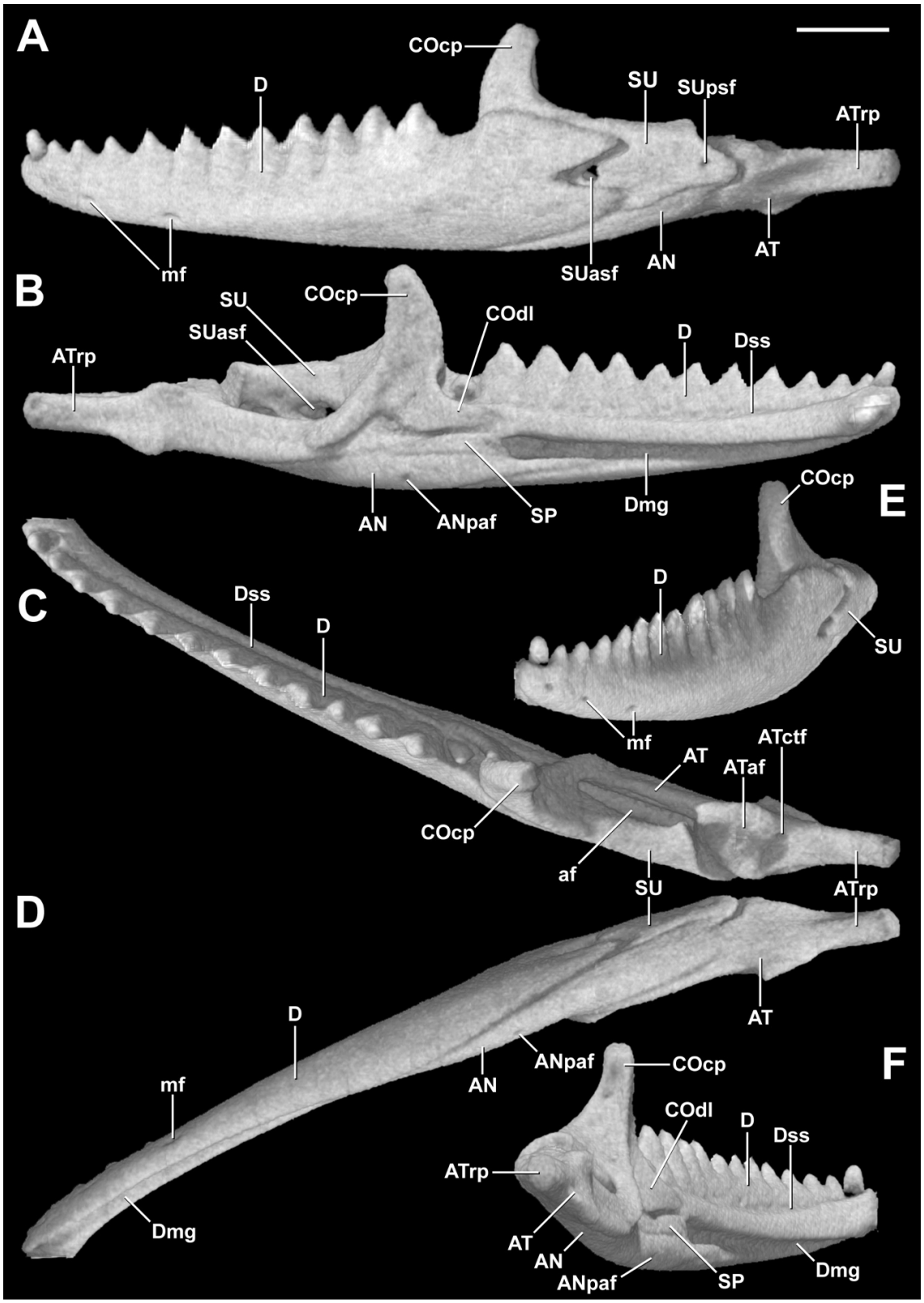

Figure 2.7: Three-dimensional reconstruction of the lower jaw of *Cryptagama aurita* (WAMR 64052) based on HRXCT data by J. Maisano. A: Lateral view. B: Medial view. C: Dorsal view. D: Ventral view. E: Anterior view. F: Posterior view. Scale bar = 1 mm.

Appendix A: Figures of Morphologic Character States for Chapter 1

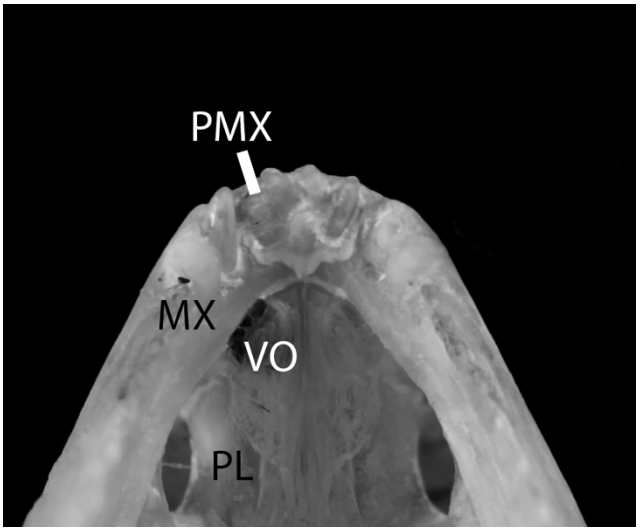

Figure A1. 1(0): WAM R162652 *Ctenophorus caudicinctus*, ventral view.

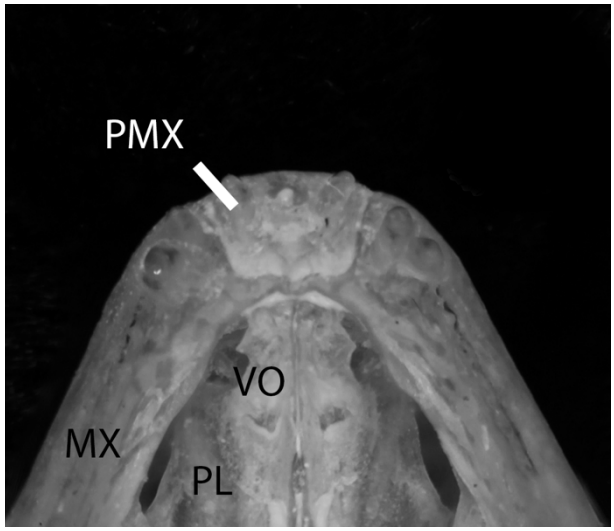

Figure A2. 1(1): WAM R165036 *Ctenophorus caudicinctus*, ventral view.

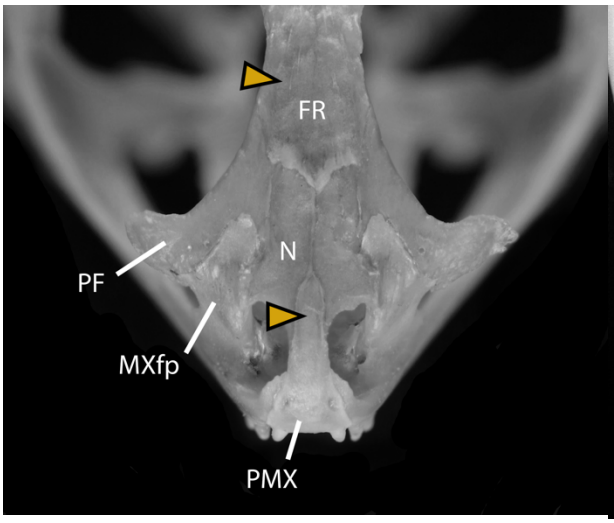

Figure A3. 2(0): WAM R167563 *Ctenophorus caudicinctus*, dorsal view.

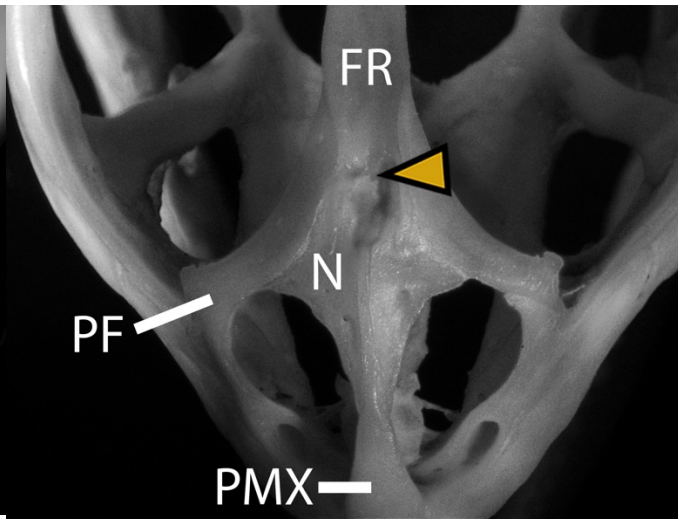

Figure A4. 2(1): VPL R8438 *Uromastyx ornatus*, dorsal view.

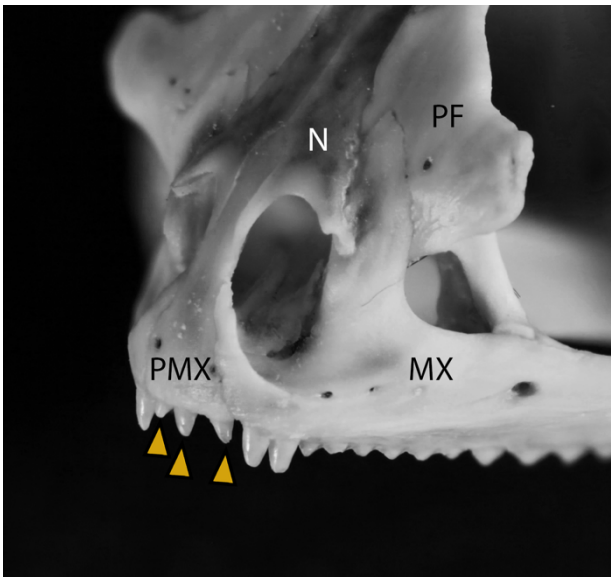

Figure A5. 3: WAM R162760
Ctenophorus caudicinctus, left anterolateral view.

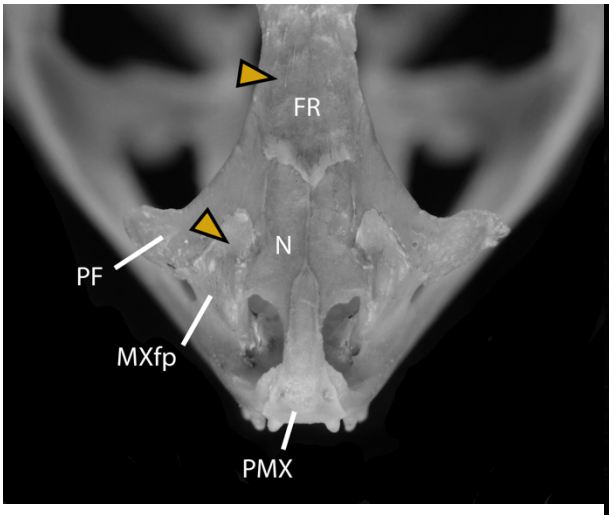

Figure A6. 4(0): WAM R167563
Ctenophorus caudicinctus, dorsal view.

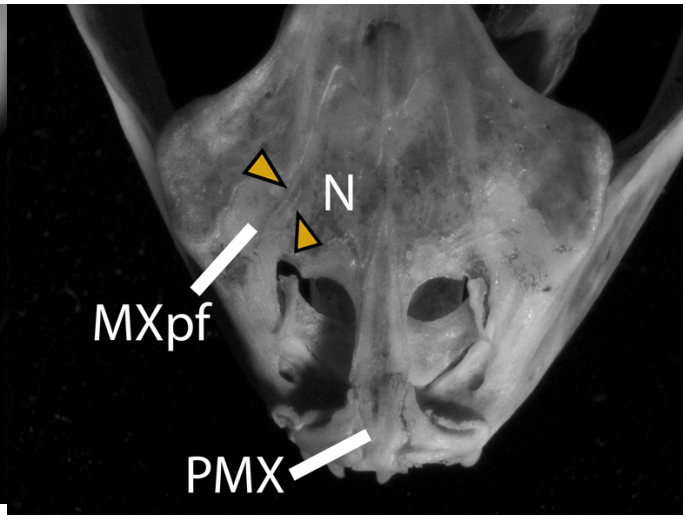

Figure A7. 4(1): TMM R uncat.
Acanthosaura sp., dorsal view.

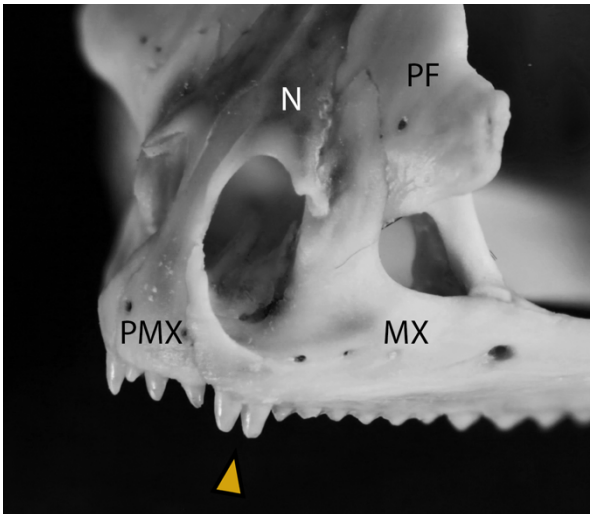

Figure A8. 5(0): WAM R162760 *Ctenophorus caudicinctus*, left anterolateral view.

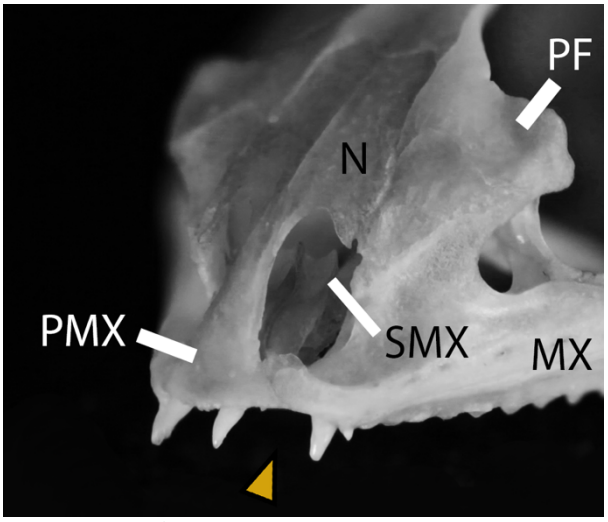

Figure A9. 5(1): WAM R111736 *Ctenophorus isolepis*, left anterolateral view.

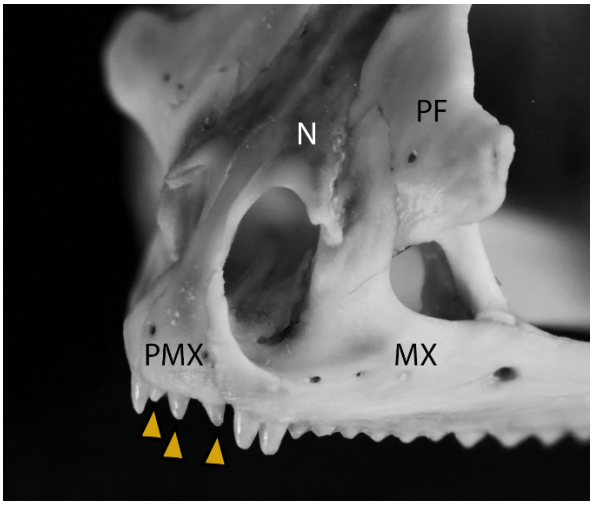

Figure A10. 6(0): WAM R162760 *Ctenophorus caudicinctus*, left anterolateral view.

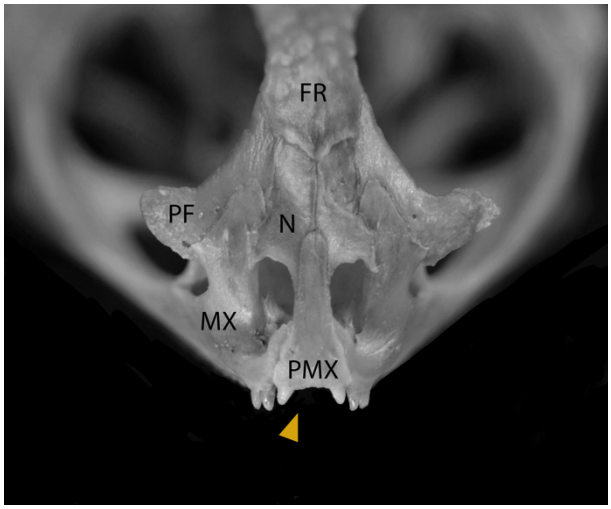

Figure A11. 6(1): WAM R167563 *Ctenophorus caudicinctus*, anterodorsal view.

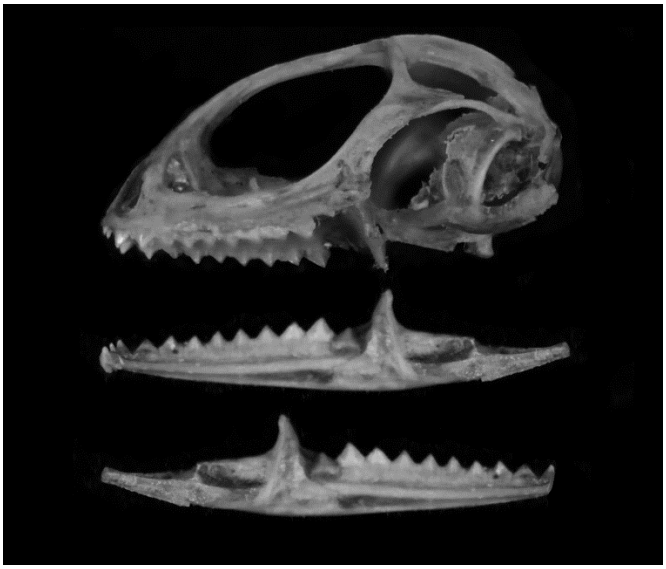

Figure A12. 7: WAM R162820 *Ctenophorus caudicinctus*, left view of skull, lingual view of right (upper) and left (lower) dentaries.

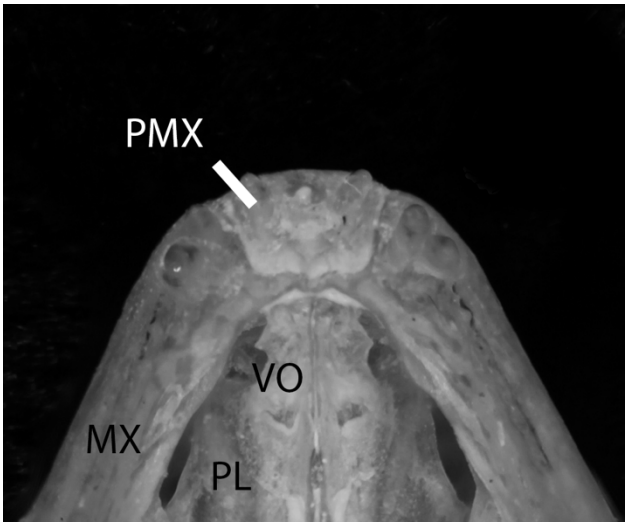

Figure A13. 8(0): WAM R165036 *Ctenophorus caudicinctus*, ventral view.

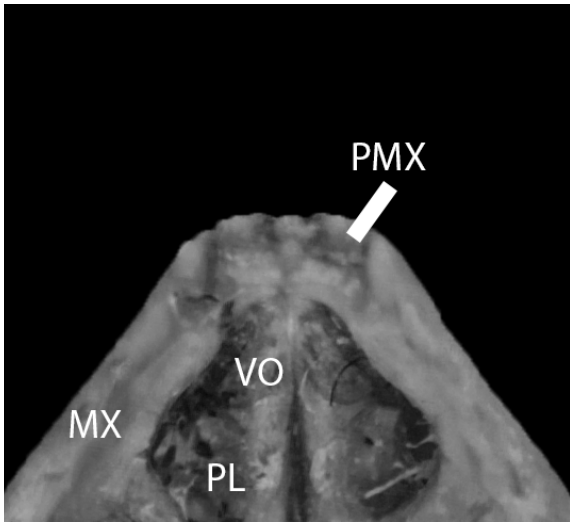

Figure A14. 8(1): WAM R162820 *Ctenophorus caudicinctus*, ventral view.

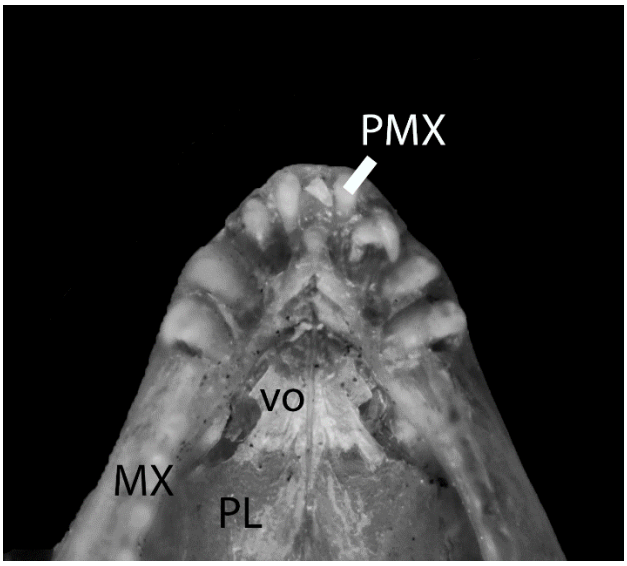

Figure A15. 8(2): WAM R162929
Lophognatus longirostrus, ventral view.

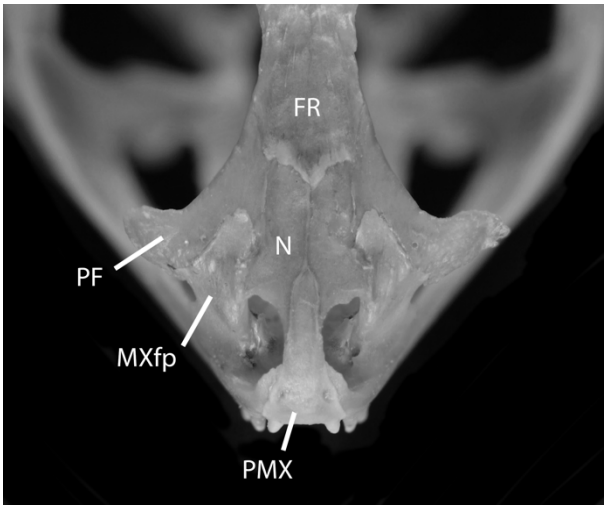

Figure A16. 9(0): WAM R167563
Ctenophorus caudicinctus, dorsal view.

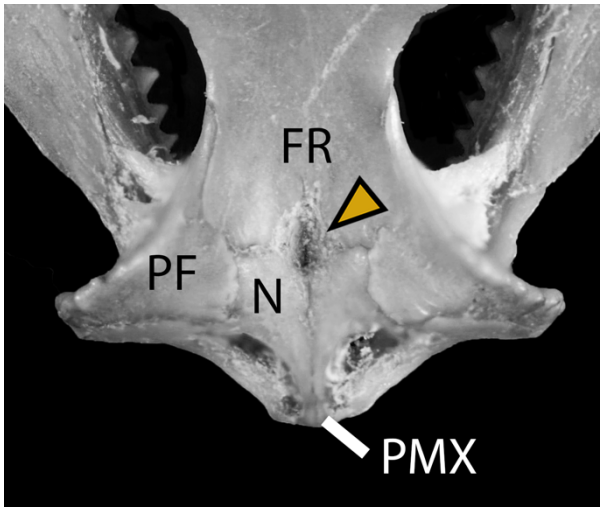

Figure A17. 9(1): WAM R1688
Moloch horridus, dorsal view.

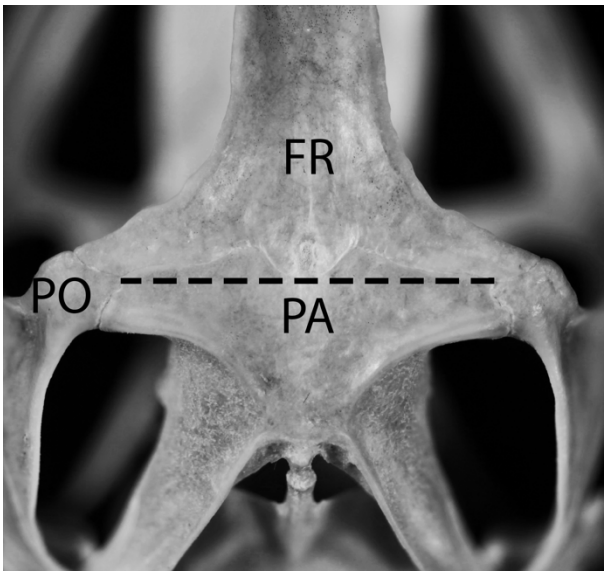

Figure A18. 10(0): TMM M-8436
Physignathus cocincinus, dorsal view.

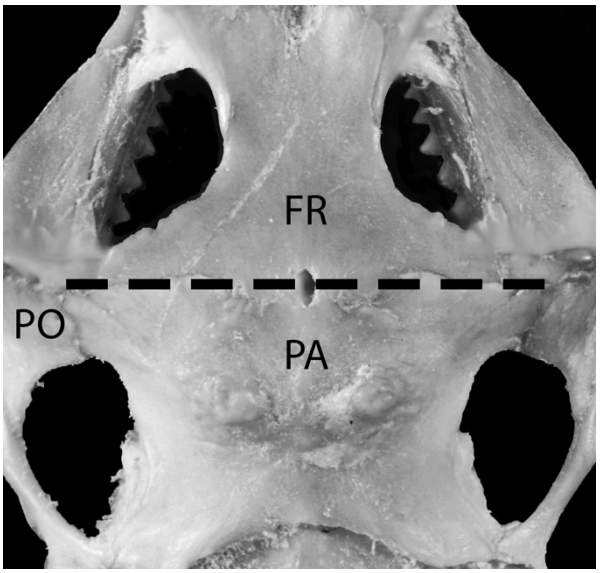

Figure A19. 10(1): WAM 1688
Moloch horridus, dorsal view.

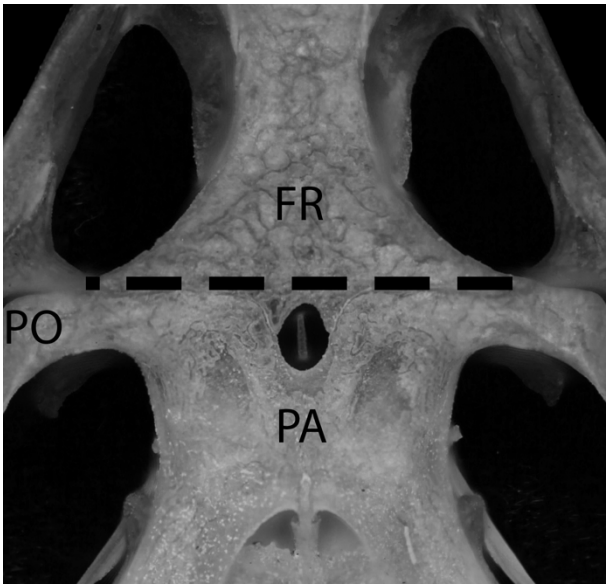

Figure A20. 10(2): WAM R165036
Ctenophorus caudicinctus, dorsal view.

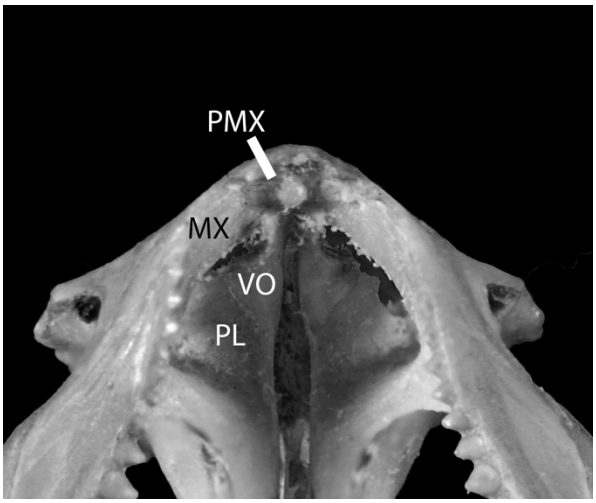

Figure A21. 11(0): WAM R1688
Moloch horridus, ventral view.

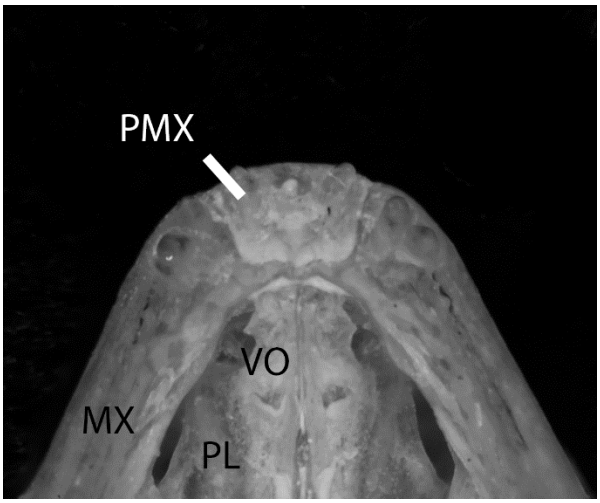

Figure A22. 11(1): WAM R165036
Ctenophorus caudicinctus, ventral view.

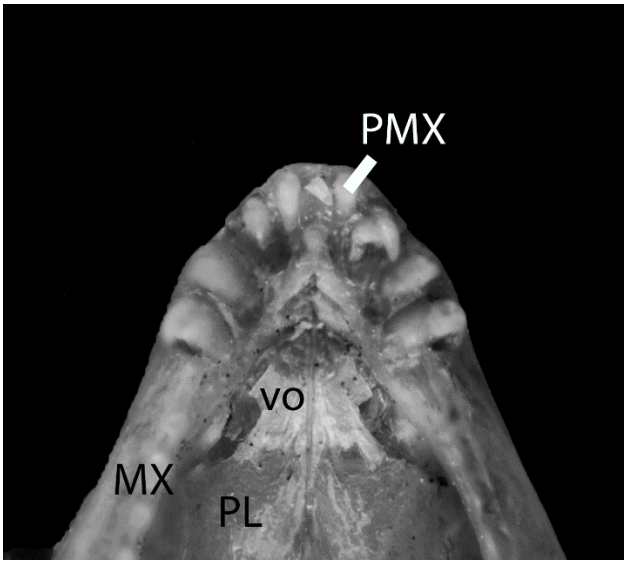

Figure A23. 11(2): WAM R162929
Lophognatus longirostrus, ventral view.

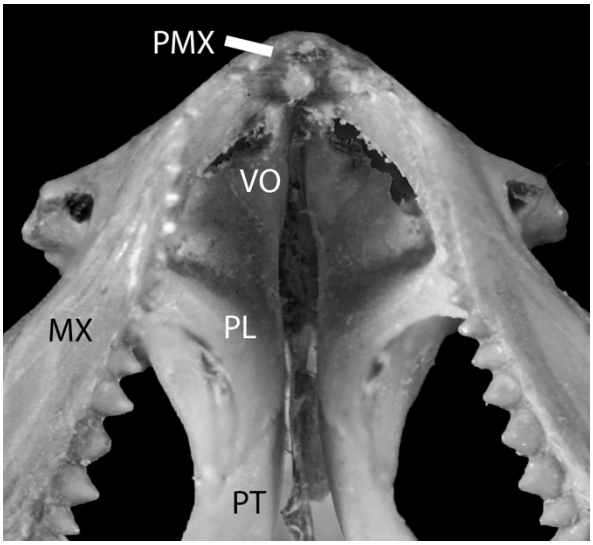

Figure A24. 12(0): WAM R1688
Moloch horridus, ventral view.

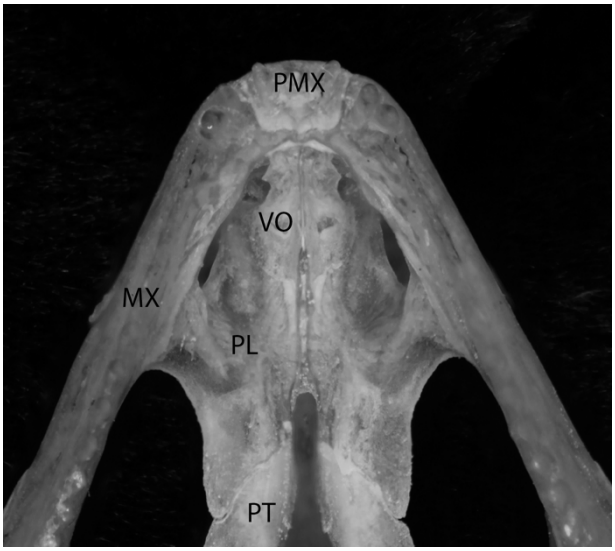

Figure A25. 12(1): WAM R165036
Ctenophorus caudicinctus, ventral view.

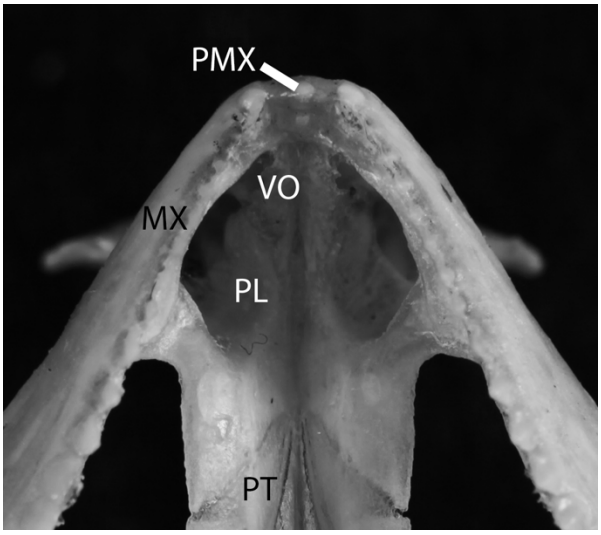

Figure A26. 12(2): WAM R111893
Ctenophorus nuchalis, ventral view.

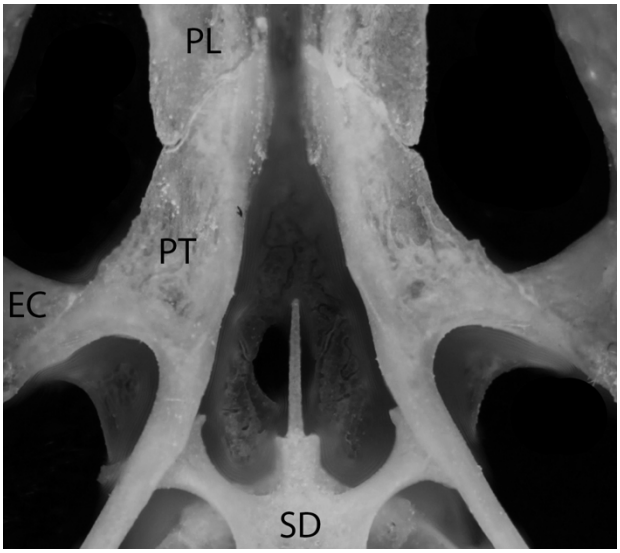

Figure A27. 13(0): WAM R165036 *Ctenophorus caudicinctus*, ventral view.

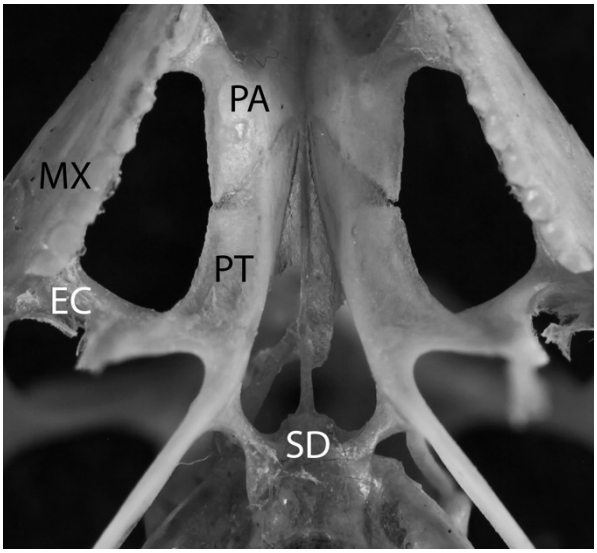

Figure A28. 13(1): WAM R111893 *Ctenophorus nuchalis*, ventral view.

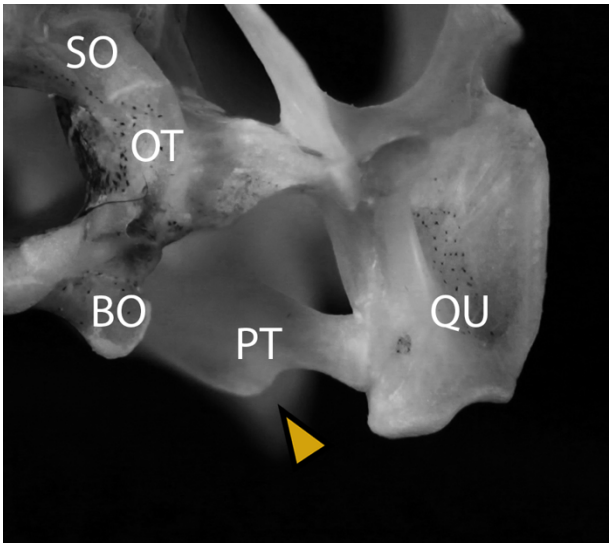

Figure A29. 14(0): WAM WAM R167672 *Ctenophorus caudicinctus*, posterior view.

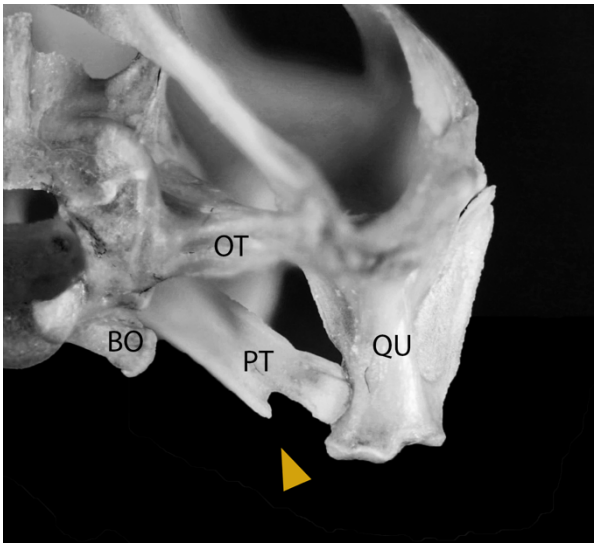

Figure A30. 14(1): WAM R167563 *Ctenophorus caudicinctus*, posterior view.

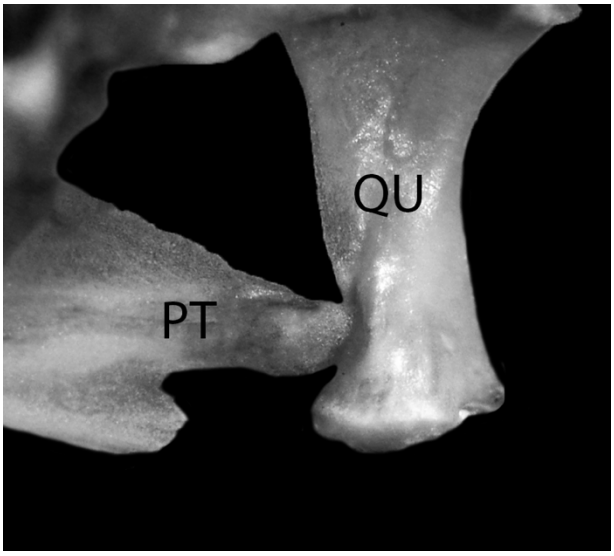

Figure A31. 15(0): WAM R111893
Ctenophorus nuchalis, posterior view.

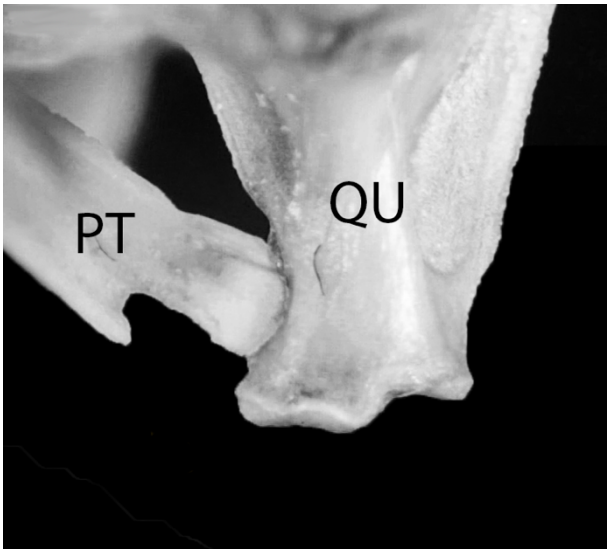

Figure A32. 15(1): WAM R167563
Ctenophorus caudicinctus, posterior view.

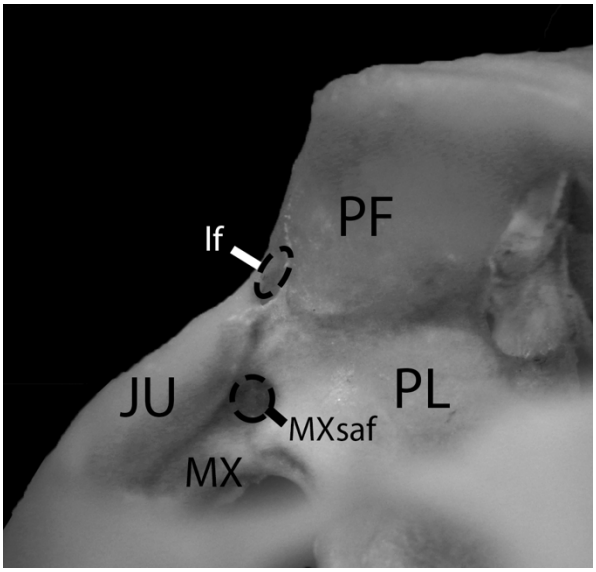

Figure A33. 16(0): WAM R8438
Uromastyx ornatus, posterior view of anterior orbit.

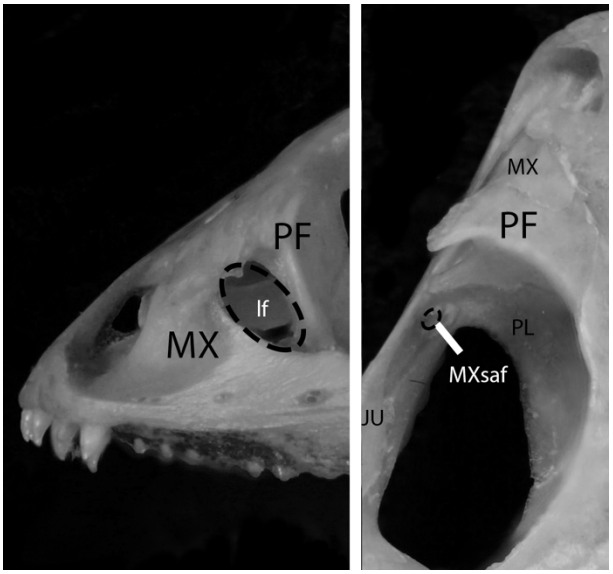

Figure A34. 16(1): WAM R111747
Ctenophorus caudicinctus, left lateral view (left) and dorsal view (right).

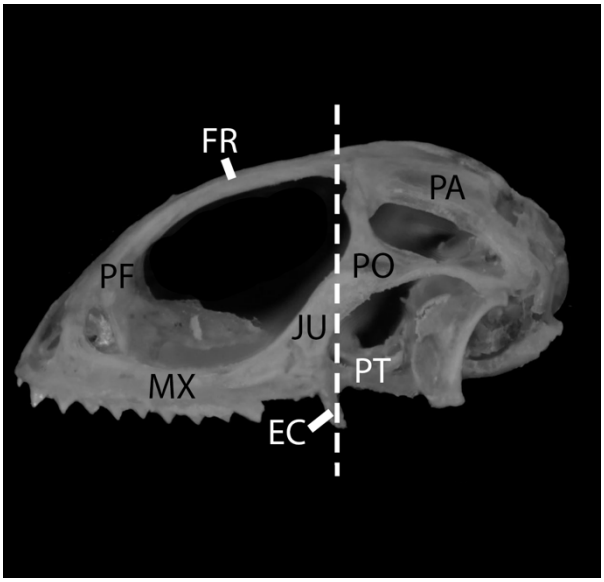

Figure A35. 17(0): WAM R162820
Ctenophorus caudicinctus, lateral view.

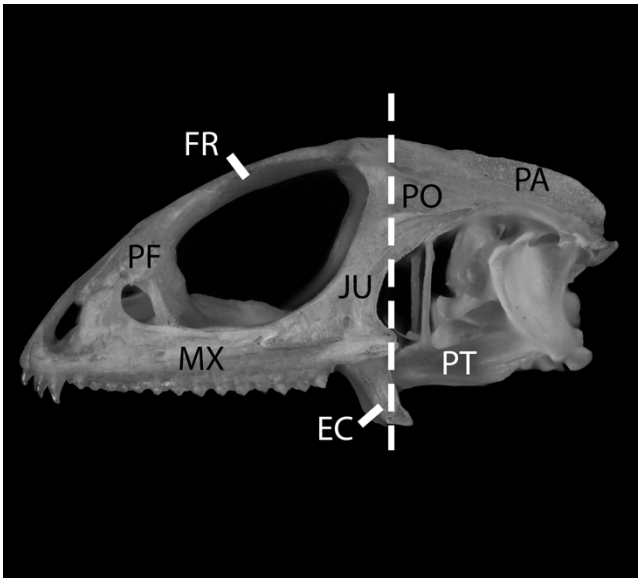

Figure A36. 17(1): WAM R165036
Ctenophorus caudicinctus, lateral view.

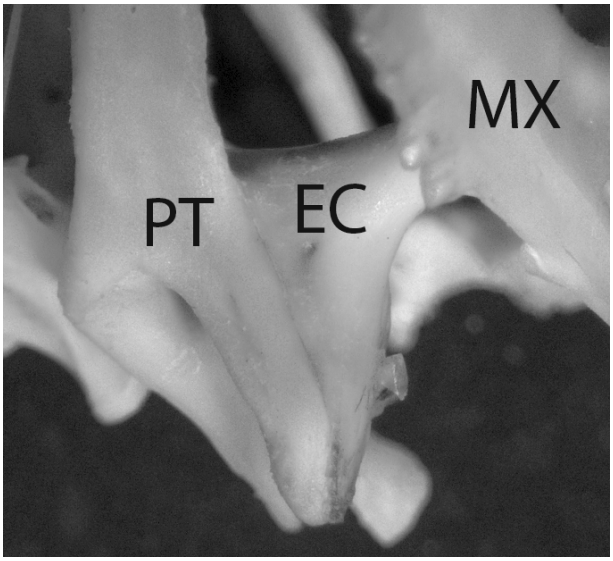

Figure A37. 18(0): WAM R112142
Pogona minor, anterior view.

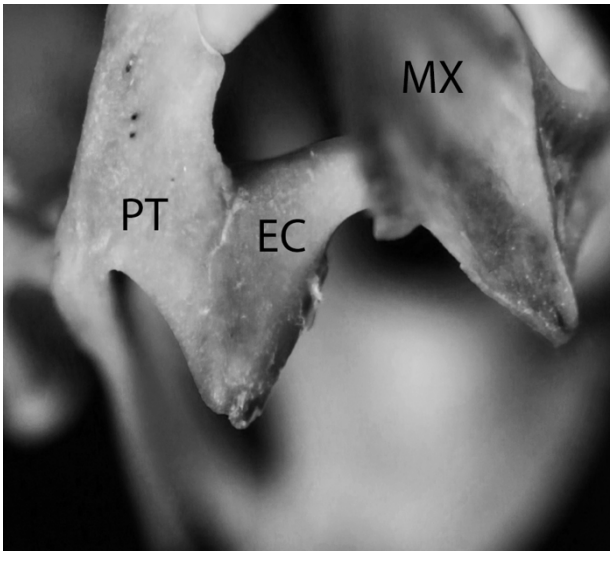

Figure A38. 18(1): WAM R162878
Ctenophrous reticulatus, anterior view.

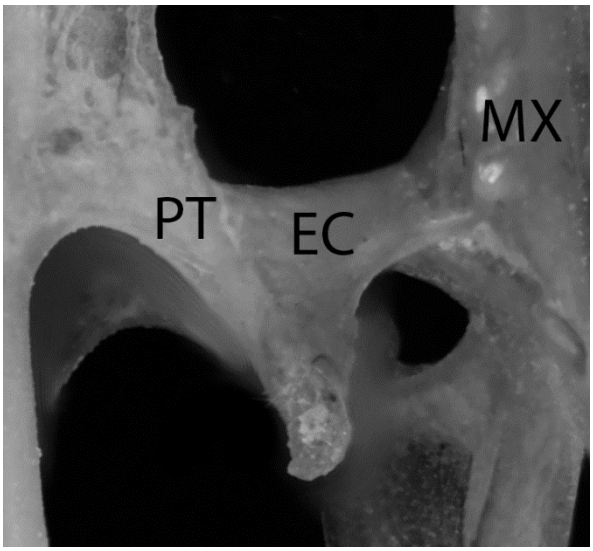

Figure A39. 18(2): WAM R165036
Ctenophorus caudicinctus, anterior view.

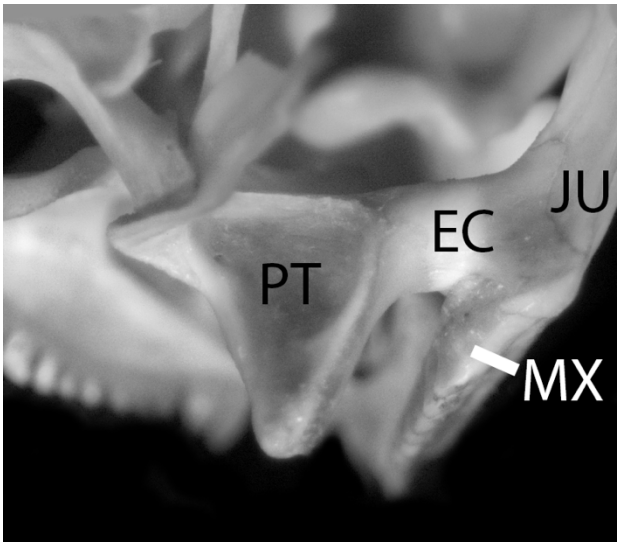

Figure A40. 19(0): WAM R112142
Pogona minor, posterior view.

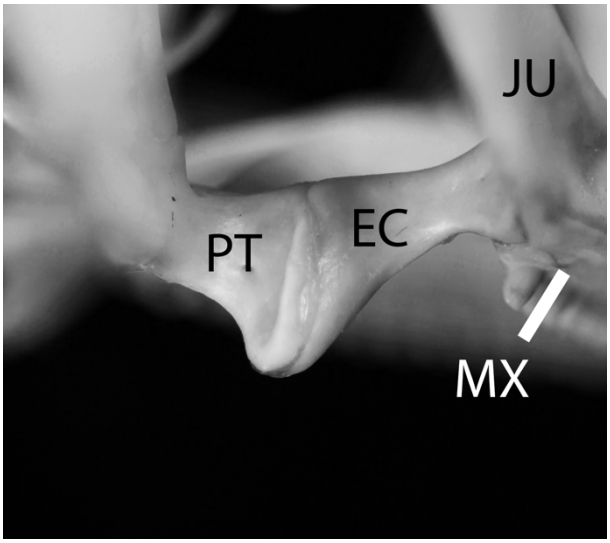

Figure A41. 19(1): TMM Uncatalogued for thesis. *Uromastyx benti*, posterior view.

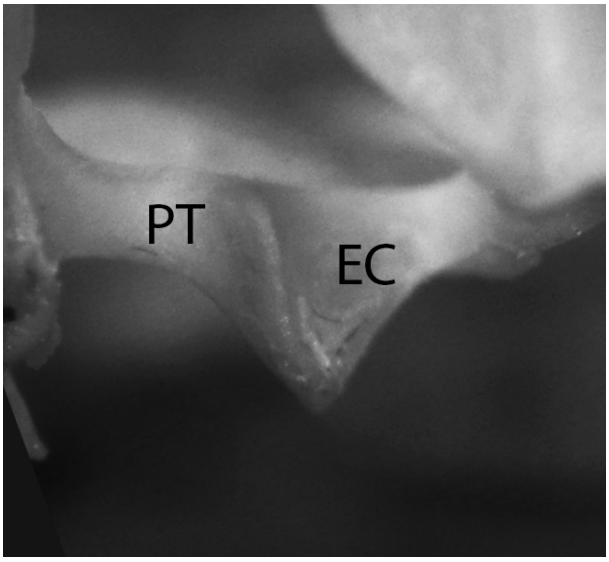

Figure A42. 19(2): WAM R167533
Ctenophorus scutulatus, posterior view.

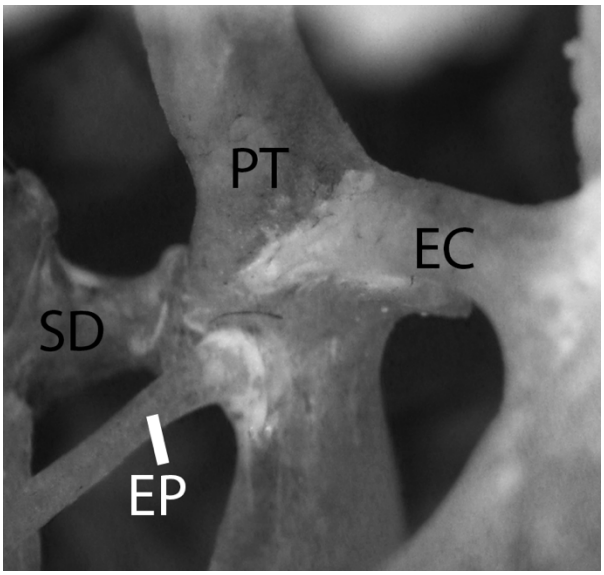

Figure A43. 20(0): WAM R149488
Moloch horridus, dorsal view.

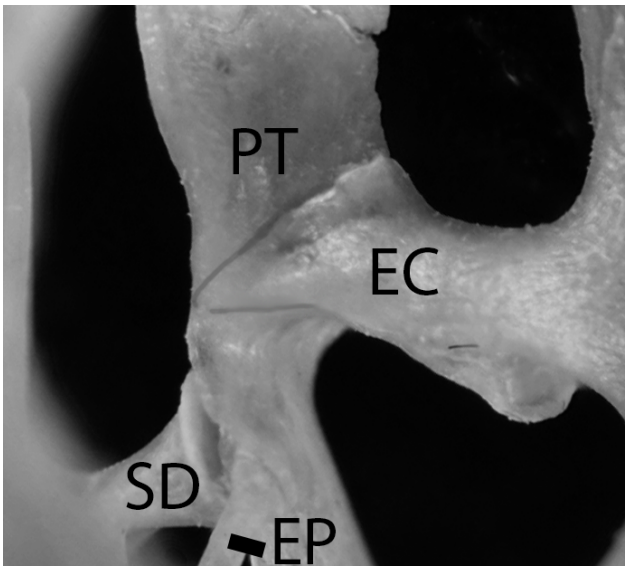

Figure A44. 20(1): WAM R167563
Ctenophorus caudicinctus, dorsal view.

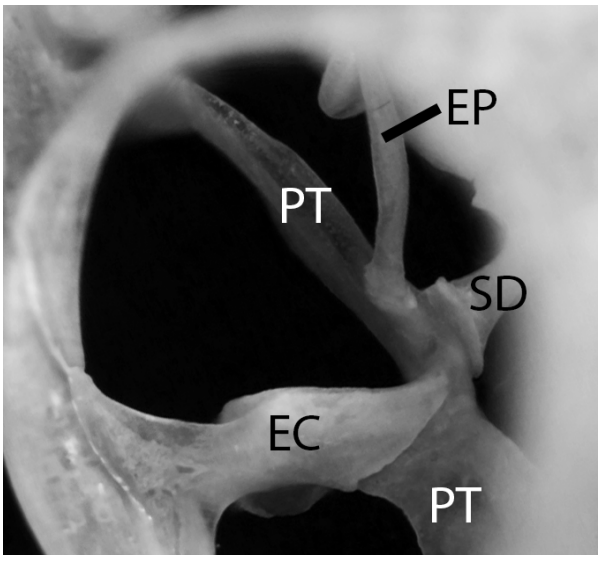

Figure A45. 21(0): WAM R167503 *Ctenophorus reticulatus*, anterodorsal view through the orbit.

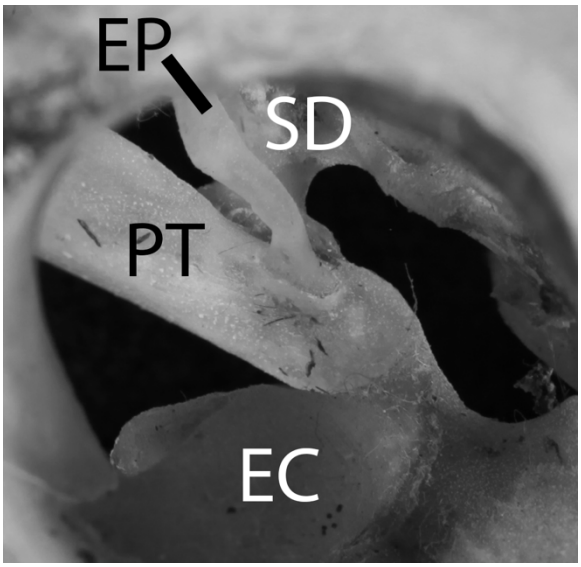

Figure A46. 21(1): WAM R47842 *Physignathus lesurii*, anterodorsal view through the orbit.

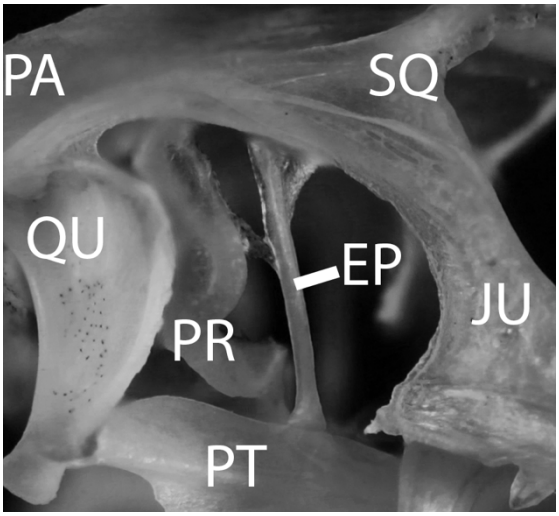

Figure A47. 22(0): WAM R167672 *Ctenophorus caudicinctus*, right lateral view.

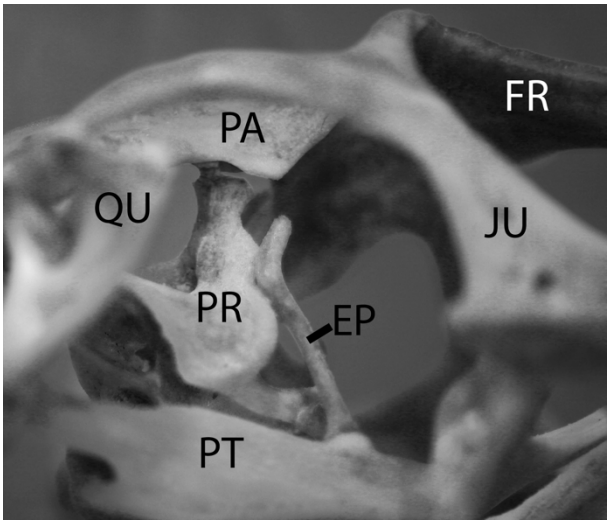

Figure A48. 22(1): WAM R162878 *Ctenophorus reticulatus*, right lateral view.

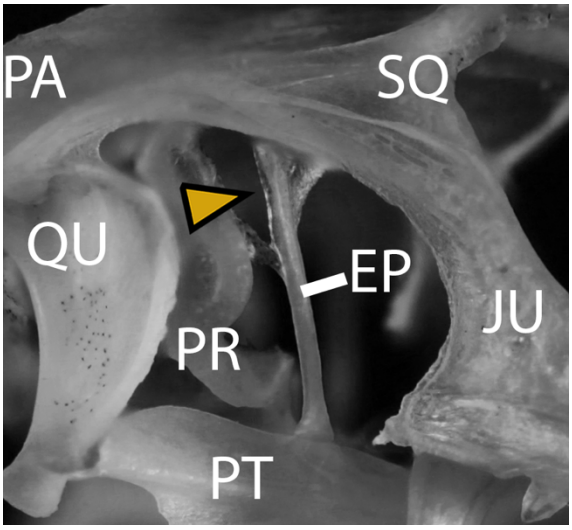

Figure A49. 23(0): WAM R167672 *Ctenophorus caudicinctus*, right lateral view.

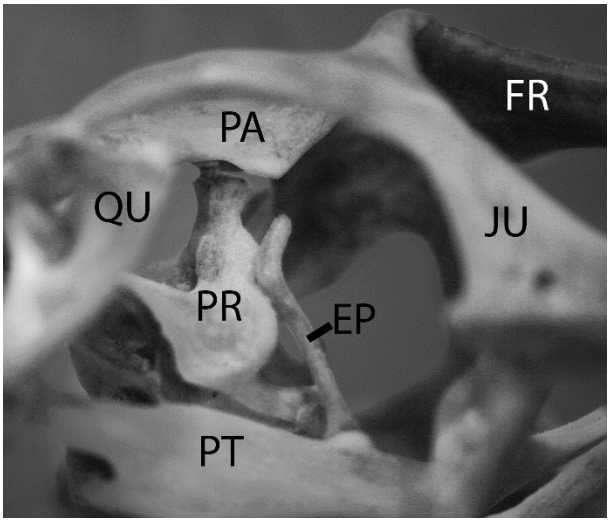

Figure A50. 23(1): WAM R162878 *Ctenophorus reticulatus*, right lateral view.

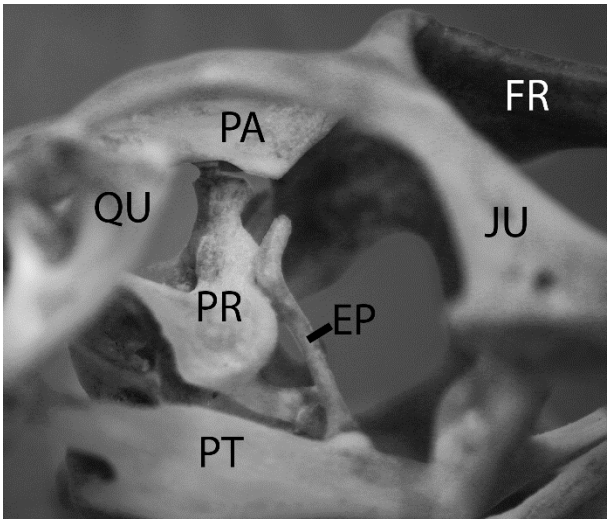

Figure A51. 24(0): WAM R162878 *Ctenophorus reticulatus*, right lateral view.

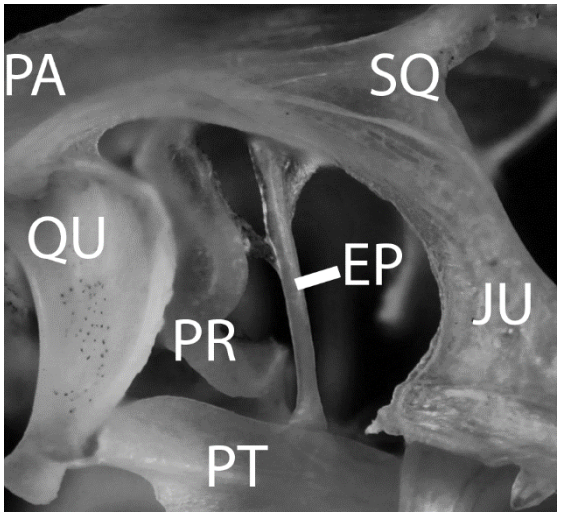

Figure A52. 24(1): WAM R167672 *Ctenophorus caudicinctus*, right lateral view.

Figure A53. 25(0): WAM R162819
Ctenophorus caudicinctus, left lateral view.

Figure A54. 25(1): WAM R167672
Ctenophorus caudicinctus, left lateral view.

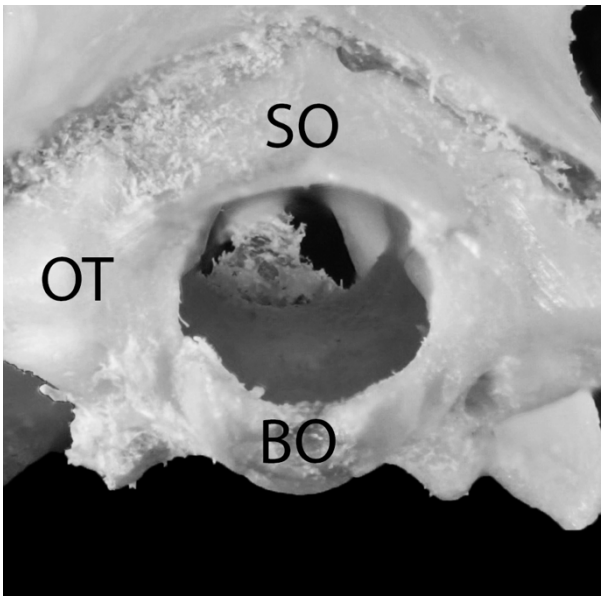

Figure A55. 26(0): WAM R1688

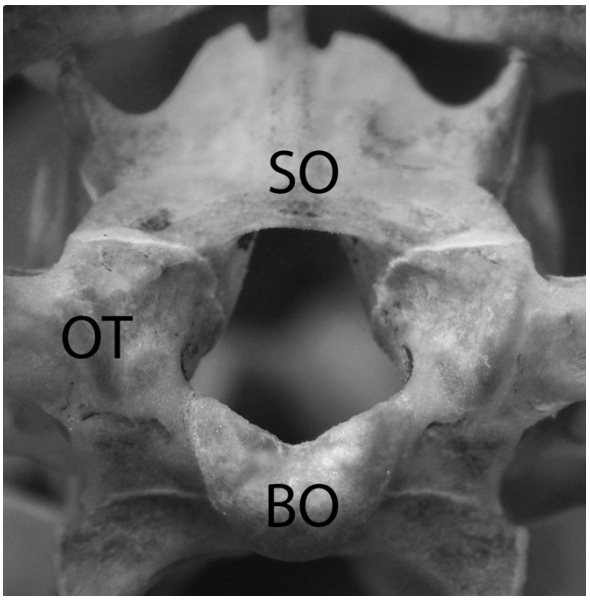

Figure A56. 26(1): WAM R162878

Moloch horridus, posterior view.

Ctenophorus reticulatus, posterior view.

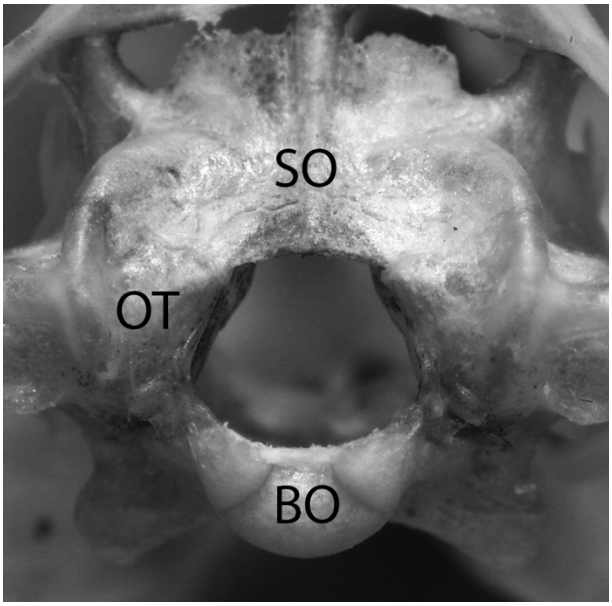

Figure A57. 26(2): WAM R111893 *Ctenophorus nuchalis*, posterior view.

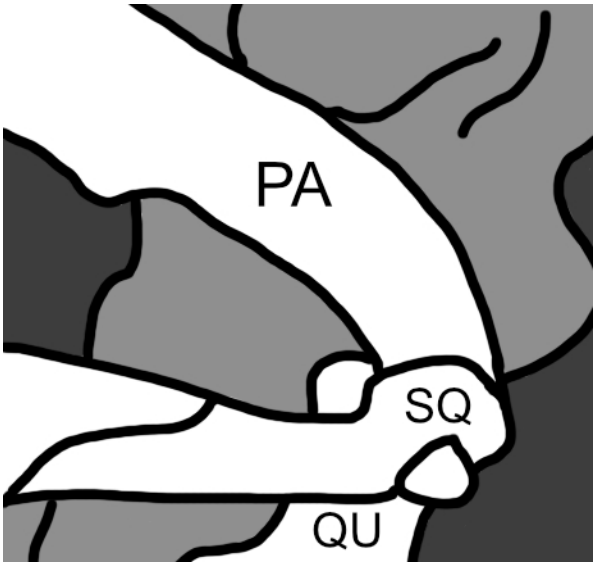

Figure A58. 27(0): Idealized character based on WAM R162878 *Ctenophorus reticulatus*, posterolateral view.

Figure A59. 27(1): WAM R162878 *Ctenophorus reticulatus*, posterolateral view.

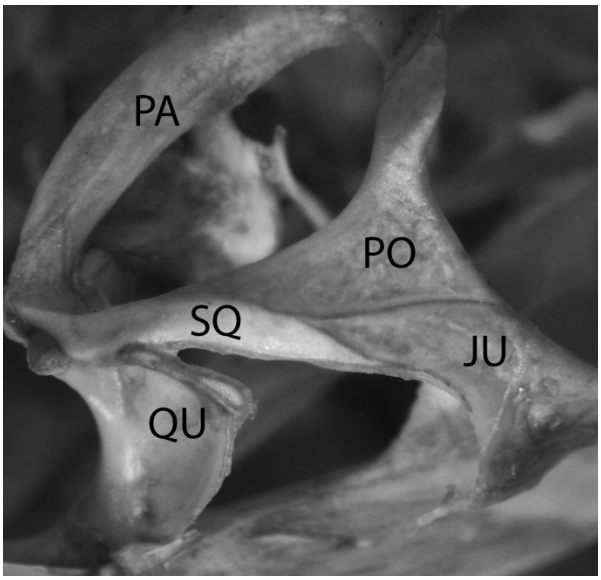

Figure A60. 28(0): WAM R111893
Ctenophorus nuchalis, posterolateral view.

Figure A61. 28(1): WAM R167672
Ctenophorus caudicinctus, posterolateral view.

Figure A62. 28(2): JIM R uncat.
Agama kirkii, posterolateral view.

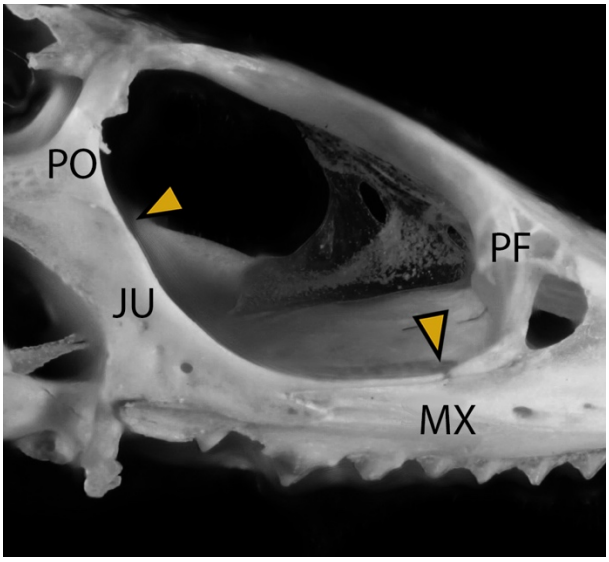

Figure A63. 29(0): WAM R162932 *Lophognathus longirostrus*, lateral view.

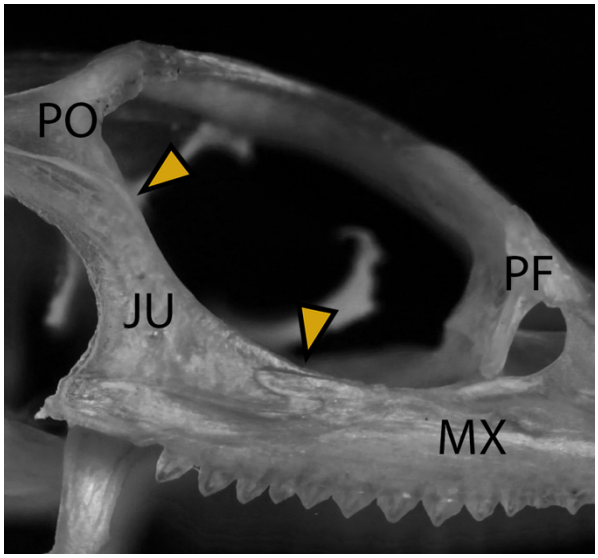

Figure A64. 29(1): WAM R167672 *Ctenophorus caudicinctus*, lateral view.

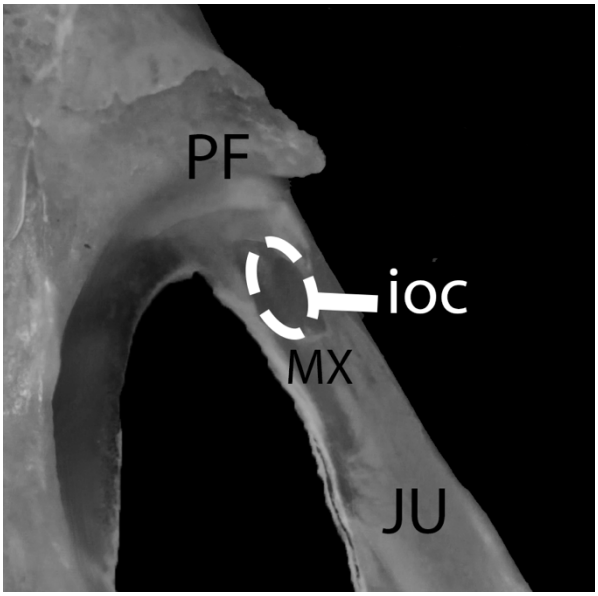

Figure A65. 30(0): WAM R1676752 *Ctenophorus caudicinctus*, dorsal view.

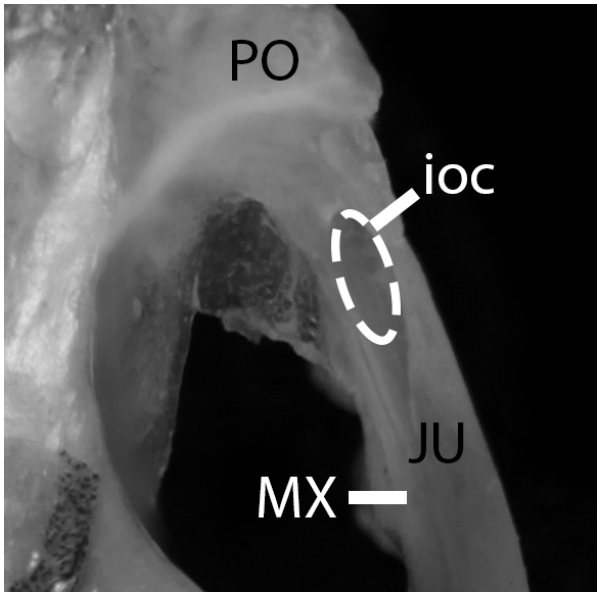

Figure A66. 30(1): WAM R162932 *Ctenophorus longirostrus*, dorsal view.

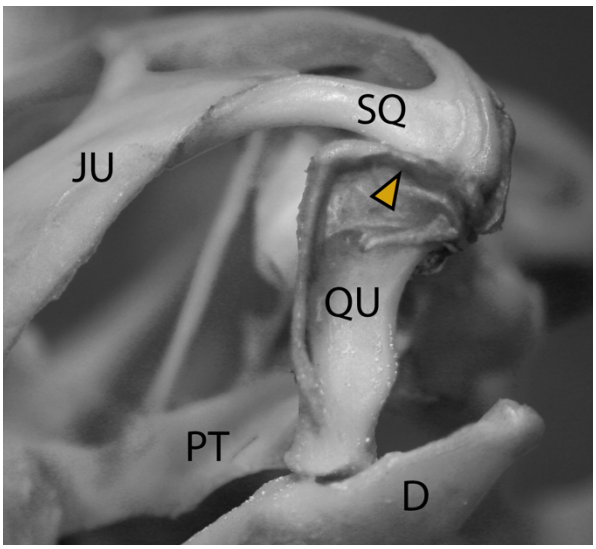

Figure A67. 31(0): WAM R8438
Uromastyx ornatus, lateral view.

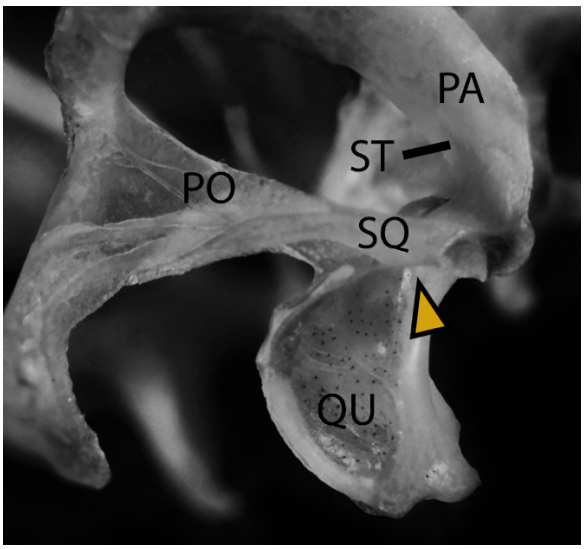

Figure A68. 31(1): WAM R167672
Ctenophorus caudicinctus, lateral view.

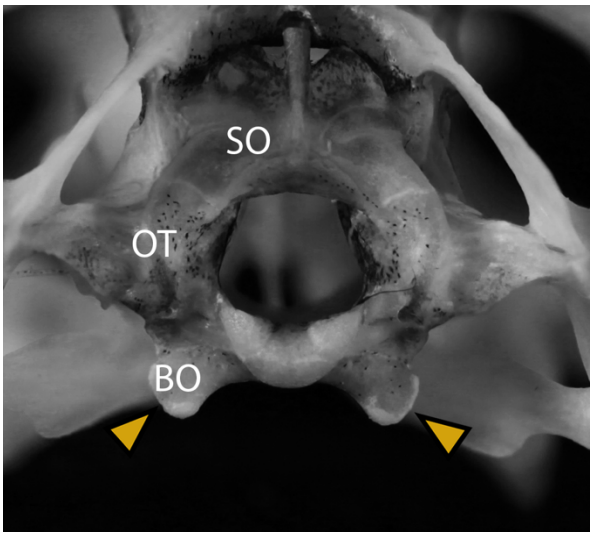

Figure A69. 32(0): WAM R167672
Ctenophorus caudicinctus, posterior view.

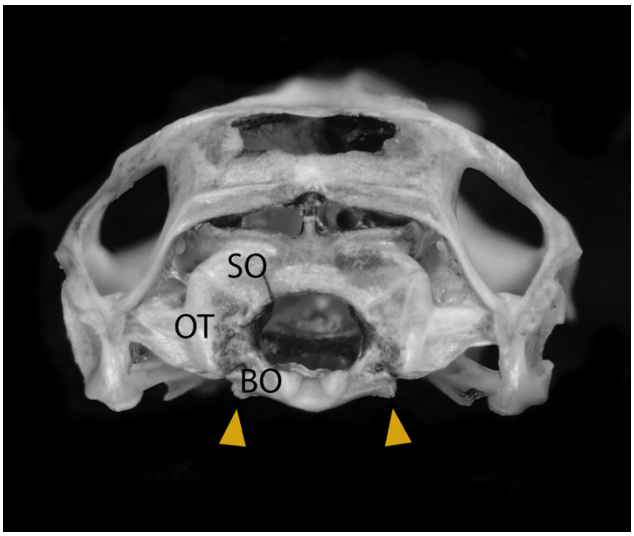

Figure A70. 32(1): WAM R162779
Ctenophorus reticulatus, posterior view.

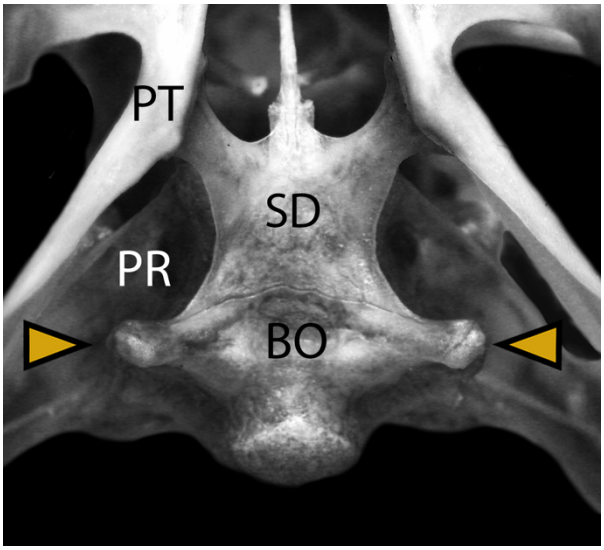

Figure A71. 33(0): WAM R165185
Ctenophorus nuchalis, ventral view.

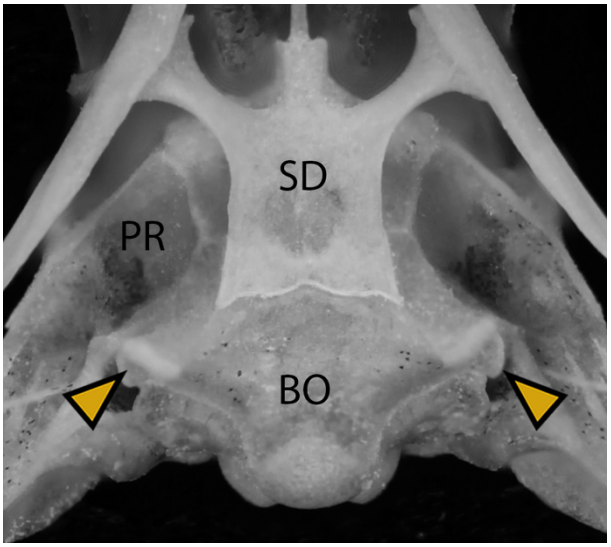

Figure A72. 33(1): WAM R165036
Ctenophorus caudicinctus, ventral view.

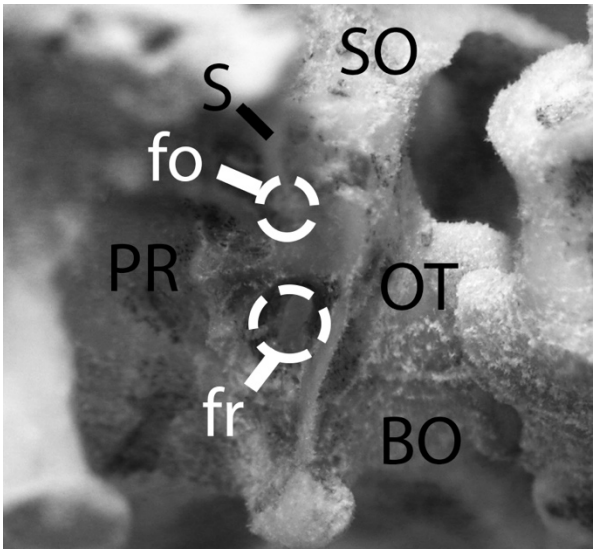

Figure A73. 34(0): WAM R1478
Calotes versicolor, posterolateral view..

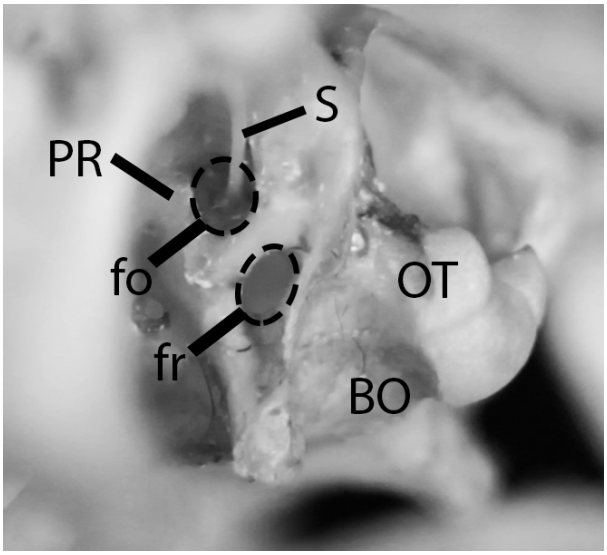

Figure A74. 34(1): WAM R156678
Ctenophrous reticulatus, posterolateral view.

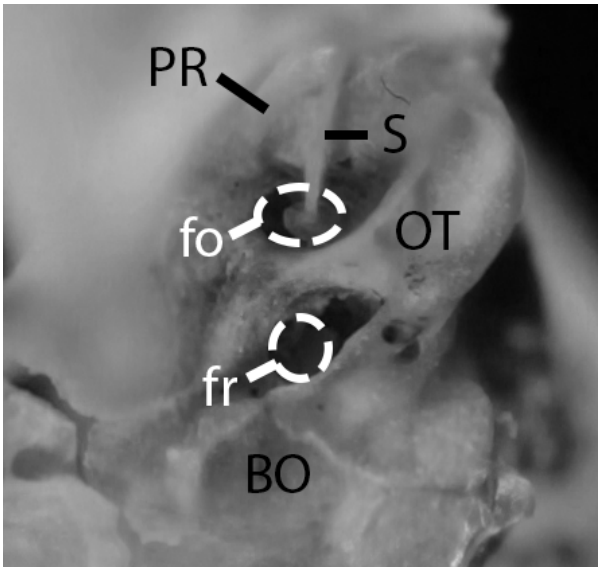

Figure A75. 34(2): WAM R uncat.
Stekkui atricolis, posterolateral view.

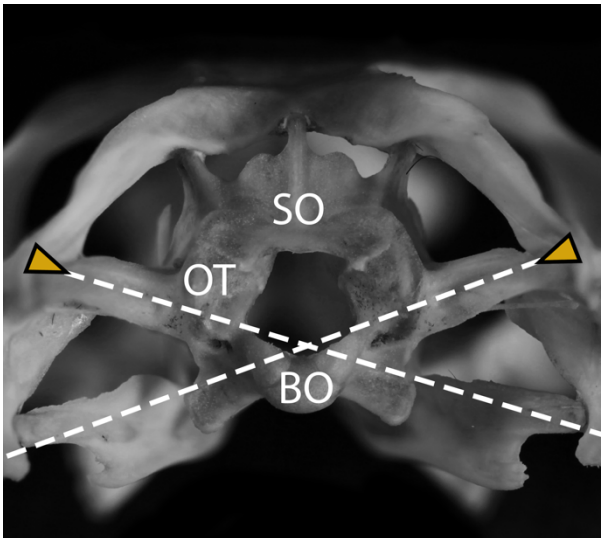

Figure A76. 35(0): WAM R162760
Ctenophorus reticulatus, posterior view.

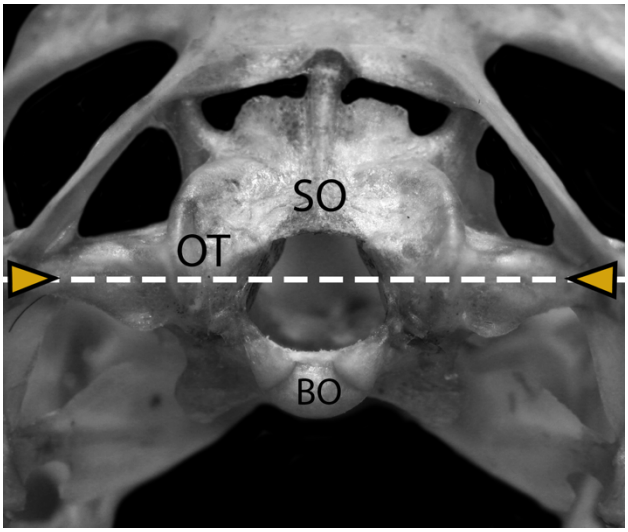

Figure A77. 35(1): WAM R111893
Ctenophorus nuchalis, posterior view.

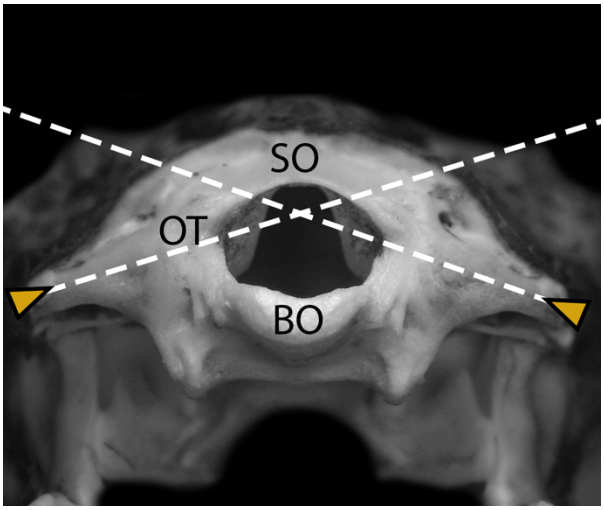

Figure A78. 35(2): WAM R149423
Moloch horridus, posterior view.

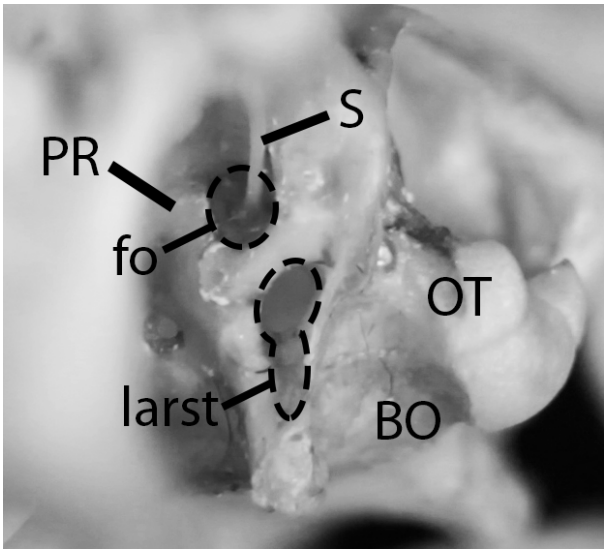

Figure A79. 36(0): WAM R156678
Ctenophorus reticulatus, posterolateral view.

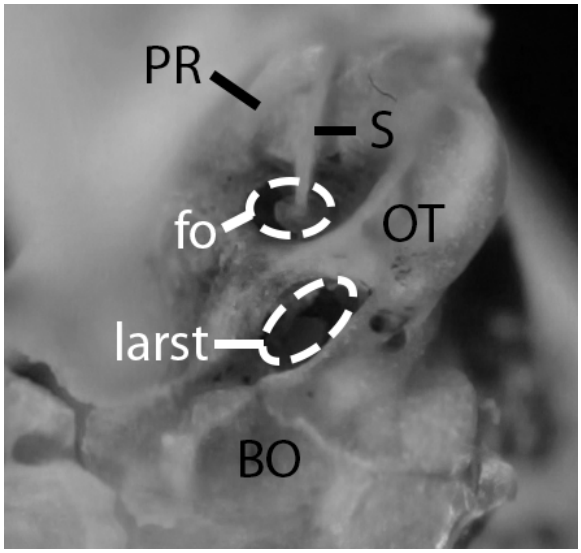

Figure A80. 36(1): WAM R uncat.
Stekkui atricolis, posterolateral view.

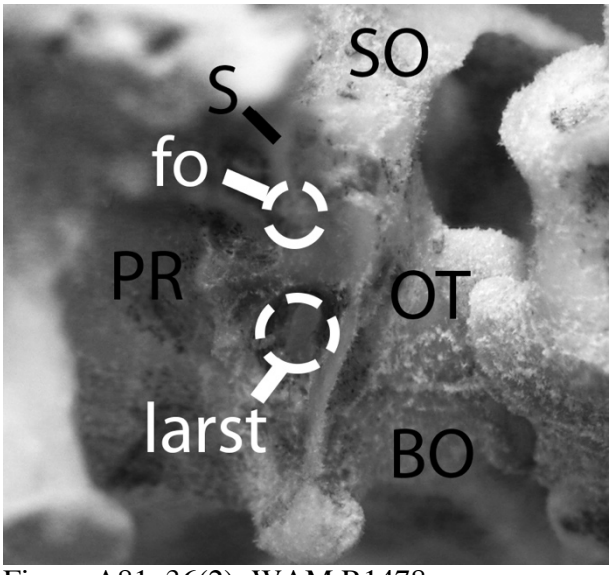

Figure A81. 36(2): WAM R1478
Calotes versicolor, posterolateral view.

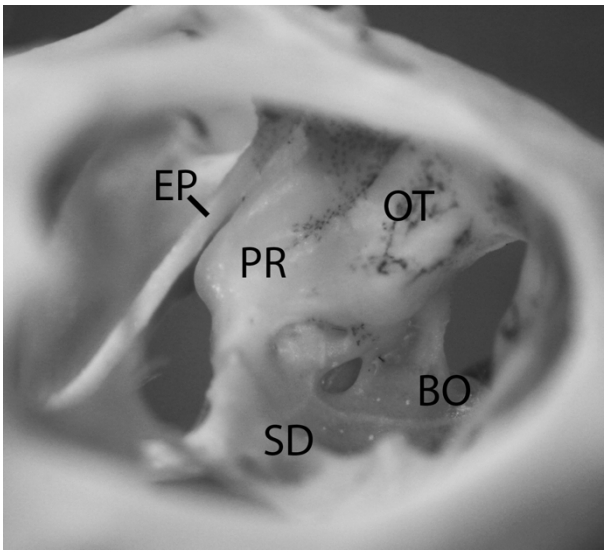

Figure A82. 37(0): WAM R8438
Uromastyx ornatus, view of right medial braincase through left lateral orbit.

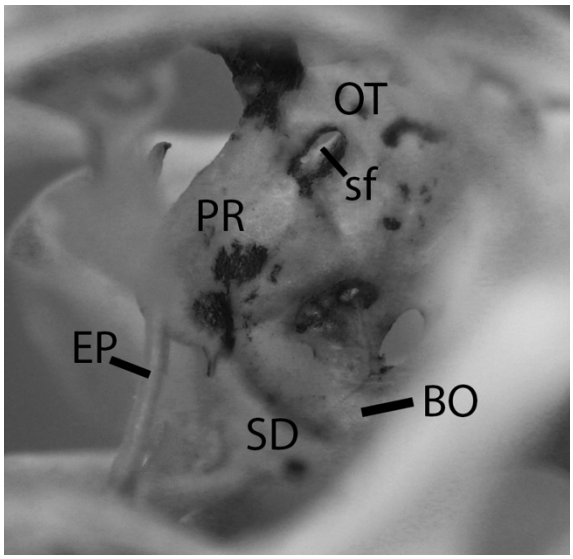

Figure A83. 37(1): WAM R16280
Ctenophorus nuchalis, view of right medial braincase through left lateral orbit.

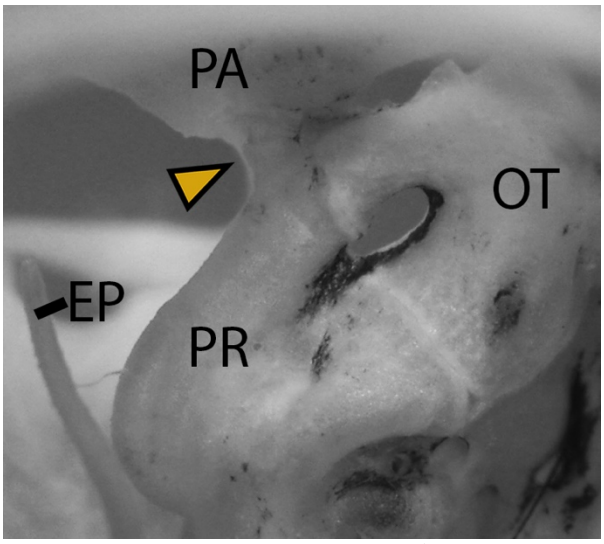

Figure A84. 34(0): WAM R16753 *Ctenophorus scutulatus*, medial view of right braincase.

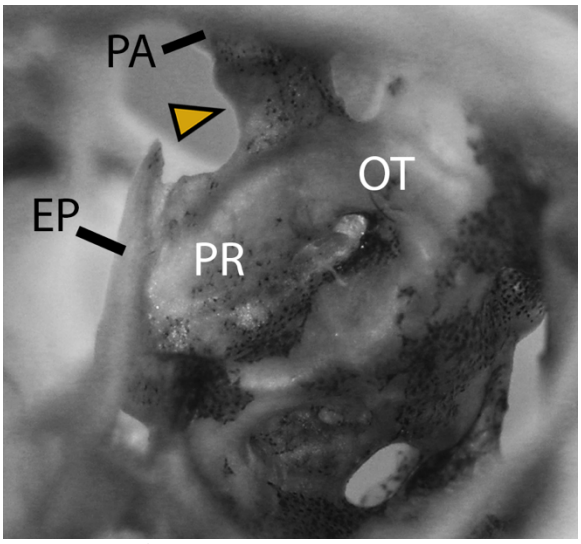

Figure A85. 38(1): WAM R111893 *Ctenophorus nuchalis*, medial view of right braincase.

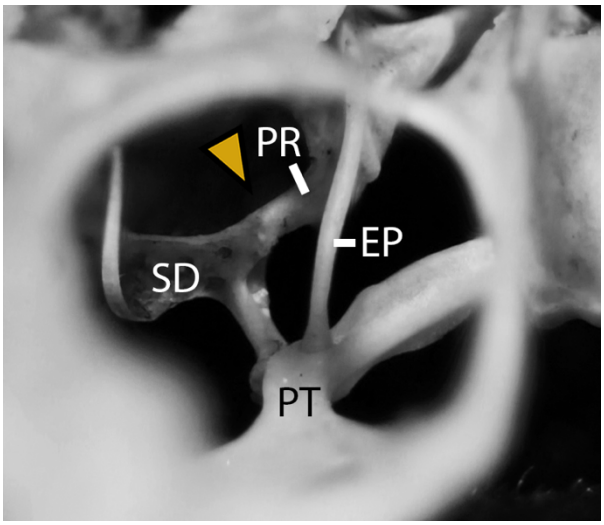

Figure A86. 39(0): TMM Uncatalogued for thesis. *Petrosaurus mearnsi*, anterolateral view.

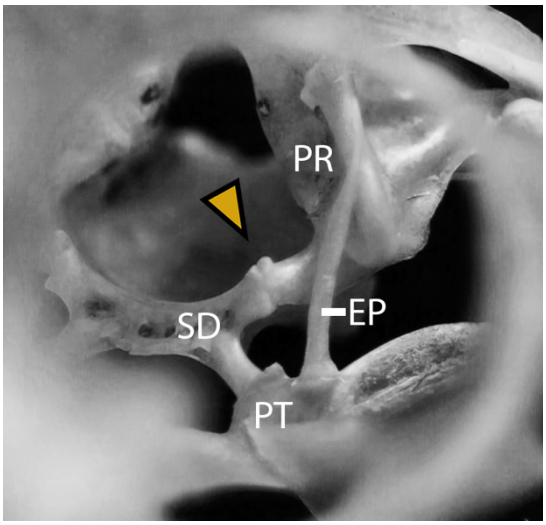

Figure A87. 39(1): WAM R167503 *Ctenophorus reticulatus*, anterolateral view.

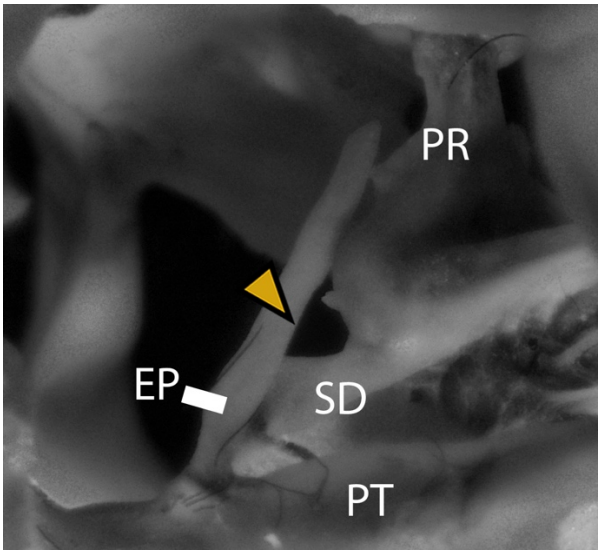

Figure A88. 39(2): WAM R162760, *Ctenophorus caudicinctus*, left lateral view.

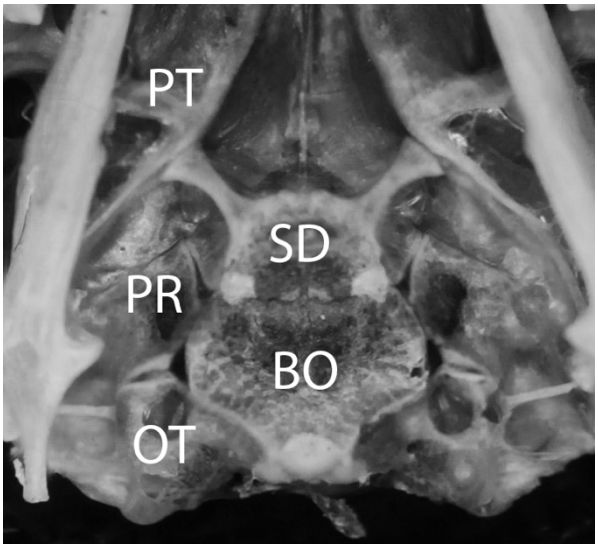

Figure A89. 40(0): WAM R162822 *Ctenophorus caudicinctus*, ventral view.

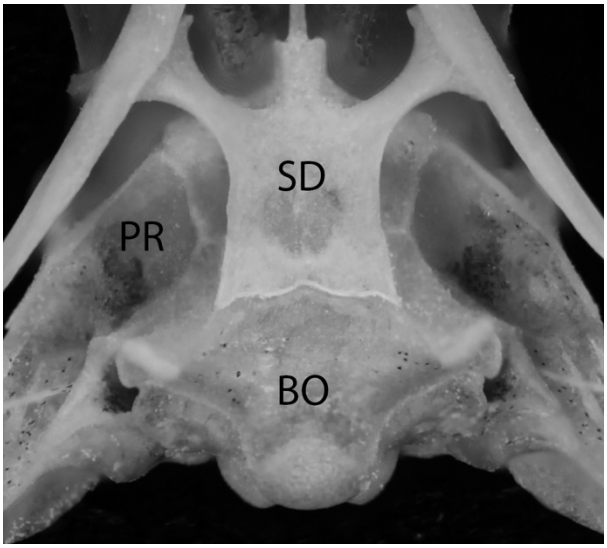

Figure A90. 40(1): WAM R165036 *Ctenophorus caudicinctus*, ventral view.

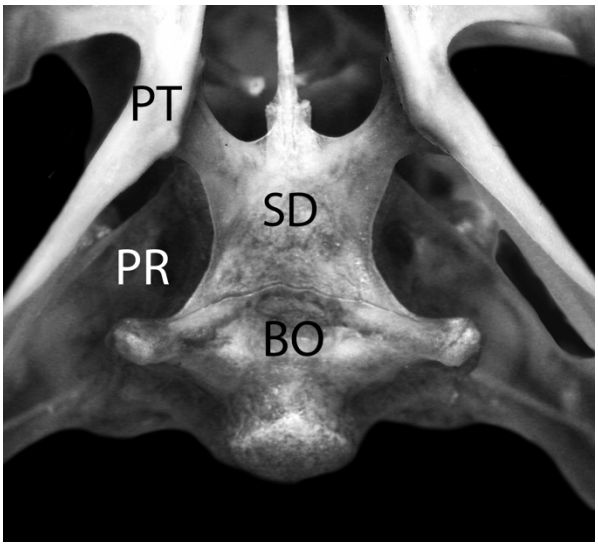

Figure A91. 40(2): WAM R165185
Ctenophorus nuchalis, ventral view.

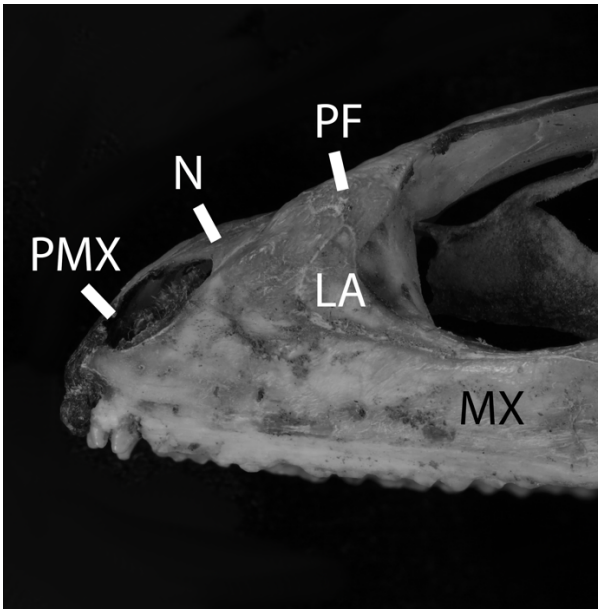

Figure A92. 41(0): VPL R47842
Physignathus lesurii, left lateral view.

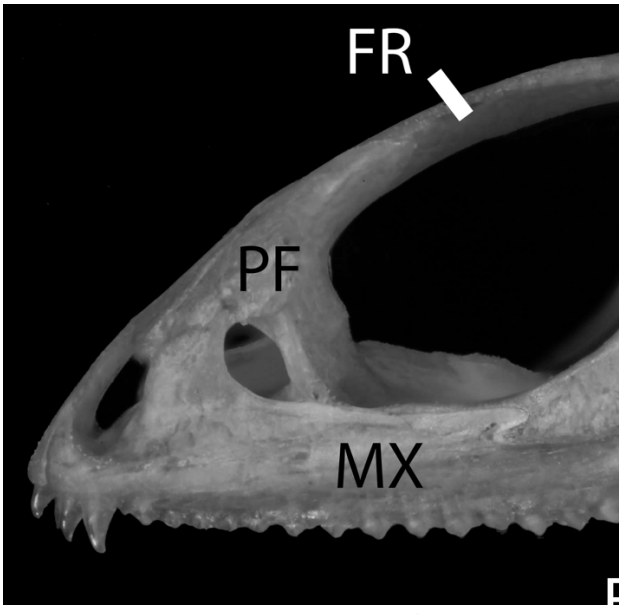

Figure A93. 41 (1): WAM R165036
Ctenophorus caudicinctus, left lateral view.

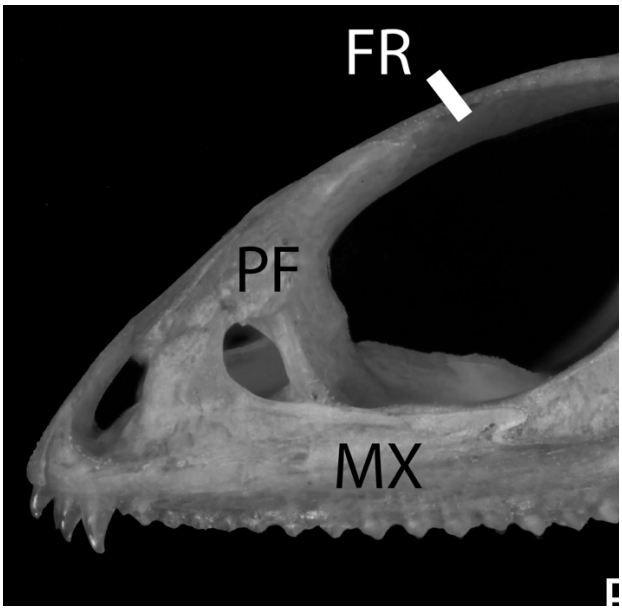

Figure A94. 42(0): WAM R165036 *Ctenophorus caudicinctus*, left lateral view.

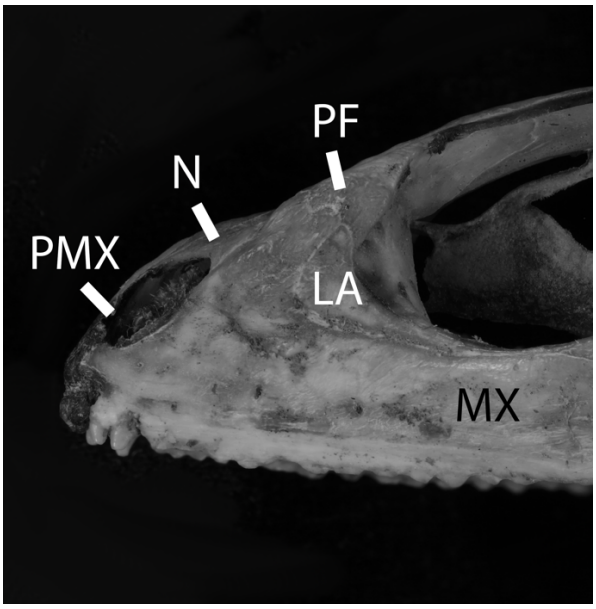

Figure A95. 42(1): WAM R27842 *Physignathus lesurii*, left lateral view.

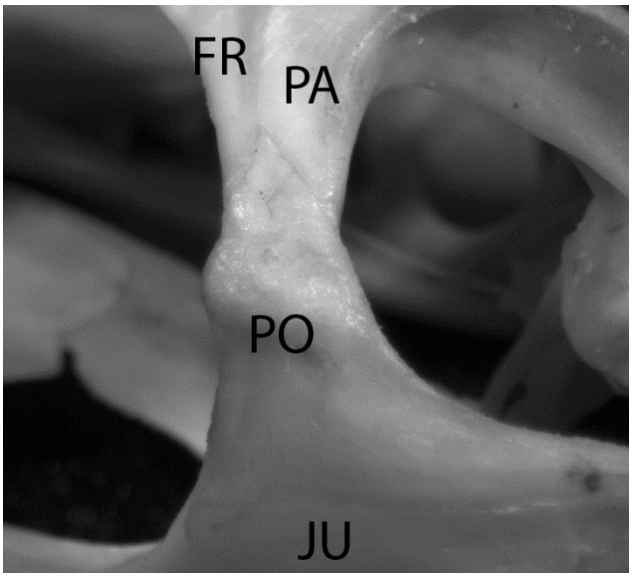

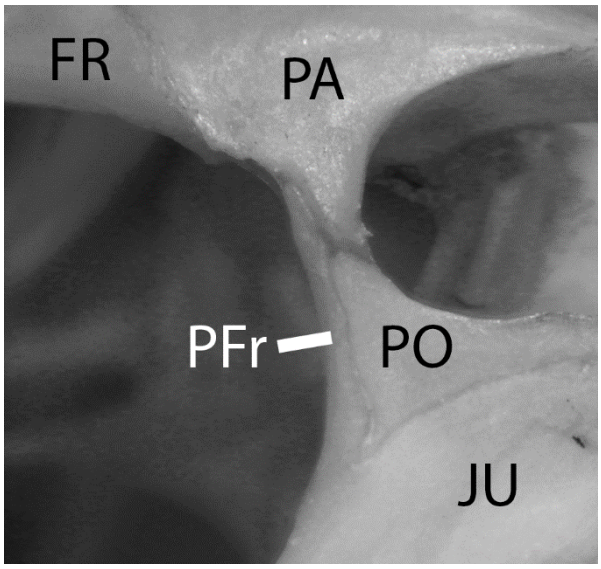

Figure A96. 43(0): WAM R112142
Pogona minor, dorsolateral view.

Figure A97. 43(1): WAM R8438
Uromastyx ornatus, dorsolateral view.

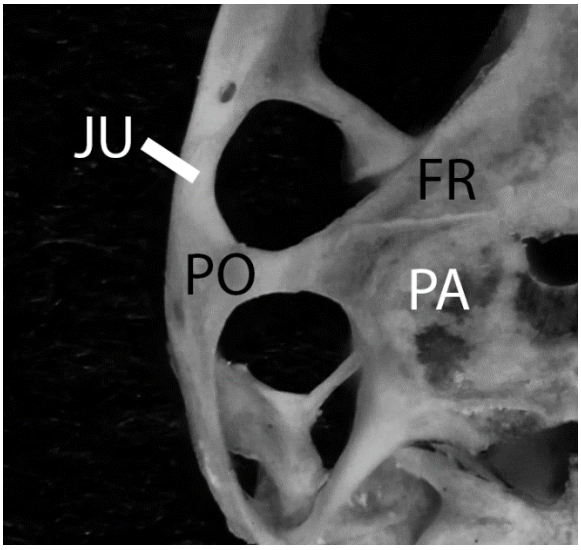

Figure A98. 44(0): WAM R162892
Ctenophorus femoralis, dorsal view.

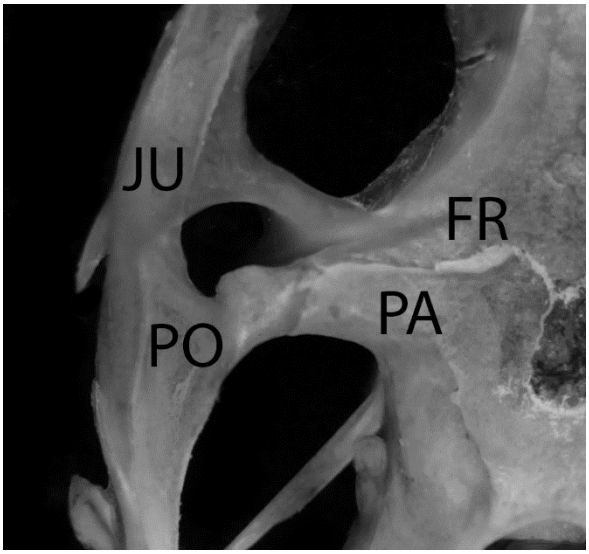

Figure A99. 44(1): WAM R167665
Ctenophorus caudicinctus, dorsal view.

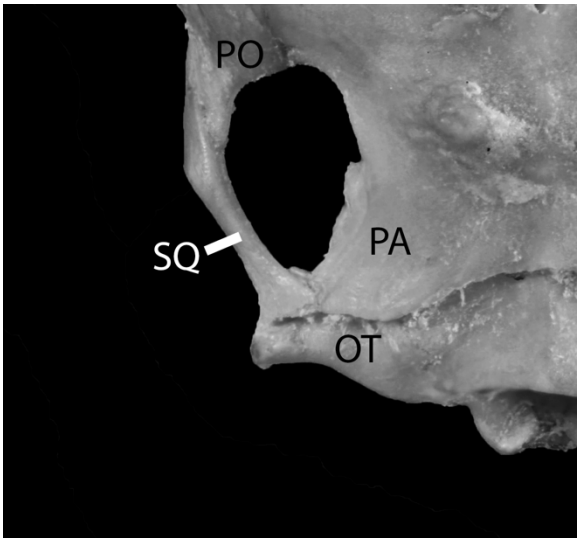

Figure A100. 43(0): WAM R1688
Moloch horridus, dorsal view.

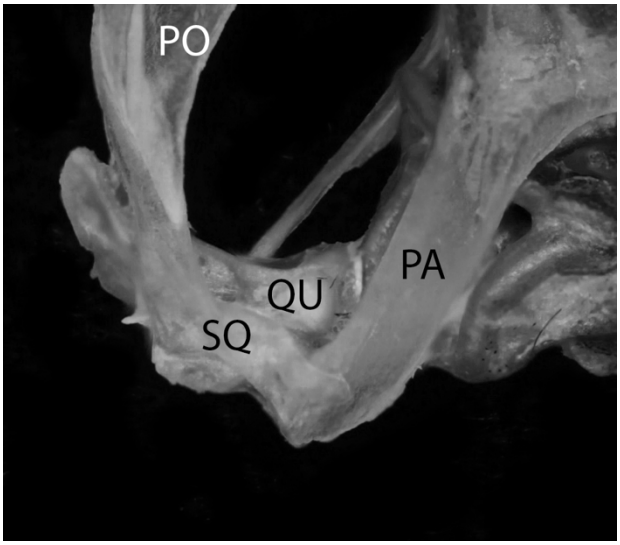

Figure A101. 44(1): WAM R167632
Ctenophorus caudicinctus, dorsal view.

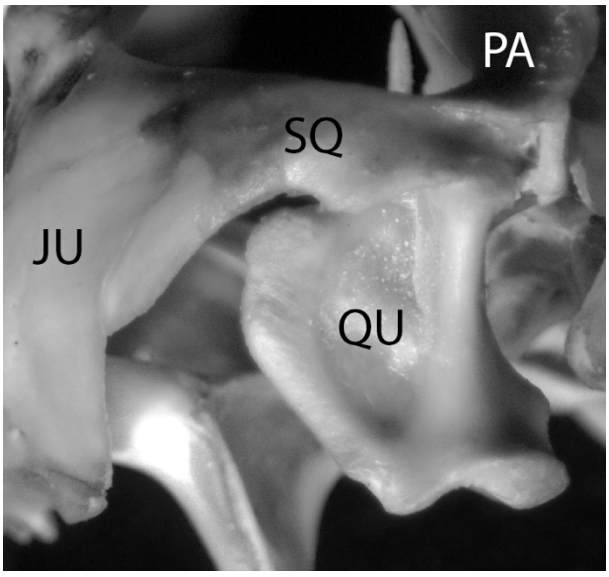

Figure A102. 46(0): WAM R112142 *Pogona minor*, posterolateral view.

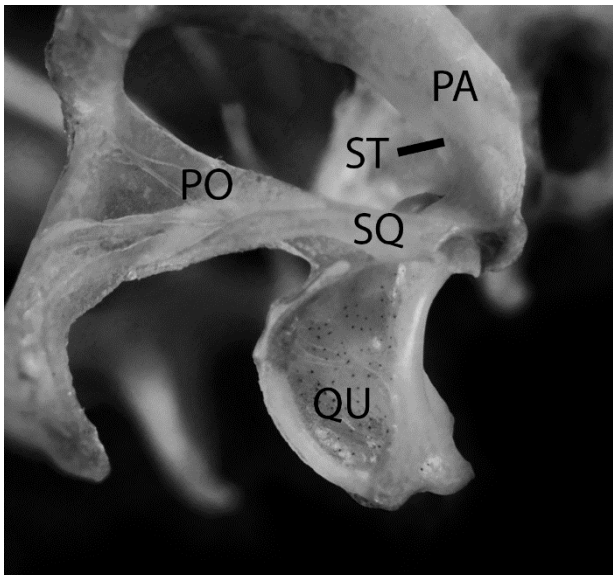

Figure A103. 46(0): WAM R167672 *Ctenophorus caudicinctus*, posterolateral view.

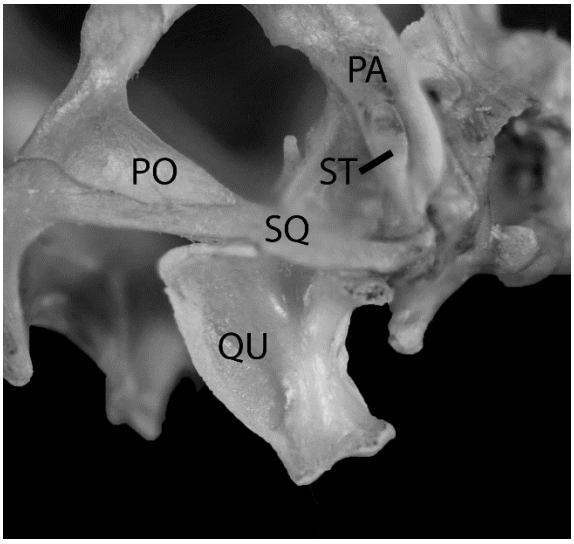

Figure A104. 46(1): WAM R1657563 *Ctenophorus caudicinctus*, posterolateral view.

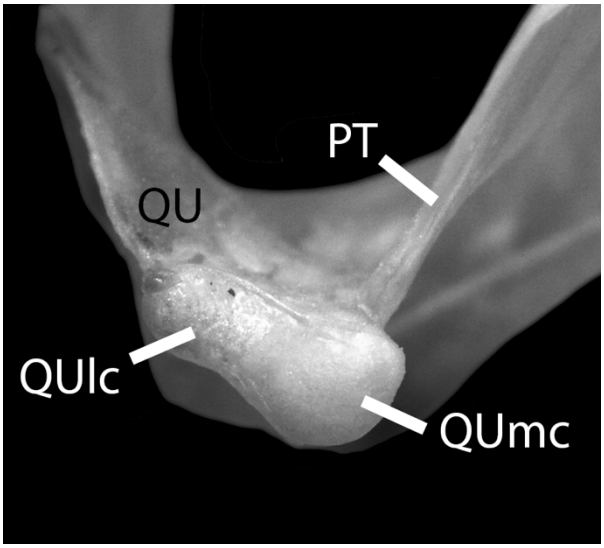

Figure A105. 47(0): WAM R165185 *Ctenophorus nuchalis*, ventral view of right quadrate.

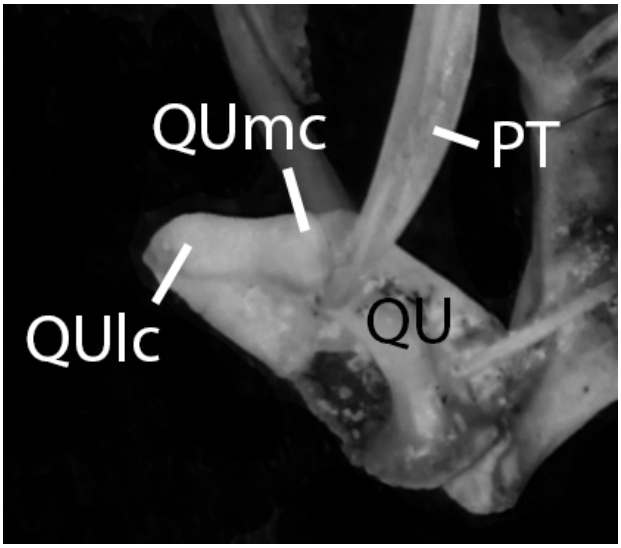

Figure A106. 47(1): WAM R2184 *Petrosaurus mearnsi*, ventral view of right quadrate.

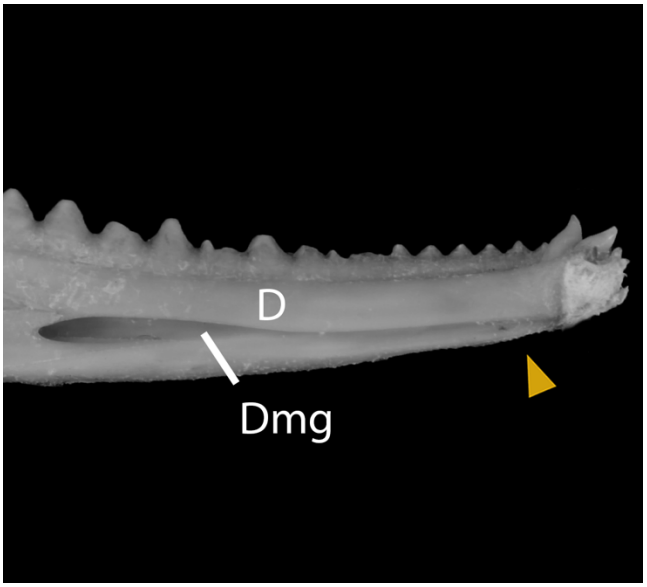

Figure A107. 48(0): WAM R112124 *Pogona minor*, lingual view.

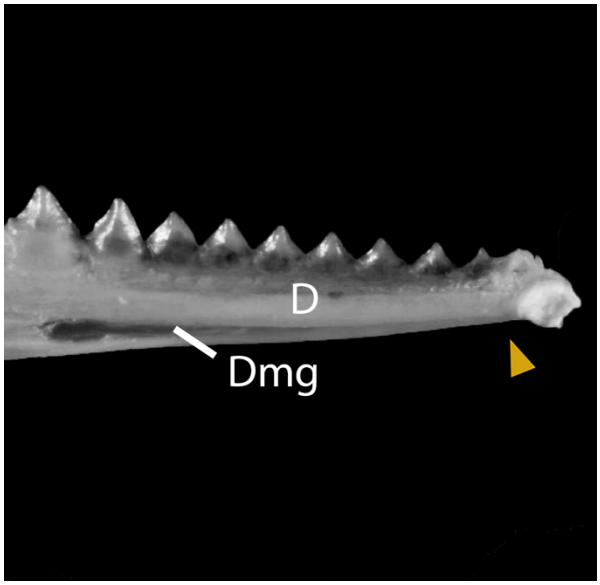

Figure A108. 48(1): WAM R162933 *Lophognathus longirostris*, lingual view.

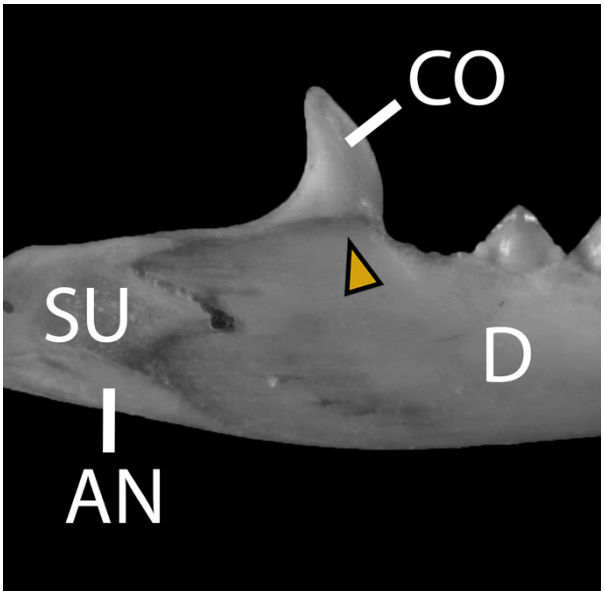

Figure A109. 49(0): WAM R162926 *Lophognathus gilberti*, right labial view.

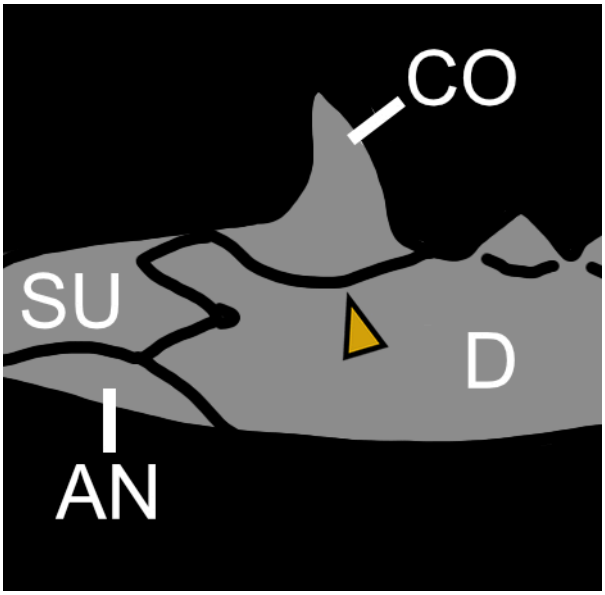

Figure A110. 49(1): modified from WAM R162926 *Lophognathus gilberti*, right labial view.

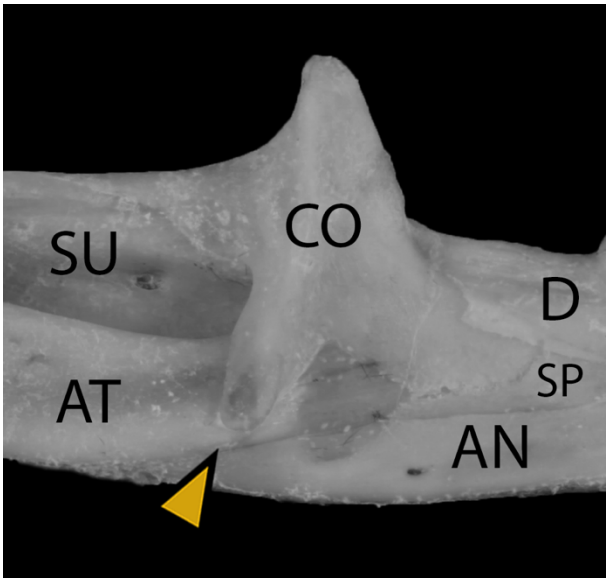

Figure A111. 50(0): WAM R112124
Pogona minor, left lingual view.

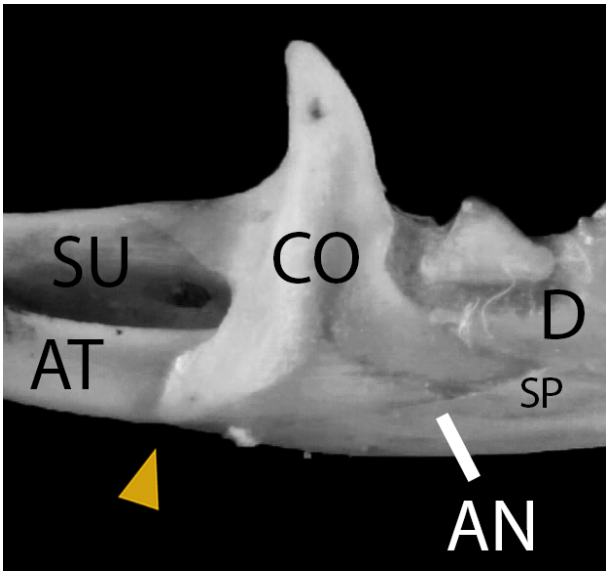

Figure A112. 50(1): WAM R162933
Lophognathus longirostris, left lingual view.

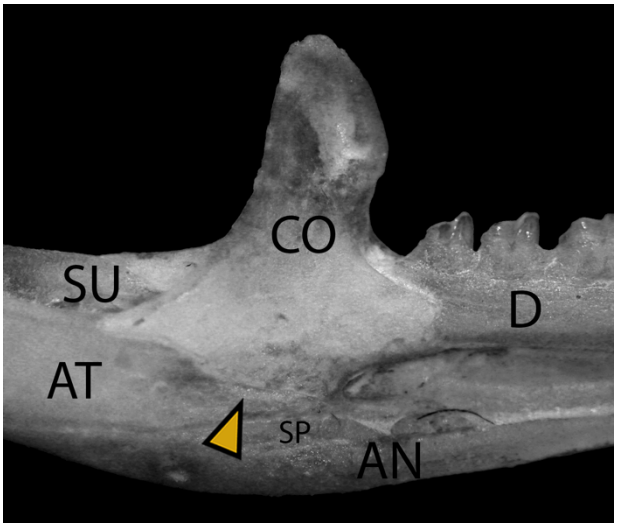

Figure A113. 50(2): WAM R149488
Moloch horridus, left lingual view.

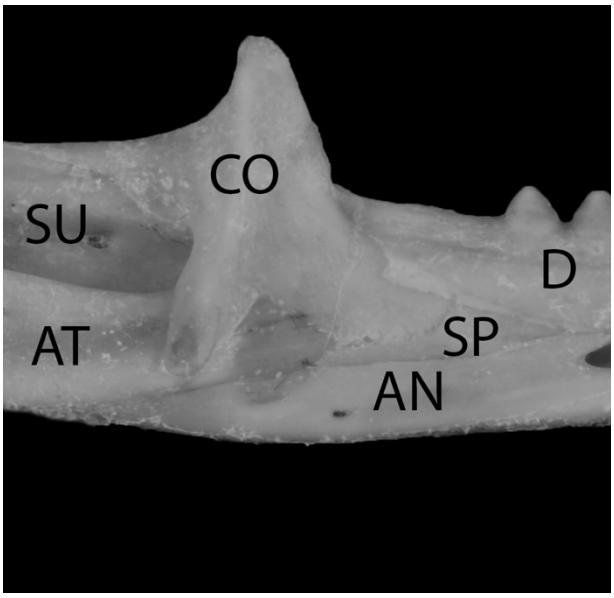

Figure A114. Character 51(0): WAM R112124 *Pogona minor*, left lingual view.

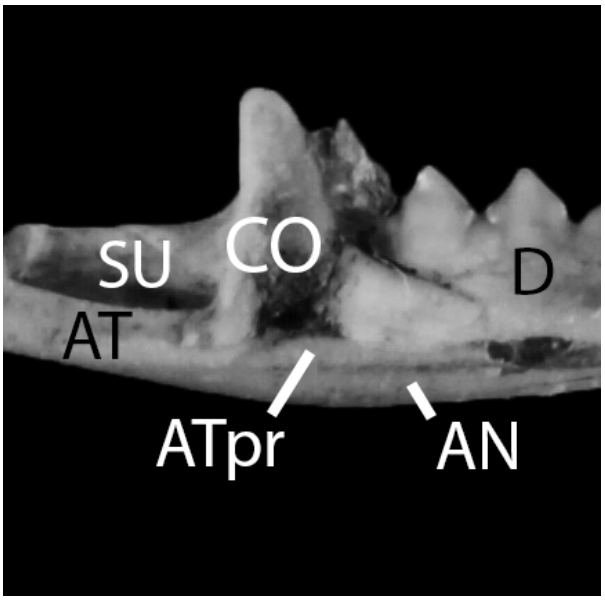

Figure A115. Character 51(1): WAM R165887 *Rankinia adelaidensis*, left lingual view.

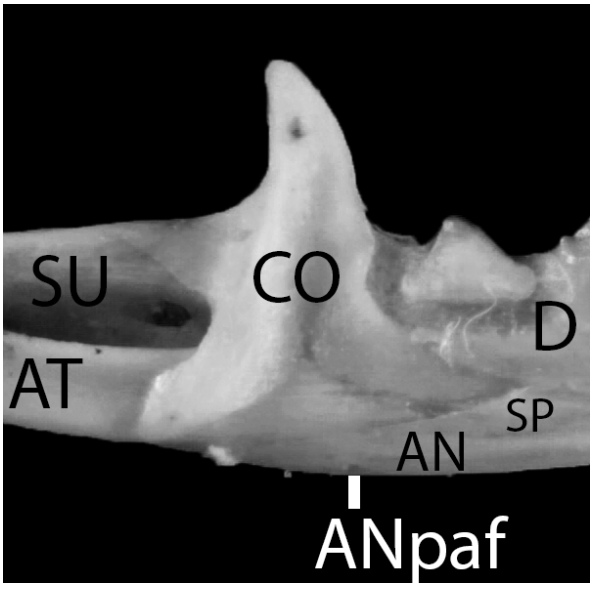

Figure A116. Character 52(0): WAM R162933 *Lophognathus longirostris*, left lingual view.

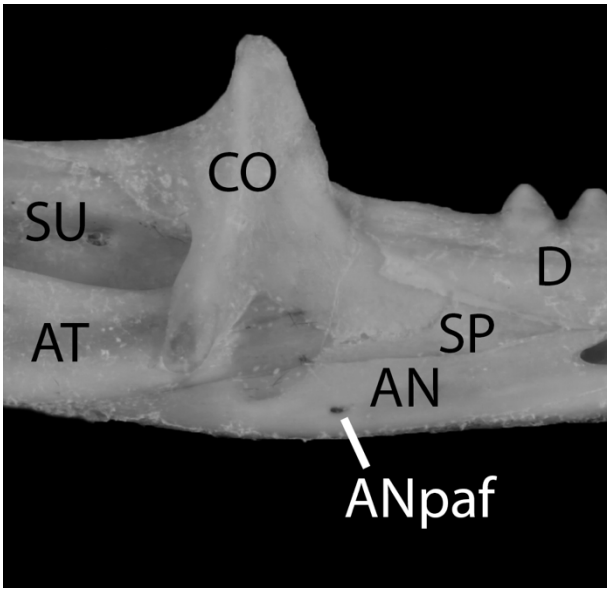

Figure A117. Character 52(1): WAM R112124 *Pogona minor*, left lingual view.

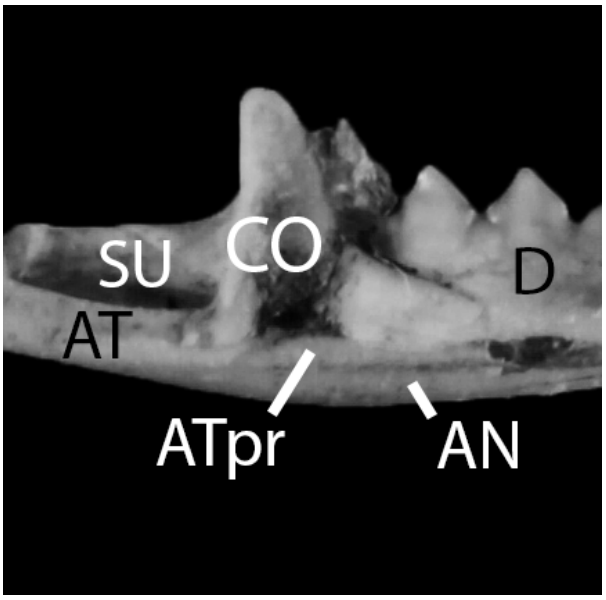

Figure A118. Character 53(0): WAM R165887 *Rankinia adelaidensis*, left lingual view.

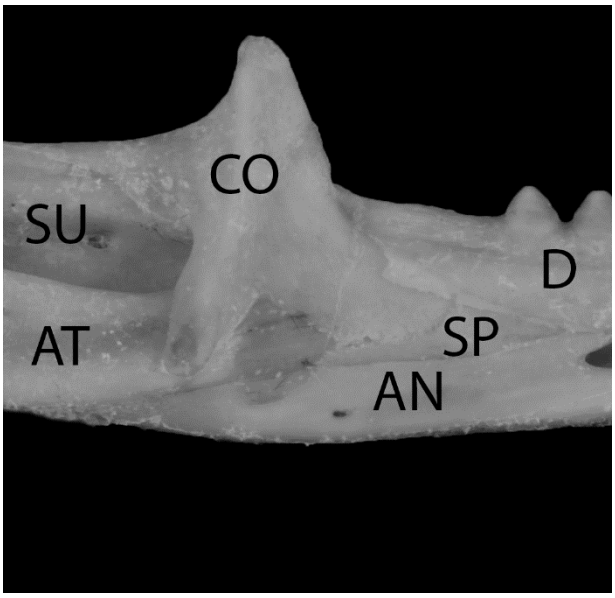

Figure A119. Character 53(1): WAM R112124 *Pogona minor*, left lingual view.

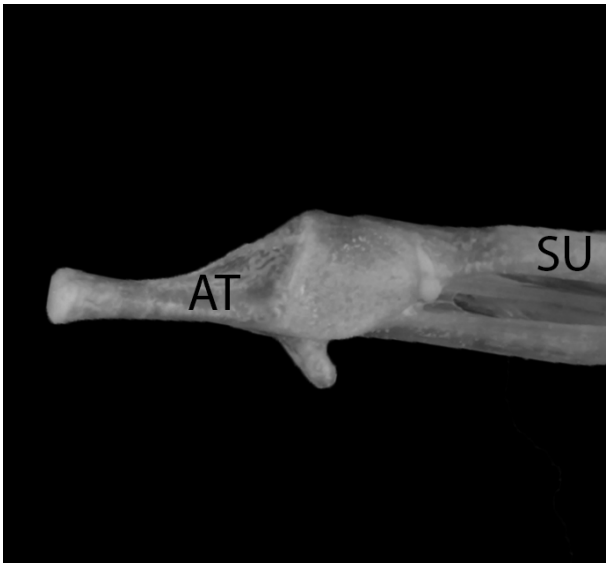

Figure A120. Character 54(0): WAM R167534 *Ctenophorus scutulatus*, left dentary dorsal view.

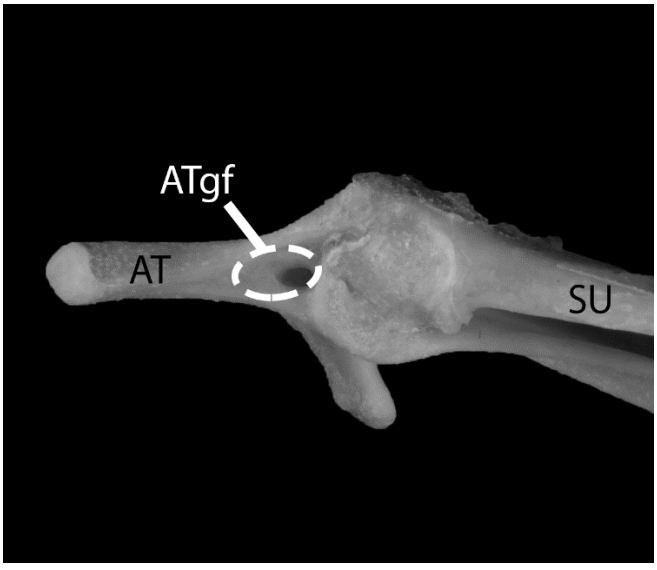

Figure A121. Character 54(1): WAM R112124 *Pogona minor*, left dentary dorsal view.

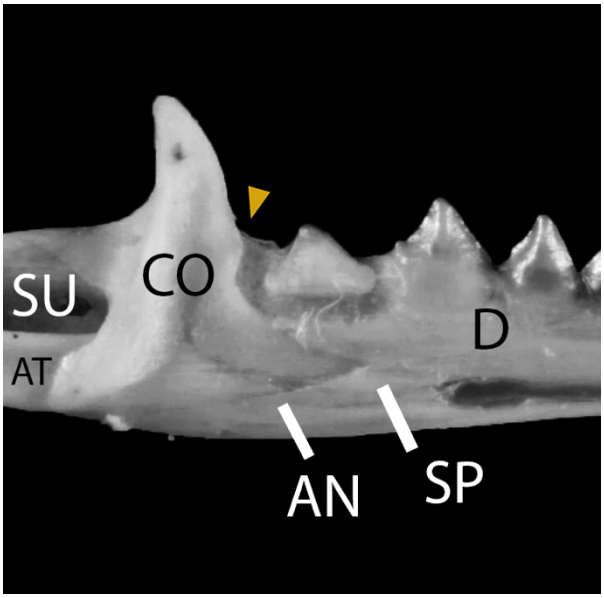

Figure A122. Character 55(0): WAM R162933 *Lophognathus longirostris*, left lingual view.

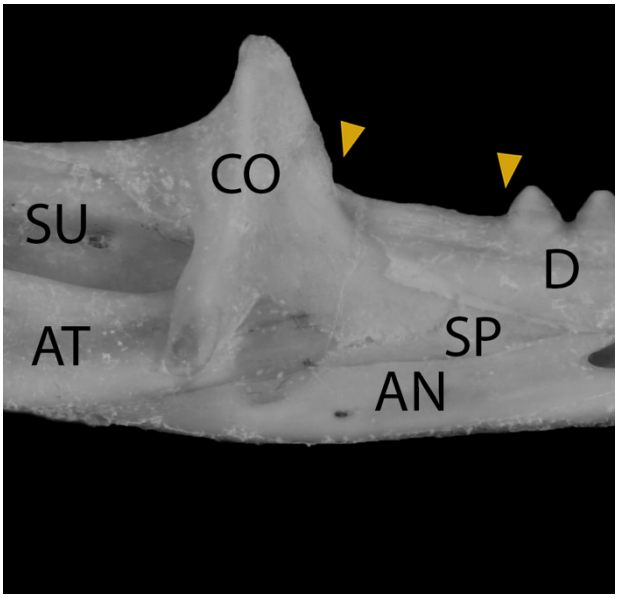

Figure A123. Character 55(1): WAM R112124 *Pogona minor*, left lingual view.

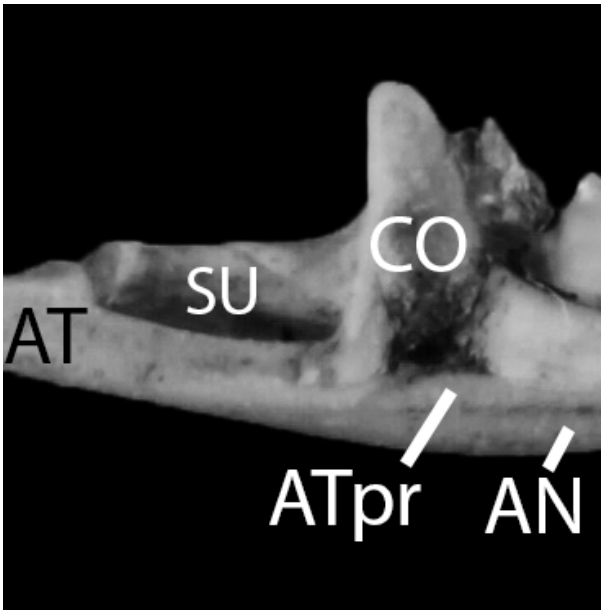

Figure A124. Character 56(0): WAM R165887 *Rankinia adelaidensis*, left lingual view.

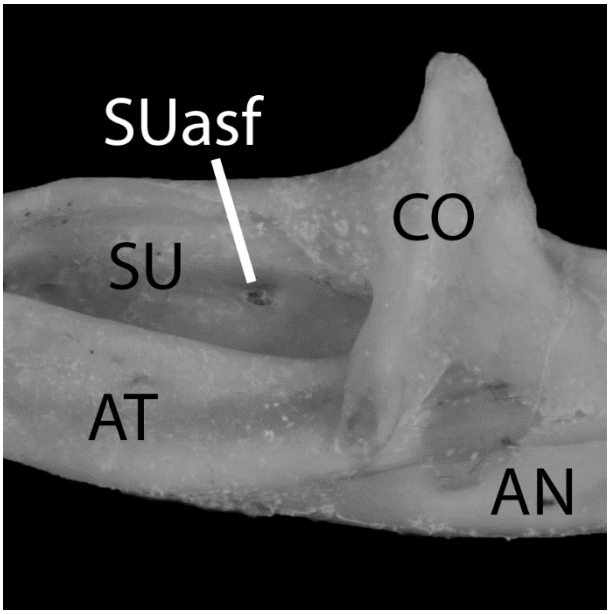

Figure A125. Character 56(1): WAM R112124 *Pogona minor*, left lingual view.

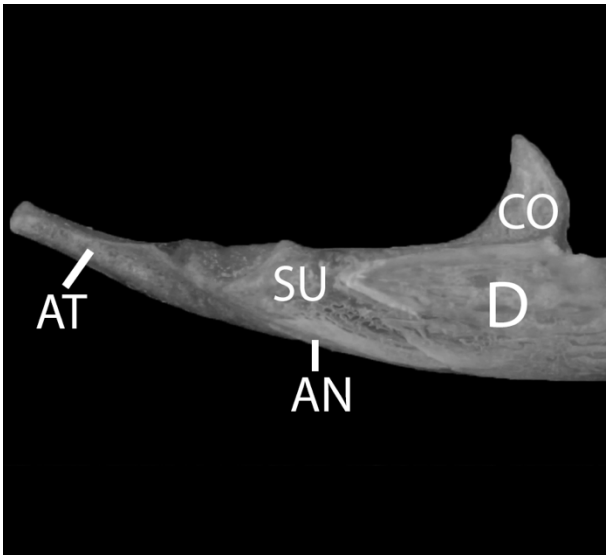

Figure A126. Character 57(0): WAM R167534 *Ctenophorus scutulatus*, right labial view.

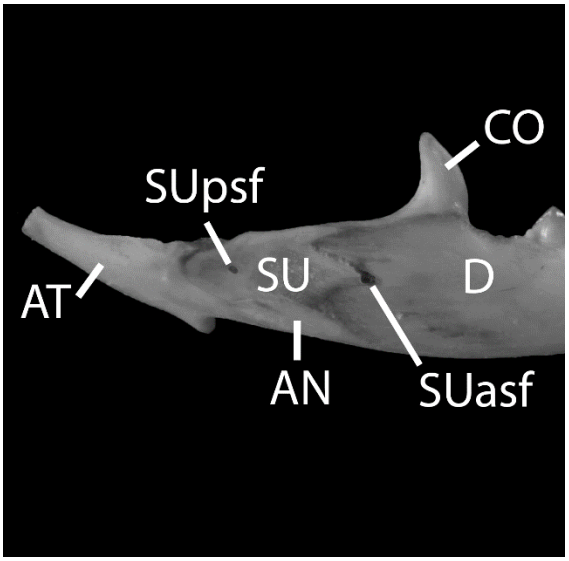

Figure A127. Character 57(1): WAM R162926 *Lophognathus gilberti*, right labial view.

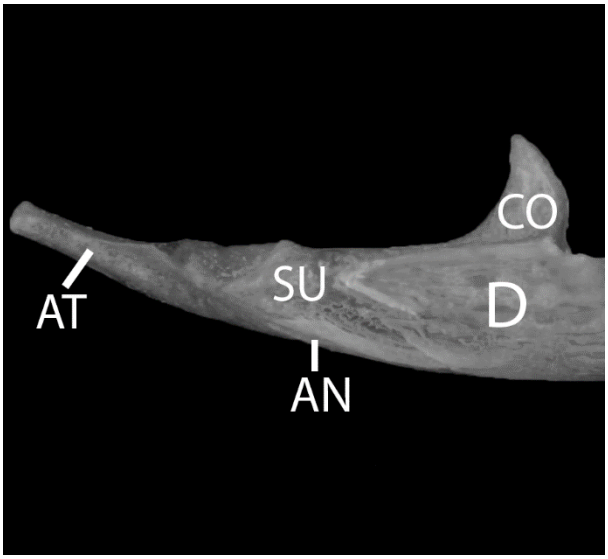

Figure A128. Character 58(0): WAM R167534 *Ctenophorus scutulatus*, right labial view.

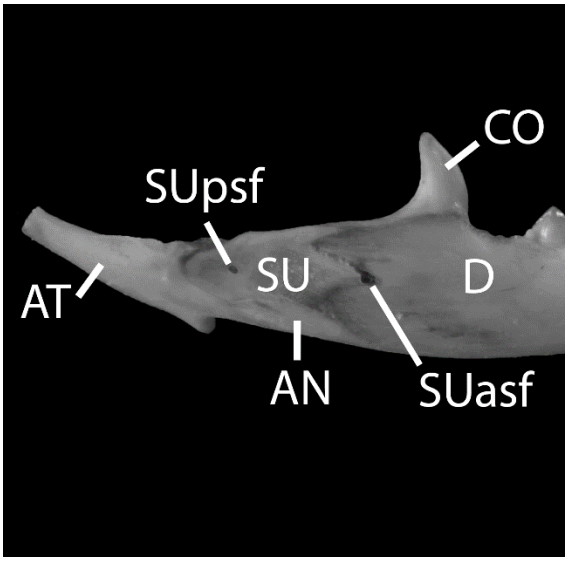

Figure A129. Character 58(1): WAM R162926 *Lophognathus gilberti*, right labial view.

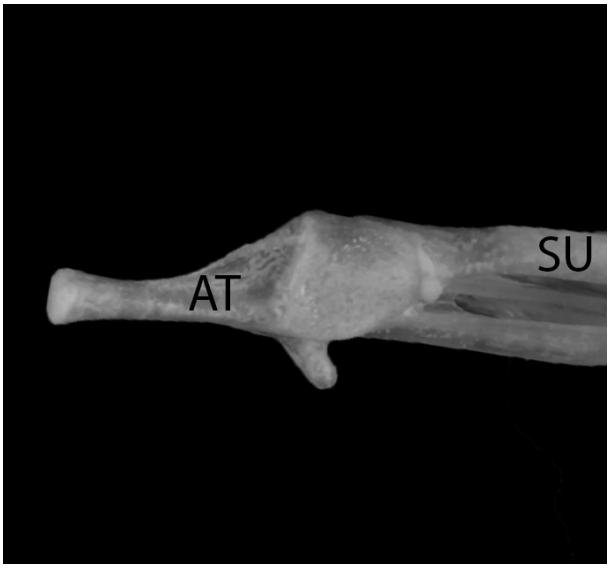

Figure A130. Character 59(0): WAM R167534 *Ctenophorus scutulatus*, left dentary dorsal view.

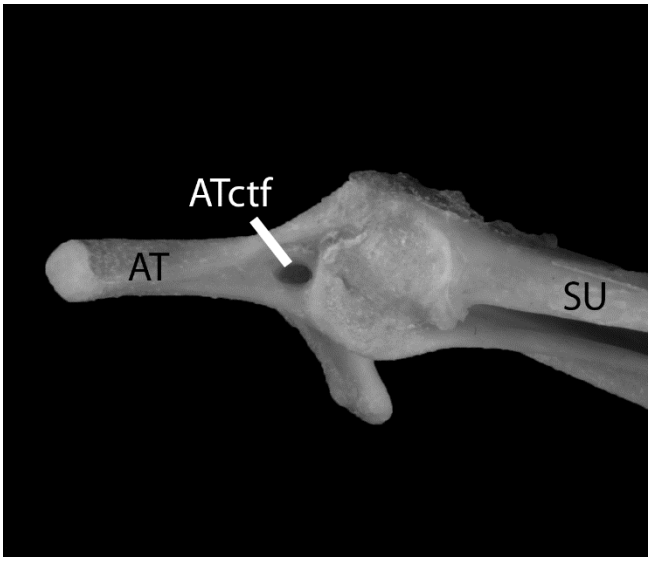

Figure A131. Character 59(1): WAM R112124 *Pogona minor*, left dentary dorsal view.

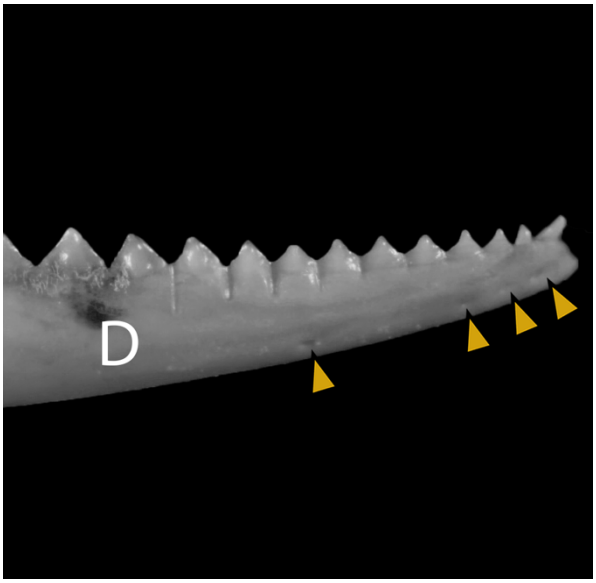

Figure A132. Character 60: WAM R162926 *Lophognathus gilberti*, right labial view.

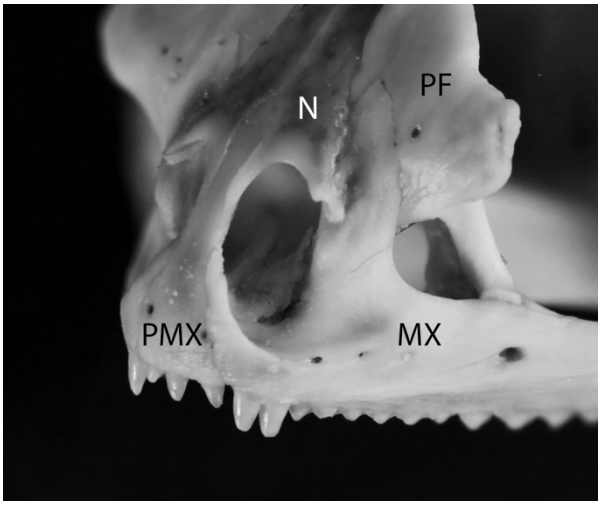

Figure A133. Character 61(0): WAM R162760 *Ctenophorus caudicinctus*, left anterolateral view.

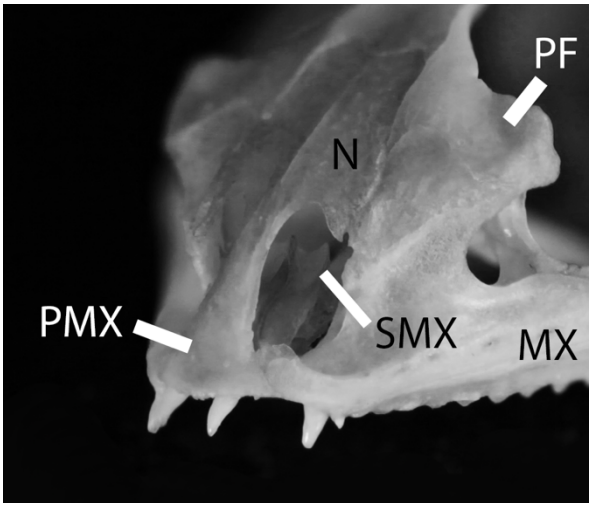

Figure A134. Character 61(1): WAM R111736 *Ctenophorus isolepis*, left anterolateral view.

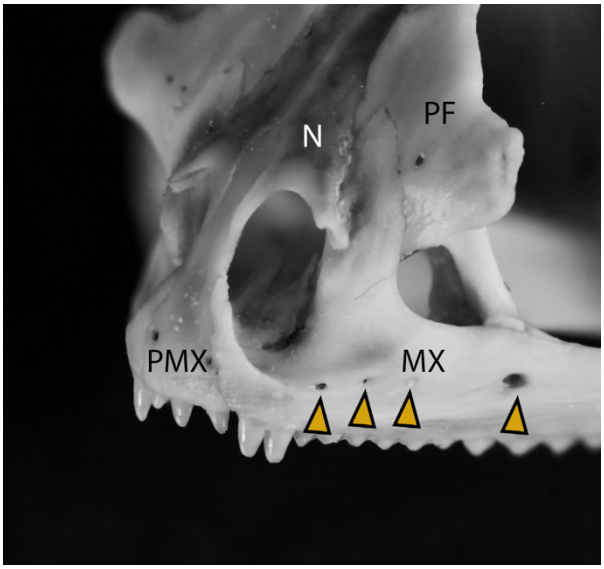

Figure A135. Character 62: WAM R162760 *Ctenophorus caudicinctus*, left anterolateral view.

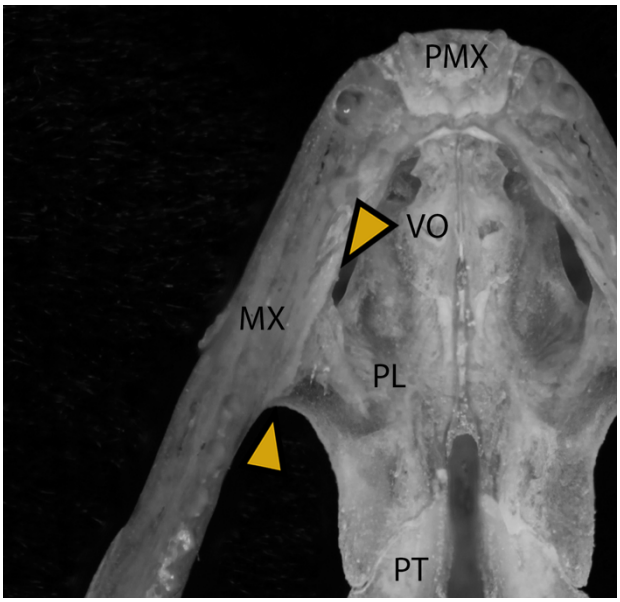

Figure A136. Character 63(0): WAM R165036 *Ctenophorus caudicinctus*, ventral view.

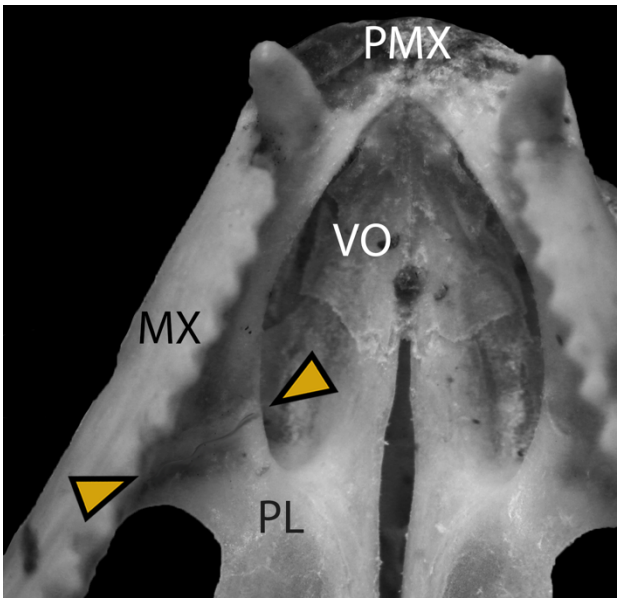

Figure A17. Character 63(1): JIM R1478 *Calotes versicolor*, ventral view.

.

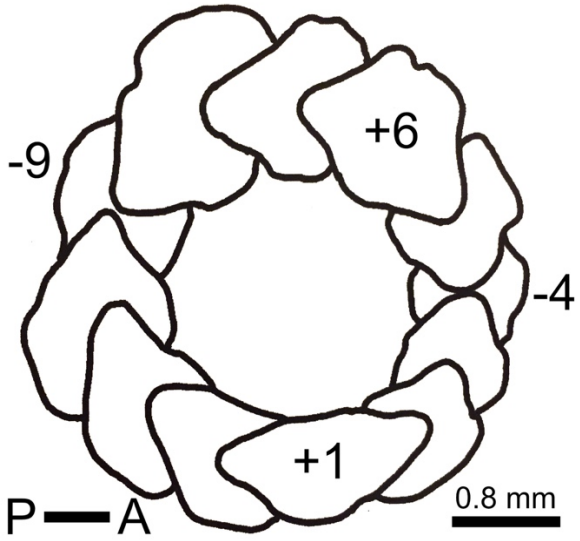

Figure A138. Character 64(0): NT R12804 *Cryptagama aurita*. P = posterior direction, A = anterior direction. Dorsal is toward the top. Lateral view.

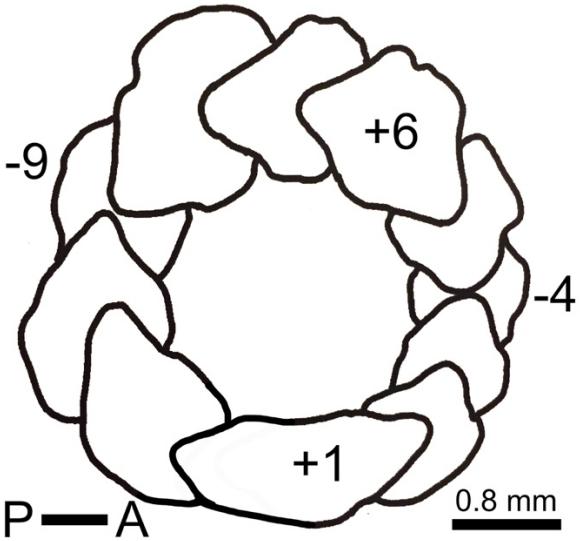

Figure A139. Character 64(1): Modified from NT R12804 *Cryptagama aurita* and based on Moody 1980, Figure 20. P = posterior direction, A = anterior direction. Dorsal is toward the top. Lateral view.

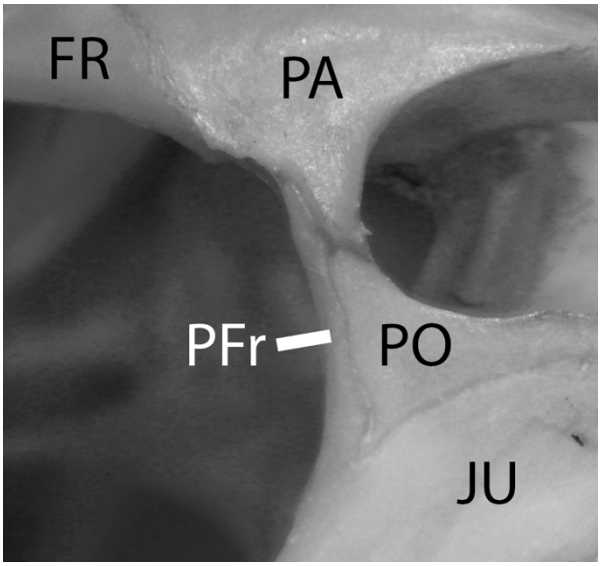

Figure A142. Character 65(0): WAM R8438 *Uromastyx ornatus*, dorsolateral view.

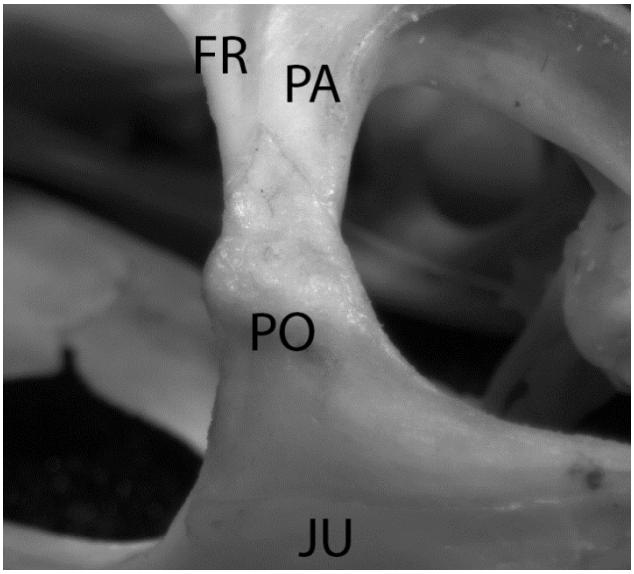

Figure A143. Character 65(1): WAM R112142 *Pogona minor*, dorsolateral view.

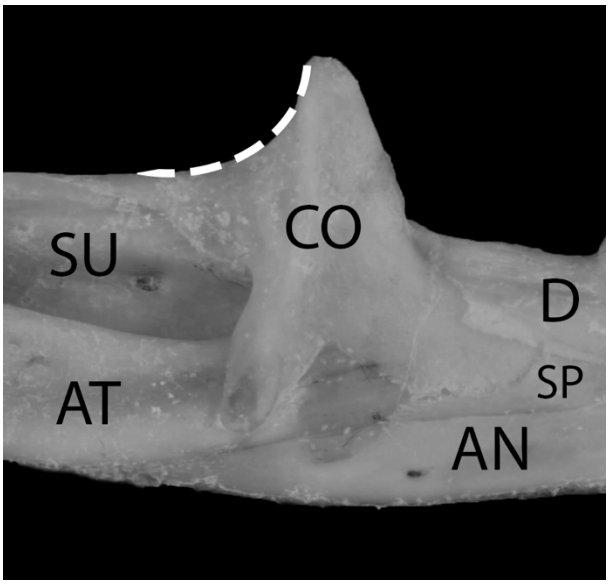

Figure A144. Character 66(0): WAM R112124 *Pogona minor*, left lingual view.

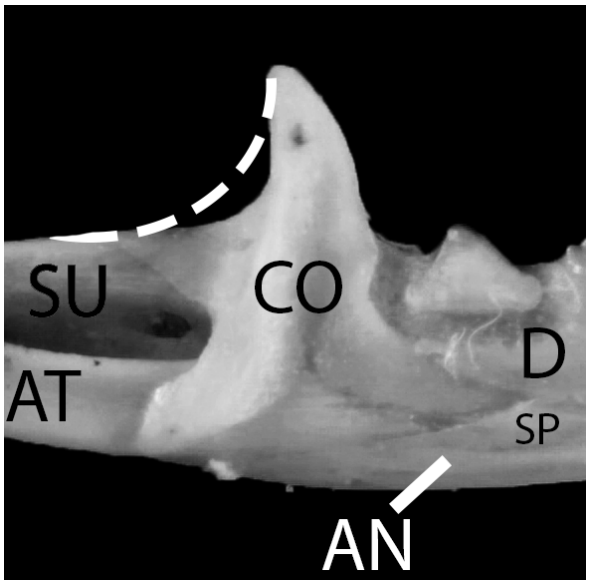

Figure A145. Character 66(1): WAM R162933 *Lophognathus longirostris*, left lingual view.

Appendix B: Complete Dataset of Australian Agamidae Morphological Character Scores

Table A2.1.1 Morphological Characters 1-10

WAM R	Genus	Species	1	2	3	4	5	6	7	8	9	10
111819	*Caimanops*	*amphiboluroides*	1	0	3	0	1	0	8	2	0	2
156705	*Caimanops*	*amphiboluroides*	1	0	2	1	1	0	8	2	0	2
162747	*Caimanops*	*amphiboluroides*	1	0	3	1	1	0	7	2	0	2
162754	*Caimanops*	*amphiboluroides*	1	?	3	?	1	0	7	2	?	2
162803	*Caimanops*	*amphiboluroides*	1	0	3	1	1	0	9	2	1	2
163197	*Chelosania*	*brunnea*	1	0	2	1	1	0	5	0	1	2
41565	*Chelosania*	*brunnea*	1	0	2	1	0	0	12	0	0	2
12100	*Chlamydosaurus*	*kingii*	1	0	4	1	1	0	7	2	0	2
12804	*Cryptagama*	*aurita*	0	0	2	1	0	0	10	0	0	2
64052	*Cryptagama*	*aurita*	1	0	3	1	0	0	4	0	0	2
165887	*Ctenophorus*	*adelaidensis*	1	0	3	1	0	1	8	0	1	2
162820	*Ctenophorus*	*caudicinctus*	1	0	2	1	1	0	5	0	0	1
162819	*Ctenophorus*	*caudicinctus*	1	0	1	1	1	0	3	0	0	2
162822	*Ctenophorus*	*caudicinctus*	1	0	2	1	1	0	6	0	0	2
167625	*Ctenophorus*	*caudicinctus*	0	0	2	1	1	0	3	0	0	2
167626	*Ctenophorus*	*caudicinctus*	1	0	2	1	1	0	3	0	0	2
167673	*Ctenophorus*	*caudicinctus*	0	0	1	1	1	0	10	0	0	2
167676	*Ctenophorus*	*caudicinctus*	1	0	3	1	1	1	6	0	0	2
167679	*Ctenophorus*	*caudicinctus*	1	0	3	1	1	0	3	0	0	2
162887	*Ctenophorus*	*caudicinctus*	1	0	1	1	1	0	12	0	0	2
167665	*Ctenophorus*	*caudicinctus*	1	0	1	1	1	0	13	0	0	2
167667	*Ctenophorus*	*caudicinctus*	1	0	1	1	1	0	11	0	0	2
167670	*Ctenophorus*	*caudicinctus*	1	0	3	1	1	0	8	0	0	2
167672	*Ctenophorus*	*caudicinctus*	1	0	3	1	1	1	9	0	0	2
111747	*Ctenophorus*	*caudicinctus*	1	0	1	1	1	0	12	0	0	2
167632	*Ctenophorus*	*caudicinctus*	1	1	1	1	1	0	12	0	0	2
165036	*Ctenophorus*	*caudicinctus*	1	0	2	1	1	0	11	0	0	2
93130	*Ctenophorus*	*caudicinctus*	1	0	1	1	1	0	11	0	0	2
167652	*Ctenophorus*	*caudicinctus*	1	0	1	1	1	0	8	0	0	2
149167	*Ctenophorus*	*clayi*	1	0	2	1	0	0	7	0	0	2
149201	*Ctenophorus*	*clayi*	1	0	2	1	1	0	7	0	0	2
149371	*Ctenophorus*	*clayi*	1	0	2	1	1	0	5	0	0	2
149425	*Ctenophorus*	*clayi*	1	0	2	1	0	0	5	0	1	2

Table A2.1.2 Morphological Characters 1-10 (continued)

WAM R	Genus	Species	1	2	3	4	5	6	7	8	9	10
149497	*Ctenophorus*	*clayi*	1	0	2	1	1	0	7	0	0	2
156957	*Ctenophorus*	*clayi*	1	0	1	1	1	0	12	0	0	2
162889	*Ctenophorus*	*femoralis*	1	0	1	1	1	0	6	0	0	2
162890	*Ctenophorus*	*femoralis*	1	0	2	1	1	0	6	0	0	2
162891	*Ctenophorus*	*femoralis*	0	0	1	1	0	0	12	0	0	2
162893	*Ctenophorus*	*femoralis*	1	0	2	1	1	0	9	0	0	2
162893	*Ctenophorus*	*femoralis*	1	0	1	1	0	0	9	0	0	2
162898	*Ctenophorus*	*isolepis isolepis*	1	0	2	1	1	0	5	0	0	2
149279	*Ctenophorus*	*isolepis gularis*	1	0	2	1	1	0	10	0	0	2
149444	*Ctenophorus*	*isolepis gularis*	1	0	2	1	1	0	10	2	0	2
149693	*Ctenophorus*	*isolepis gularis*	1	0	4	1	1	0	2	2	0	2
162896	*Ctenophorus*	*isolepis*	1	0	3	1	1	0	5	2	0	2
149094	*Ctenophorus*	*isolepis gularis*	1	0	4	1	1	0	10	2	0	2
149574	*Ctenophorus*	*isolepis gularis*	1	0	4	1	0	0	7	2	0	2
149689	*Ctenophorus*	*isolepis gularis*	1	0	1	1	1	0	9	2	0	2
149710	*Ctenophorus*	*isolepis gularis*	0	0	1	1	1	0	10	2	0	2
149943	*Ctenophorus*	*isolepis gularis*	1	0	0	1	0	0	12	2	0	2
162895	*Ctenophorus*	*isolepis*	1	0	1	1	1	0	5	2	0	2
149179	*Ctenophorus*	*isolepis gularis*	1	0	3	1	1	0	6	2	0	2
149677	*Ctenophorus*	*isolepis gularis*	1	0	5	1	1	0	11	2	0	2
149917	*Ctenophorus*	*isolepis gularis*	1	0	1	1	1	0	11	2	0	2
162894	*Ctenophorus*	*isolepis*	1	0	1	1	1	0	8	2	0	2
111736	*Ctenophorus*	*isolepis*	1	0	1	1	1	0	7	0	0	2
111894	*Ctenophorus*	*isolepis gularis*	1	0	0	1	1	0	12	0	0	2
149161	*Ctenophorus*	*isolepis gularis*	0	0	1	1	1	0	11	2	0	2
111903	*Ctenophorus*	*isolepis isolepis*	0	0	1	1	1	0	12	2	0	2
156956	*Ctenophorus*	*isolepis isolepis*	?	0	2	1	1	1	10	2	0	2
164149	*Ctenophorus*	*maculatus maculatus*	0	0	2	1	1	0	5	0	0	2
167526	*Ctenophorus*	*maculatus badius*	1	0	1	1	1	0	8	0	0	2
167582	*Ctenophorus*	*maculatus badius*	1	0	1	1	1	0	9	0	0	2
164148	*Ctenophorus*	*maculatus maculatus*	1	0	1	1	0	0	11	0	0	2
162817	*Ctenophorus*	*nuchalis*	1	0	3	1	1	1	4	0	1	1
162805	*Ctenophorus*	*nuchalis*	1	0	3	1	0	1	4	1	0	2
111880	*Ctenophorus*	*nuchalis*	0	?	2	1	0	0	5	0	1	2
111905	*Ctenophorus*	*nuchalis*	0	0	2	1	0	0	7	1	0	2
111752	*Ctenophorus*	*nuchalis*	0	0	3	1	1	0	6	0	1	2
156675	*Ctenophorus*	*reticulatus*	0	0	2	1	0	0	7	0	0	2

Table A2.1.3 Morphological Characters 1-10 (continued)

WAM R	Genus	Species	1	2	3	4	5	6	7	8	9	10
111893	*Ctenophorus*	*nuchalis*	1	0	2	1	0	0	5	0	1	1
19288	*Ctenophorus*	*ornatus*	?	?	?	?	?	?	?	?	?	?
165705	*Ctenophorus*	*butleri*	1	0	2	1	0	0	9	0	0	2
162795	*Ctenophorus*	*reticulatus*	1	0	3	1	1	1	5	1	0	1
162744	*Ctenophorus*	*reticulatus*	1	0	3	1	0	1	4	0	0	1
162821	*Ctenophorus*	*reticulatus*	0	0	3	1	1	1	4	0	0	1
162759	*Ctenophorus*	*reticulatus*	1	0	3	1	1	1	4	1	0	1
162779	*Ctenophorus*	*reticulatus*	1	0	2	1	1	0	5	0	0	2
162856	*Ctenophorus*	*reticulatus*	1	0	4	1	1	0	2	1	0	2
162881	*Ctenophorus*	*reticulatus*	1	0	2	1	1	0	5	0	0	2
167575	*Ctenophorus*	*reticulatus*	1	0	2	1	1	0	6	1	0	2
167589	*Ctenophorus*	*reticulatus*	0	0	2	1	0	0	7	1	0	2
167590	*Ctenophorus*	*reticulatus*	0	0	2	1	1	0	7	1	0	2
156678	*Ctenophorus*	*reticulatus*	0	0	1	1	1	0	12	0	0	2
167591	*Ctenophorus*	*reticulatus*	1	0	2	1	0	0	7	1	0	2
167503	*Ctenophorus*	*reticulatus*	1	0	2	1	1	0	9	0	0	2
162855	*Ctenophorus*	*reticulatus*	1	0	2	1	1	0	7	0	0	2
167551	*Ctenophorus*	*reticulatus*	1	0	2	1	1	0	11	1	0	2
167514	*Ctenophorus*	*reticulatus*	0	0	2	1	0	0	11	0	0	2
167563	*Ctenophorus*	*reticulatus*	0	0	3	1	0	1	8	1	0	2
162760	*Ctenophorus*	*reticulatus*	1	0	2	1	0	0	10	1	0	2
162878	*Ctenophorus*	*reticulatus*	1	0	3	1	1	0	6	1	0	2
167567	*Ctenophorus*	*reticulatus*	0	0	2	1	1	0	11	0	0	2
162900	*Ctenophorus*	*rubens*	1	0	1	1	1	0	4	2	0	2
162901	*Ctenophorus*	*rubens*	?	0	1	1	1	0	6	2	0	2
167532	*Ctenophorus*	*scutulatus*	1	0	2	1	1	0	5	0	0	2
167533	*Ctenophorus*	*scutulatus*	1	0	2	1	1	0	7	2	0	2
167529	*Ctenophorus*	*sctutulatus*	1	0	2	1	1	0	11	2	0	2
162906	*Diporiphora*	*bennettii*	1	0	2	1	1	0	9	2	0	2
162905	*Diporiphora*	*bennettii*	1	0	1	1	1	0	7	2	0	2
156958	*Diporiphora*	*winneckei*	1	0	2	1	1	0	9	2	0	2
162928	*Lophognathus*	*gilberti*	1	0	5	0	0	0	13	2	0	2
162926	*Lophognathus*	*gilberti*	1	0	5	1	0	0	13	2	0	2
162929	*Lophognathus*	*gilberti*	1	0	5	1	0	0	13	2	0	2
162927	*Lophognathus*	*gilberti*	1	?	5	?	1	0	13	2	?	2
162930	*Lophognathus*	*gilberti*	1	0	5	0	0	0	12	0	0	2
162932	*Lophognathus*	*longirostris*	1	0	4	1	1	0	8	2	0	2

Table A2.1.4 Morphological Charcters 1-10 (continued)

WAM R	Genus	Species	1	2	3	4	5	6	7	8	9	10
162933	*Lophognathus*	*longirostris*	1	0	5	1	1	0	9	2	0	2
162934	*Lophognathus*	*longirostris*	1	0	5	1	0	0	13	2	0	2
162931	*Lophognathus*	*longirostris*	1	0	5	1	0	0	13	2	0	2
162935	*Lophognathus*	*longirostris*	1	0	5	1	1	0	14	2	0	2
167530	*Lophognathus*	*longirostris*	1	0	5	1	0	0	17	0	0	2
163198	*Moloch*	*horridus*	0	?	5	?	1	0	0	0	?	?
149488	*Moloch*	*horridus*	0	0	2	1	1	0	5	0	0	1
149923	*Moloch*	*horridus*	0	?	3	?	1	0	9	?	?	?
27737B	*Moloch*	*horridus*	0	0	2	1	1	0	9	0	0	1
97222	*Moloch*	*horridus*	0	0	1	1	1	0	7	0	0	1
162857	*?*	*?*	1	?	3	?	1	1	4	?	?	?
167556	*Ctenophorus*	*?*	0	0	2	1	0	0	7	0	0	2
165138	*?*	*?*	1	0	4	1	1	0	9	0	0	2
162802	*?*	*?*	1	0	2	1	0	0	7	1	0	2
164273	*?*	*?*	1	0	2	1	1	0	9	2	0	2
111994	*?*	*?*	1	0	2	1	0	0	11	0	0	2
47842	*Physignathus*	*lesueurii*	1	0	0	0	0	0	4	0	1	2
111733	*Pogona*	*minor*	1	0	2	1	1	0	5	0	0	2
156884	*Pogona*	*minor minima*	1	0	2	1	1	0	12	0	0	2
156920	*Pogona*	*minor*	1	?	3	?	0	1	8	0	?	?
111737	*Pogona*	*minor*	1	0	2	1	1	0	9	0	0	2
162801	*Pogona*	*minor*	1	0	2	1	1	0	9	0	0	2
112142	*Pogona*	*minor*	1	0	2	1	1	0	11	0	0	1

Table A2.2.1 Morphological Characters 11-25

WAM R	11	12	13	14	15	16	17	18	19	20	21	22	23	24	25
111819	2	1	1	0	1	1	1	2	0	0	0	1	1	1	1
156705	1	0	0	1	1	1	1	2	0	0	0	1	1	0	1
162747	1	0	0	0	1	1	0	2	0	0	0	0	1	1	1
162754	1	0	0	0	1	1	0	2	0	0	?	?	?	0	1
162803	2	0	0	0	1	1	1	2	0	0	0	1	1	1	1
163197	2	2	1	0	1	1	1	1	0	1	0	1	2	1	0
41565	2	2	1	0	1	1	1	1	0	0	0	1	1	0	0
12100	2	1	0	0	1	?	1	2	0	0	0	0	0	0	0
12804	1	0	0	0	1	1	0	1	0	0	0	1	1	1	0
64052	0	0	0	0	1	1	0	1	0	1	0	1	1	1	1
165887	2	1	0	0	1	1	0	2	0	1	0	1	1	1	1
162820	2	1	0	0	1	1	0	2	0	0	0	1	1	1	1
162819	2	1	0	0	1	1	0	1	0	0	0	1	1	1	1
162822	2	1	0	1	1	1	0	2	0	?	?	?	?	1	1
167625	2	2	0	0	1	1	0	1	0	0	0	1	1	1	1
167626	2	1	0	0	1	1	0	2	0	1	0	1	1	1	1
167673	2	0	0	0	1	1	0	2	0	0	0	1	1	1	1
167676	1	0	0	0	1	1	0	2	0	0	0	1	1	1	1
167679	1	0	0	0	1	1	0	2	0	1	0	1	1	1	1
162887	2	1	0	0	1	1	0	1	0	0	0	1	1	1	1
167665	2	1	0	0	1	1	0	1	0	0	0	1	1	1	1
167667	2	0	0	0	1	1	1	2	0	0	0	1	1	1	1
167670	2	1	0	0	1	1	0	1	0	1	0	1	1	1	1
167672	2	1	0	0	1	1	1	2	0	0	0	1	1	1	1
111747	1	0	0	?	?	1	1	2	0	1	0	?	?	1	1
167632	2	0	0	0	1	1	1	2	0	0	0	1	1	1	1
165036	2	1	0	0	1	1	1	2	0	0	0	1	1	1	1
93130	2	1	0	1	1	1	1	1	0	1	0	1	1	1	1
167652	1	0	0	0	1	1	1	2	0	1	0	1	1	0	1
149167	2	1	0	0	1	1	0	2	0	0	?	?	?	1	1
149201	1	0	0	0	0	1	0	2	0	0	0	1	1	1	1
149371	1	0	0	0	1	1	0	2	0	0	0	1	1	0	1
149425	1	1	0	0	1	1	0	2	0	0	0	1	1	1	1
149497	1	0	0	0	1	1	0	2	0	0	0	1	1	1	1
156957	2	1	0	0	1	1	0	2	0	1	0	1	1	1	1
162889	2	1	0	0	1	1	0	2	0	0	0	1	1	1	1
162890	1	0	0	0	1	1	0	2	0	0	0	?	?	1	1

Table A2.2.2 Morphologial Characters 11-25 (continued)

WAM R	11	12	13	14	15	16	17	18	19	20	21	22	23	24	25
162891	1	0	0	1	1	1	0	2	0	0	0	1	1	1	1
162893	1	1	0	1	1	1	0	2	0	0	0	1	1	1	1
162893	2	1	0	1	1	1	0	1	0	0	0	1	1	1	1
162898	1	0	0	1	1	1	0	2	0	0	0	1	1	1	1
149279	1	0	0	0	1	1	0	2	0	1	0	1	1	1	1
149444	1	0	0	0	1	1	0	2	0	0	0	1	1	1	1
149693	1	0	0	1	1	1	0	1	0	0	0	1	1	1	1
162896	1	0	0	1	1	1	0	2	0	1	0	1	1	1	1
149094	1	0	0	0	1	1	0	1	0	0	0	1	1	1	1
149574	1	0	0	0	1	1	0	1	0	0	0	1	1	1	1
149689	1	1	0	0	1	1	0	1	0	0	0	1	1	1	1
149710	1	0	0	1	1	1	0	2	0	0	0	1	1	1	1
149943	1	0	0	0	1	1	0	1	0	?	0	1	1	1	1
162895	1	0	0	1	1	1	0	2	0	1	0	1	1	1	1
149179	1	0	0	1	1	1	0	2	0	1	0	1	1	1	0
149677	1	0	0	1	1	1	0	1	0	0	0	1	1	1	1
149917	1	0	0	1	1	1	0	1	0	1	0	1	1	1	1
162894	1	0	0	1	1	1	0	1	0	0	0	1	1	1	1
111736	1	0	0	1	1	1	0	2	0	0	0	1	1	1	1
111894	1	0	0	1	1	1	0	1	0	0	0	1	1	1	1
149161	1	0	0	0	1	1	0	2	0	0	0	1	1	1	1
111903	1	1	0	1	1	1	0	1	0	1	0	1	1	1	1
156956	1	0	0	1	1	1	0	2	0	0	0	1	1	1	1
164149	2	1	0	?	1	1	0	?	?	1	0	1	1	1	1
167526	2	1	0	1	1	1	0	2	0	0	0	1	1	1	1
167582	2	0	0	0	1	1	0	2	?	0	0	1	1	1	1
164148	1	0	0	1	1	1	0	2	0	0	0	1	1	1	1
162817	1	1	0	1	1	1	0	1	0	0	0	1	1	1	1
162805	1	0	0	1	1	1	0	1	0	0	0	1	1	1	1
111880	1	0	0	1	1	1	0	1	0	0	0	1	1	1	1
111905	2	1	0	1	1	1	0	1	0	1	0	1	1	1	0
111752	1	0	0	0	1	1	0	1	0	1	0	1	1	1	0
156675	1	0	0	1	1	1	1	1	0	0	0	1	1	1	1
111893	1	1	0	1	1	1	0	1	0	1	0	1	1	1	1
19288	?	?	?	?	?	?	?	?	?	?	?	?	?	?	?
165705	1	0	0	0	1	1	0	1	0	1	0	1	1	1	1
162795	2	1	0	1	0	1	0	?	0	1	0	1	1	1	1

Table A2.2.3 Morphological Characters 11-25 (continued)

WAM R	11	12	13	14	15	16	17	18	19	20	21	22	23	24	25
162744	2	0	0	1	0	1	0	?	?	?	?	?	?	1	1
162821	2	1	0	0	1	1	0	1	0	1	0	1	1	1	1
162759	2	1	0	1	1	1	0	1	0	?	0	1	1	1	1
162779	2	1	0	1	1	1	0	2	0	0	0	1	1	1	1
162856	2	1	0	0	1	1	?	2	0	1	0	1	1	1	1
162881	2	1	0	1	1	1	0	2	0	1	0	1	1	1	1
167575	1	0	0	1	1	1	?	2	0	1	0	1	1	0	1
167589	2	1	0	1	1	1	0	2	0	1	0	1	1	1	1
167590	2	0	0	1	1	1	0	1	0	1	0	1	1	1	1
156678	1	0	0	1	1	1	0	2	0	1	0	1	1	1	1
167591	1	0	0	1	1	1	0	1	0	1	0	1	1	0	1
167503	2	1	0	1	1	1	?	1	0	1	0	1	1	1	1
162855	2	1	0	1	1	1	1	2	0	0	0	1	1	1	1
167551	2	1	0	1	1	1	1	2	0	1	0	1	1	1	1
167514	2	1	0	1	1	1	0	1	0	1	0	1	1	1	1
167563	2	2	1	1	1	1	1	0	1	1	0	1	1	0	1
162760	2	1	0	1	1	1	1	1	0	1	0	1	1	1	1
162878	2	1	0	1	1	1	1	1	0	1	0	1	1	0	1
167567	1	0	0	1	1	1	1	2	0	1	0	1	1	0	1
162900	1	0	0	1	1	1	0	1	0	1	0	1	1	0	1
162901	1	0	0	0	1	1	0	?	0	0	0	1	1	1	1
167532	1	1	0	1	1	1	0	1	0	0	0	1	1	1	1
167533	2	2	0	1	1	1	0	1	0	1	0	1	1	1	1
167529	2	2	0	1	1	1	0	1	0	0	0	1	1	1	1
162906	2	1	0	1	1	1	0	1	0	0	0	1	1	1	1
162905	2	1	0	1	1	1	1	1	0	0	0	1	1	1	1
156958	2	1	0	0	1	1	?	1	0	0	0	1	1	1	1
162928	1	0	0	1	1	1	0	2	0	0	0	1	1	1	1
162926	1	0	0	0	1	1	0	2	0	0	0	1	1	1	1
162929	2	1	0	1	1	1	1	2	0	1	0	0	0	1	1
162927	?	?	0	?	?	1	0	2	0	?	?	?	?	1	1
162930	1	0	0	1	1	1	0	2	0	1	0	1	1	1	1
162932	1	0	0	0	1	1	0	1	0	1	0	1	1	1	1
162933	1	1	0	0	1	1	0	1	0	0	0	1	1	1	1
162934	1	0	0	0	1	1	1	1	0	0	0	0	0	1	1
162931	1	0	0	0	1	1	1	1	0	0	0	?	?	1	1
162935	1	0	0	0	1	1	1	1	0	0	0	?	?	1	1

Table A2.2.4 Morphological Characters 11-25 contined

WAM R	11	12	13	14	15	16	17	18	19	20	21	22	23	24	25
167530	2	2	0	1	1	1	1	1	0	1	0	1	1	0	0
163198	1	0	0	0	1	1	1	?	?	0	0	?	?	?	?
149488	1	0	0	0	1	1	1	?	?	0	0	0	0	1	0
149923	1	0	0	0	1	1	1	?	?	?	0	1	1	?	0
27737B	1	0	0	0	1	1	0	?	?	0	0	1	1	1	0
97222	1	0	0	0	1	1	1	?	?	?	?	?	?	1	0
162857	2	1	0	0	?	?	0	2	0	?	0	1	1	1	1
167556	2	1	0	1	1	1	0	2	0	0	0	1	1	0	1
165138	1	1	0	0	1	1	1	1	0	0	0	1	1	1	1
162802	2	1	0	1	1	1	0	2	0	0	0	1	2	0	1
164273	2	1	0	1	1	1	0	2	0	0	0	1	2	1	1
111994	2	1	0	1	1	1	1	2	0	1	0	1	1	1	1
47842	2	0	0	0	1	1	1	1	0	1	0	0	0	1	0
111733	2	1	0	?	?	1	0	2	0	?	?	?	?	?	?
156884	2	1	0	1	1	1	1	2	0	1	0	1	1	1	1
156920	2	1	0	1	1	1	?	1	0	1	0	1	1	?	?
111737	2	1	0	1	1	1	1	1	2	0	0	1	1	1	1
162801	2	1	0	1	1	1	1	1	0	1	0	1	1	1	1
112142	1	1	0	1	1	1	1	1	0	1	0	1	1	1	1

Table A2.3.1 Morphological Characters 25-40

WAM R	26	27	28	29	30	31	32	33	34	35	36	37	38	39	40
111819	2	1	0	0	0	1	?	?	0	1	1	1	1	1	0
156705	2	1	1	0	0	1	1	0	1	0	1	1	1	2	0
162747	2	1	1	0	0	1	1	0	0	1	1	1	1	2	1
162754	?	1	0	0	0	1	?	?	?	?	?	?	?	?	?
162803	2	1	1	1	0	1	1	1	0	1	1	1	1	1	0
163197	2	1	1	1	1	1	1	0	0	1	0	1	1	2	0
41565	2	1	1	0	1	1	1	1	0	0	0	1	1	2	2
12100	2	1	1	1	1	1	0	0	2	0	1	1	1	2	0
12804	2	1	0	1	0	1	1	0	1	0	1	1	1	1	2
64052	2	0	0	1	0	1	1	1	1	0	0	1	0	1	2
165887	2	1	1	1	0	1	1	?	1	0	1	1	1	0	1
162820	2	1	1	1	0	1	?	?	1	1	1	1	1	1	2
162819	2	1	1	1	0	1	1	?	0	1	1	1	1	1	2
162822	2	1	1	1	0	1	1	?	0	1	1	1	?	?	2
167625	2	?	1	1	0	1	1	?	0	1	1	1	1	1	2
167626	2	1	1	1	0	1	1	?	0	1	1	1	1	1	2
167673	2	1	1	1	0	1	1	0	1	1	1	1	1	?	1
167676	2	1	1	1	0	1	1	0	0	1	1	1	1	1	2
167679	2	1	1	1	0	1	1	0	0	1	1	1	1	1	2
162887	2	1	1	1	0	1	1	0	0	1	1	1	1	1	2
167665	2	1	1	0	0	1	0	0	0	1	1	1	1	1	2
167667	2	1	1	1	0	1	1	0	1	1	1	1	1	1	2
167670	2	1	1	1	0	1	0	0	1	1	1	1	1	1	2
167672	2	1	1	1	0	0	1	?	0	1	1	1	1	2	1
111747	2	1	1	1	0	1	?	?	?	1	?	1	1	?	?
167632	2	1	1	0	0	1	0	?	0	1	0	1	1	1	1
165036	2	1	1	0	1	1	0	1	0	1	0	1	1	2	1
93130	2	?	1	1	0	1	0	0	0	1	1	1	1	2	1
167652	2	1	1	1	0	1	0	1	0	1	1	1	1	2	1
149167	2	1	1	1	0	1	1	0	?	1	?	?	?	?	2
149201	2	1	1	0	0	1	0	1	1	1	1	1	1	0	2
149371	2	1	0	1	0	1	1	0	1	1	1	1	0	0	2
149425	2	1	1	1	1	0	0		1	1	1	1	0	0	2
149497	2	1	1	1	0	1	1	0	1	1	1	1	1	0	2
156957	2	1	1	1	0	1	1	0	1	1	1	1	1	1	2
162889	2	1	0	0	0	1	?	?	?	1	?	1	1	0	1
162890	2	1	0	1	0	1	?	?	1	1	1	1	0	0	2

Table A2.3.2 Morphological Characters 25-40 (continued)

WAM R	26	27	28	29	30	31	32	33	34	35	36	37	38	39	40
162891	2	1	1	0	0	1	0	1	1	1	1	1	1	1	2
162893	2	1	0	0	0	1	0	1	1	1	1	1	1	1	2
162893	2	1	1	0	0	1	0	1	1	1	1	1	1	1	2
162898	2	1	0	0	0	1	1	1	1	1	1	1	1	1	2
149279	2	1	0	0	1	1	0	0	0	1	1	1	1	1	1
149444	2	1	0	0	1	1	0	1	0	1	1	1	1	1	1
149693	2	?	0	0	1	1	1	1	0	1	1	1	1	1	1
162896	2	1	0	0	1	1	0	0	1	1	1	1	1	1	2
149094	2	1	0	0	1	1	0	1	0	0	1	1	1	1	1
149574	2	1	0	0	1	1	?	?	0	1	1	1	1	1	2
149689	2	?	0	0	1	1	0	1	0	1	1	1	1	1	1
149710	2	?	1	0	1	1	0	0	1	1	1	1	1	1	2
149943	2	1	0	0	1	1	0	0	0	1	1	1	1	?	1
162895	2	1	0	1	0	1	1	0	0	1	1	1	1	1	2
149179	2	1	0	0	0	1	0	1	1	0	0	1	1	1	1
149677	2	1	0	0	1	1	1	0	0	1	1	1	1	1	1
149917	2	1	0	0	1	1	0	1	0	1	1	1	1	1	2
162894	2	1	0	0	1	1	0	1	1	1	1	1	1	1	1
111736	2	1	0	0	1	1	1	1	0	1	1	1	1	2	1
111894	2	1	1	0	1	1	0	1	0	1	1	1	1	2	2
149161	2	1	0	0	1	1	0	1	0	1	1	1	1	1	1
111903	2	1	0	0	1	1	?	1	0	1	1	1	1	?	?
156956	2	1	0	0	1	1	0	0	0	1	1	1	1	?	1
164149	2	1	1	0	0	1	1	0	?	1	?	1	1	0	?
167526	2	1	1	0	0	1	1	0	1	1	1	1	1	0	1
167582	2	1	0	0	0	1	0	0	1	1	1	?	?	?	1
164148	2	1	1	0	0	1	0	0	1	1	1	1	1	0	2
162817	2	1	0	1	0	1	?	?	1	1	1	?	0	0	2
162805	2	1	0	1	0	1	1	0	1	1	1	1	1	1	1
111880	2	1	0	1	0	1	0	0	0	1	0	1	1	2	2
111905	2	1	0	1	0	1	1	0	0	1	1	1	1	2	1
111752	2	1	0	1	0	1	1	0	0	1	0	1	1	1	1
156675	2	1	0	1	0	1	1	0	0	1	0	1	1	2	1
111893	2	1	0	1	0	1	1	0	0	1	0	1	1	2	1
19288	?	?	?	?	?	?	?	?	?	?	?	?	?	?	?
165705	2	1	1	0	0	1	0	1	2	1	1	1	1	2	0
162795	2	1	0	1	0	1	?	?	1	1	1	1	0	0	2

Table A2.3.3 Morphological Characters 25-40 (continued)

WAM R	26	27	28	29	30	31	32	33	34	35	36	37	38	39	40
162744	2	1	1	1	0	1	?	?	1	1	1	1	?	?	2
162821	2	1	1	1	0	1	?	?	?	1	?	1	0	0	2
162759	2	1	1	1	0	1	1	0	1	1	1	1	1	?	2
162779	2	1	1	1	0	1	1	?	1	1	1	1	1	0	2
162856	2	1	1	1	0	1	?	0	1	1	1	1	1	0	2
162881	2	1	1	1	0	1	1	0	1	1	1	1	1	0	1
167575	2	1	1	1	0	1	0	?	1	1	1	1	1	2	0
167589	2	1	1	1	0	1	1	0	1	1	1	1	1	1	1
167590	2	1	0	1	0	1	1	0	0	1	0	1	1	2	1
156678	2	1	1	1	0	1	0	0	1	1	1	1	1	1	1
167591	2	1	1	1	0	1	1	0	1	0	1	1	1	2	2
167503	2	1	1	0	0	1	0	0	1	1	0	1	1	1	1
162855	2	1	1	1	0	1	0	1	1	1	1	1	1	1	1
167551	2	1	1	1	0	1	1	0	1	0	1	1	1	1	1
167514	2	1	1	1	0	1	0	?	1	1	1	1	1	2	1
167563	2	1	1	1	0	1	1	0	1	0	1	1	1	2	1
162760	2	1	1	0	0	1	1	0	1	0	1	1	1	2	1
162878	2	1	1	1	0	1	1	0	1	0	1	1	1	2	1
167567	2	1	1	1	0	1	1	1	0	0	1	1	1	2	1
162900	2	?	1	1	0	1	1	0	1	1	1	1	1	0	1
162901	2	1	0	1	0	1	0	0	1	1	1	1	?	?	1
167532	2	1	1	0	0	1	1	1	1	1	1	1	1	1	1
167533	2	1	1	0	0	1	1	1	1	1	1	1	1	1	1
167529	2	0	1	1	0	1	0	0	1	1	1	1	1	2	0
162906	2	?	1	1	0	1	1	1	1	1	1	1	1	1	2
162905	2	?	1	0	0	1	1	?	1	1	1	1	1	1	1
156958	2	1	1	1	0	1	0	0	1	1	1	1	1	2	2
162928	2	1	1	0	1	1	1	1	?	1	?	1	1	1	1
162926	2	1	1	0	1	1	1	0	0	0	1	1	1	2	1
162929	2	1	1	0	1	1	1	0	0	0	1	1	1	2	2
162927	?	1	1	?	?	?	?	?	?	?	?	?	?	?	?
162930	2	1	1	0	1	1	1	?	0	1	1	1	1	1	2
162932	2	1	1	0	1	1	1	1	1	1	1	1	1	1	1
162933	2	1	1	0	1	1	1	1	0	1	1	1	1	1	2
162934	2	1	1	0	1	1	1	1	1	1	1	1	1	1	2
162931	2	1	1	0	1	1	1	1	0	1	1	1	1	1	1
162935	2	1	1	0	1	1	1	0	1	1	1	1	1	1	1

Table A2.3.4 Morphological Characters 25-40 (continued)

WAM R	26	27	28	29	30	31	32	33	34	35	36	37	38	39	40
167530	2	1	1	0	1	1	1	1	0	0	1	1	1	2	1
163198	0		?	0	1	1	0	0	1	1	1	?	?	?	?
149488	1	1	0	1	1	1	0	?	1	2	1	1	1	2	1
149923	0	1	?	0	1	1	0	0	1	1	1	?	1	1	1
27737B	1	?	0	0	1	1	0	?	1	1	1	1	1	1	1
97222	?	?	0	1	0	1	?	?	?	?	?	?	?	?	1
162857	2	1	1	?	?	1	?	?	1	1	1	1	0	1	2
167556	2	1	1	1	1	1	1	1	1	1	1	1	1	1	1
165138	2	1	1	1	0	1	1	1	2	1	2	1	1	2	2
162802	2	1	1	1	0	1	1	?	0	1	0	1	1	2	1
164273	2	1	1	1	0	1	0	?	1	1	1	1	1	2	2
111994	2	1	1	1	0	1	1	?	0	0	0	1	1	2	1
47842	1	1	1	0	1	1	0	1	1	0	1	1	1	2	0
111733	?	?	?	?	?	?	?	?	?	?	?	?	?	?	?
156884	2	1	1	0	1	1	1	0	0	1	0	1	1	1	1
156920	2	?	?	1	0	1	1	1	1	0	1	1	1	1	1
111737	2	1	1	0	0	1	1	0	0	1	0	1	1	2	1
162801	2	1	1	0	1	1	1	0	0	1	0	1	1	2	1
112142	2	1	1	0	1	1	1	0	0	0	0	1	1	2	0

Table A2.4.1 Morphological Characters 41-55

WAM R	41	42	43	44	45	46	47	48	49	50	51	52	53	54	55
111819	1	0	0	1	1	1	0	1	0	0	1	1	1	1	0
156705	1	0	0	1	1	0	0	1	0	0	1	1	1	1	0
162747	1	0	0	1	1	1	0	1	0	0	1	1	1	1	1
162754	1	0	0	0	1	1	0	1	0	0	1	0	1	1	0
162803	1	0	0	1	1	1	0	1	0	0	1	1	1	1	0
163197	1	0	0	0	0	0	0	1	0	1	1	1	1	1	1
41565	1	0	0	0	1	0	0	1	0	0	1	1	1	1	1
12100	1	0	0	1	0	1	0	1	0	0	0	2	1	1	1
12804	1	0	0	1	0	0	0	1	0	0	1	1	1	1	0
64052	1	0	0	1	0	0	0	1	0	0	0	1	1	1	0
165887	1	0	1	1	1	1	0	1	0	0	0	0	1	1	0
162820	1	0	0	1	0	1	0	1	0	0	0	0	1	1	0
162819	1	0	0	1	1	1	0	1	0	0	0	1	1	1	0
162822	1	0	0	0	0	1	0	1	0	0	?	1	1	?	0
167625	1	0	0	0	1	1	0	1	0	0	0	0	1	1	0
167626	1	0	0	1	1	1	0	1	0	1	0	0	1	1	0
167673	1	0	0	0	0	0	0	1	0	0	0	0	1	1	0
167676	1	0	0	1	0	0	0	1	0	1	0	?	1	1	0
167679	1	0	0	1	1	0	0	1	0	0	0	0	1	1	0
162887	1	0	0	0	1	0	0	1	0	1	0	1	1	1	0
167665	1	0	0	1	1	0	0	1	0	1	0	0	1	1	0
167667	1	0	0	0	1	0	0	1	0	1	0	1	1	1	0
167670	1	0	0	1	1	0	0	1	0	1	0	0	1	1	1
167672	1	0	0	0	1	0	0	1	0	1	0	1	1	1	1
111747	1	0	0	1	1	0	0	1	0	1	0	1	1	1	1
167632	1	0	0	1	1	0	0	1	0	1	0	1	1	1	1
165036	1	0	0	0	1	0	0	1	0	1	0	1	1	1	1
93130	1	0	0	1	1	0	0	1	0	1	0	1	1	1	1
167652	1	0	0	1	1	0	0	1	0	1	0	1	1	1	1
149167	1	0	0	0	0	1	0	1	0	0	0	0	1	1	0
149201	1	0	0	1	1	0	0	1	0	0	1	0	1	1	0
149371	1	0	0	1	1	1	0	1	0	0	0	0	1	1	0
149425	1	0	0	1	1	1	0	1	0	0	1	1	1	1	0
149497	1	0	0	1	1	0	0	1	0	0	1	0	1	1	0
156957	1	0	0	1	0	0	0	1	0	0	0	1	1	1	0
162889	?	?	0	0	1	1	0	1	0	1	1	0	1	1	0
162890	?	?	0	0	0	1	0	1	0	0	0	0	1	1	0

Table A2.4.2 Morphological Characters 41-55 (continued)

WAM R	41	42	43	44	45	46	47	48	49	50	51	52	53	54	55
162891	1	0	0	0	0	1	0	1	0	1	0	0	1	1	0
162893	1	0	0	0	1	0	0	1	0	1	1	0	1	1	0
162893	1	0	0	0	0	1	0	1	0	1	1	0	1	1	0
162898	1	0	0	0	0	0	0	1	0	1	0	0	1	1	0
149279	1	0	0	0	0	0	0	1	0	0	0	1	1	1	0
149444	1	0	0	1	0	1	0	1	0	1	0	0	1	1	0
149693	1	0	0	1	0	1	0	1	0	0	0	0	1	1	0
162896	1	0	0	0	1	1	0	1	0	1	1	1	1	1	0
149094	1	0	0	1	0	1	0	1	0	0	1	0	1	1	0
149574	1	0	0	1	0	0	0	1	0	0	0	0	1	1	0
149689	1	0	0	1	0	1	0	1	0	0	1	0	1	1	0
149710	1	0	0	1	0	1	0	1	0	0	1	0	1	1	0
149943	1	0	0	1	0	0	0	1	0	0	0	0	1	1	0
162895	1	0	0	1	0	0	0	1	0	0	0	0	1	1	0
149179	1	0	0	1	0	0	0	1	0	1	0	0	1	1	0
149677	1	0	0	0	0	0	0	1	0	0	0	1	1	1	0
149917	1	0	0	1	0	0	0	1	0	0	1	0	1	1	0
162894	1	0	0	0	0	0	0	1	0	1	1	1	1	1	0
111736	1	0	0	0	0	0	0	1	0	0	1	1	1	1	1
111894	1	0	0	0	0	0	0	1	0	0	1	1	1	1	1
149161	1	0	0	1	0	0	0	1	0	1	0	0	1	1	1
111903	1	0	0	0	1	0	0	1	0	0	1	1	1	1	1
156956	1	0	0	0	0	0	0	1	0	1	0	1	1	1	1
164149	1	0	0	0	0	1	0	1	0	?	0	1	1	1	?
167526	1	0	0	1	1	0	0	1	0	1	1	0	1	1	0
167582	1	0	0	0	1	0	0	1	0	0	1	0	1	1	?
164148	1	0	0	0	1	1	0	1	0	0	0	0	0	1	1
162817	1	0	0	0	1	?	0	1	0	1	0	1	1	1	0
162805	1	0	0	0	1	0	0	1	0	1	0	1	1	1	0
111880	1	0	0	0	1	1	0	1	0	1	1	1	1	1	0
111905	1	0	0	0	1	1	0	1	0	0	0	1	1	1	0
111752	1	0	0	0	1	1	0	1	0	0	1	1	1	1	1
156675	1	0	0	0	1	1	0	1	0	0	1	1	1	1	0
111893	1	0	0	0	1	1	0	1	0	1	0	1	1	1	0
19288	?	?	?	?	?	?	?	1	?	?	?	?	?	1	?
165705	1	0	0	1	0	1	0	1	0	0	0	1	0	1	1
162795	1	0	0	0	0	1	0	1	0	1	?	0	?	?	0

Table A2.4.3 Morphological Characters 41-55 (continued)

WAM R	41	42	43	44	45	46	47	48	49	50	51	52	53	54	55
162744	1	0	0	0	1	0	0	1	0	1	0	1	1	?	?
162821	1	0	0	0	0	?	1	1	0	1	0	0	1	1	0
162759	1	0	0	0	1	0	0	1	0	1	0	1	1	1	0
162779	1	0	0	0	1	0	0	1	0	1	0	0	1	1	0
162856	1	0	0	0	1	1	0	1	0	1	0	0	1	1	0
162881	1	0	0	1	1	1	0	1	0	1	1	1	1	1	0
167575	1	0	0	1	1	0	0	1	0	1	0	1	1	1	0
167589	1	0	0	1	1	0	0	1	0	1	0	1	1	1	0
167590	1	0	0	0	1	1	0	1	0	1	0	1	1	1	1
156678	1	0	0	1	1	0	0	1	0	1	0	0	1	1	0
167591	1	0	0	1	1	0	0	1	0	1	0	0	1	1	0
167503	1	0	0	1	1	0	0	1	0	1	0	1	1	1	0
162855	1	0	0	0	1	0	0	1	0	1	0	1	1	1	0
167551	1	0	0	1	1	0	0	1	0	1	0	1	1	1	1
167514	1	0	0	1	1	1	0	1	0	1	0	0	1	1	1
167563	1	0	0	1	0	1	0	1	0	1	0	1	1	1	1
162760	1	0	0	0	1	0	0	1	0	1	0	1	1	1	1
162878	1	0	0	0	1	0	0	1	0	1	0	1	1	1	1
167567	1	0	0	0	1	0	0	1	0	1	0	1	0	1	1
162900	1	0	0	0	1	1	0	1	0	1	0	0	1	1	0
162901	1	0	0	0	0	1	0	1	0	1	1	0	1	1	0
167532	1	1	0	1	1	0	0	1	0	0	0	1	1	1	0
167533	1	0	0	1	1	1	0	1	0	0	0	1	1	1	0
167529	1	0	0	1	1	0	0	1	0	0	0	1	1	1	0
162906	1	0	0	0	1	0	0	1	0	0	0	1	1	1	0
162905	1	0	0	0	1	0	0	1	0	1	0	1	1	1	0
156958	1	0	0	0	1	1	0	1	0	1	0	1	1	1	0
162928	1	0	0	0	0	1	0	1	0	0	1	0	1	1	0
162926	1	0	0	0	0	1	0	1	0	0	1	1	1	1	0
162929	1	0	0	0	0	1	0	1	0	1	1	1	1	1	0
162927	?	?	0	0	0	?	?	1	0	0	1	0	1	1	0
162930	1	0	0	0	1	1	0	1	0	0	1	0	1	1	0
162932	1	0	0	1	1	1	0	1	0	0	1	0	1	1	0
162933	1	0	0	1	1	1	0	1	0	1	1	1	1	1	0
162934	1	0	0	1	1	0	0	1	0	0	1	1	1	1	0
162931	1	0	0	0	0	1	0	1	0	0	1	1	1	1	0
162935	1	0	0	1	1	1	0	1	0	0	1	1	1	1	0

Table A2.4.4 Morphological Characters 41-55 (continued)

WAM R	41	42	43	44	45	46	47	48	49	50	51	52	53	54	55
167530	1	1	0	0	1	2	2	1	0	0	1	1	1	1	1
163198	?	?	?	?	?	1	0	1	0	2	0	1	1	0	1
149488	1	0	0	1	1	0	0	1	0	2	0	1	1	0	1
149923	?	?	?	?	1	1	0	1	0	2	0	0	0	0	0
27737B	1	0	0	1	1	0	0	1	0	2	0	0	1	0	0
97222	1	0	0	1	?	0	0	?	?	?	?	?	?	?	?
162857	?	?	?	?	1	1	0	1	0	0	1	0	1	1	0
167556	1	0	0	0	0	0	0	1	0	0	1	1	1	1	0
165138	1	0	0	1	1	0	0	1	0	0	1	1	1	1	1
162802	1	0	0	0	1	0	0	1	0	0	1	1	1	1	1
164273	1	0	0	0	1	1	0	1	0	0	0	1	1	1	0
111994	1	0	1	0	1	0	0	1	0	0	1	1	1	1	1
47842	0	0	0	0	1	0	0	0	0	0	1	1	1	1	1
111733	1	0	0	0	0	?	?	1	0	0	1	0	1	1	0
156884	1	0	0	1	0	0	0	1	0	0	1	1	1	1	1
156920	1	0	?	?	1	0	0	1	0	0	1	0	1	1	0
111737	1	0	0	0	0	0	0	1	0	0	1	1	1	1	0
162801	1	0	0	0	0	0	0	1	0	0	0	1	1	1	0
112142	1	0	0	0	1	0	0	1	0	0	0	1	1	1	1

Table A2.5.1 Morphological Characters 55-60

WAM R	56	57	58	59	60
111819	0	1	1	1	5
156705	0	1	1	1	6
162747	0	1	1	1	3
162754	0	1	1	1	4
162803	0	1	1	1	4
163197	0	1	0	1	4
41565	0	1	1	1	0
12100	0	1	1	1	5
12804	0	1	1	0	3
64052	0	1	1	0	3
165887	0	1	1	1	5
162820	0	1	0	1	3
162819	0	1	1	1	3
162822	0	1	0	?	3
167625	0	1	0	1	1
167626	0	1	0	1	3
167673	0	1	0	1	4
167676	0	1	0	1	3
167679	0	1	0	1	3
162887	0	1	0	1	4
167665	0	1	0	1	5
167667	0	1	0	1	4
167670	0	1	0	1	3
167672	0	1	0	1	4
111747	0	1	1	1	4
167632	0	1	0	1	4
165036	0	1	1	1	3
93130	0	1	1	1	3
167652	0	1	0	1	3
149167	0	1	1	1	4
149201	0	1	1	1	4
149371	0	1	1	1	5
149425	0	1	0	1	7
149497	0	1	1	1	5
156957	0	1	1	1	4
162889	0	1	1	1	5
162890	0	1	1	1	5

Table A2.5.2 Morphological Characters 55-60

WAM R	56	57	58	59	60
162891	0	1	1	1	5
162893	0	1	1	1	5
162893	0	1	1	1	3
162898	0	1	1	1	5
149279	0	1	1	1	3
149444	0	1	1	1	6
149693	0	1	1	1	5
162896	0	1	1	1	4
149094	0	1	1	1	3
149574	0	1	1	1	3
149689	0	1	1	1	4
149710	0	1	1	1	3
149943	0	1	1	0	3
162895	0	1	1	1	4
149179	0	1	1	1	4
149677	0	1	1	1	3
149917	0	1	1	1	5
162894	0	1	1	1	5
111736	0	1	1	1	3
111894	0	1	1	1	4
149161	0	1	1	1	3
111903	0	1	1	1	4
156956	0	1	1	1	2
164149	0	1	1	?	4
167526	0	1	1	1	4
167582	0	1	1	?	2
164148	0	1	1	1	3
162817	0	1	1	1	3
162805	0	1	1	1	5
111880	0	1	1	1	5
111905	0	1	1	1	4
111752	0	1	1	1	5
156675	0	1	1	1	5
111893	0	1	1	1	3
19288	?	1	1	1	2
165705	0	1	1	1	3

Table A2.5.3 Morphological Characters 55-60

WAM R	56	57	58	59	60
162795	?	1	0	?	4
162744	0	1	1	?	3
162821	0	1	1	0	4
162759	0	1	1	0	3
162779	0	1	1	0	4
162856	0	1	1	0	4
162881	0	1	1	0	3
167575	0	1	1	0	3
167589	0	1	1	0	3
167590	0	1	1	0	3
156678	0	1	1	0	4
167591	0	1	1	0	4
167503	0	1	1	0	4
162855	0	1	1	0	4
167551	0	1	1	0	5
167514	0	1	1	0	4
167563	0	1	1	0	3
162760	0	1	1	0	3
162878	0	1	1	1	3
167567	1	1	1	0	4
162900	0	1	1	1	3
162901	0	1	1	1	5
167532	0	1	1	1	4
167533	0	1	1	1	4
167529	0	1	1	1	6
162906	0	1	1	1	4
162905	0	1	1	1	3
156958	0	1	1	1	4
162928	0	1	1	1	4
162926	0	1	1	1	4
162929	0	1	1	1	6
162927	0	?	?	1	4
162930	0	1	1	1	5
162932	0	1	1	1	?
162933	0	1	1	1	6
162934	0	1	1	1	5

Table A2.5.4 Morphological Characters 55-60

WAM R	56	57	58	59	60
162931	0	1	1	1	4
162935	0	1	1	1	5
167530	0	1	1	1	3
163198	0	1	1	1	2
149488	0	0	1	1	3
149923	0	1	1	1	4
27737B	0	1	1	1	3
97222	?	?	?	?	?
162857	0	1	1	1	4
167556	0	1	1	1	4
165138	0	1	1	1	4
162802	0	1	1	1	4
164273	0	1	1	1	4
111994	0	1	1	1	4
47842	0	1	1	1	1
111733	0	1	1	1	5
156884	0	1	1	0	5
156920	0	1	1	1	4
111737	0	1	1	1	3
162801	0	1	1	1	5
112142	0	1	1	1	?

Glossary: Anatomical Abbreviations

aar, anterior ampullar recess;
af, adductor fossa;
AN, angular;
ANpaf, posterior angular foramen;
AT, articular;
ATap, articular angular process;
ATaf, dorsal articular facet;
ATctf, chorda tympani foramen;
ATrp, retroarticular process;
avsc, anterior vertical semicircular canal;
BO, basioccipital;
BOoc, occipital condyle;
CO, coronoid;
COcp, coronoid process;
COdl, coronoid mandible lappet;
cac, cavum capsularis;
cb1, ceratobranchial 1;
ch, ceratohyal;
coc, cochlear cavity;
cr, cochlear recess;
D, mandible;
Dc, mandible canal;
Dmc, Meckelian canal;
Dmg, Meckelian groove;
Dss, subdental shelf;
EC, ectopterygoid;
EClap, Ectopterygoid lateral articulation process;
ECmap, Ectopterygoid medial articulation process;
en, external naris;
EP, epipterygoid;
EX, extracolumella;
fm, foramen magnum;
fo, foramen ovale
FR, frontal;
fv, fenestra vomeronasalis;
hh, hypohyal;
hsc, horizontal semicircular canal;
ip, incisura prootica
iv, interpterygoid vacuity
JU, jugal;
JUmnf, jugal maxillary nerve foramen;
JUmp, jugal maxillary process;
JUpop, jugal postorbital process;
LA, lacrimal;
lf, lacrimal fenestra;

mf, mental foramen;
MX, maxilla;
MXaaf, anterior inferior alveolar foramen;
MXc, maxillary canal;
MXfp, maxilla facial process;
MXlr, maxilla lateral ridge;
MXpp, maxilla premaxillary process;
MXs, maxillary shelf;
MXsaf, superior alveolar foramen;
NA, nasal;
OB, orbitosphenoid;
OT, otooccipital;
OTlarst, recessus scalae tympani lateral aperture;
OTmarst, recessus scalae tympani medial aperture;
OTpp, paroccipital process;
PA, parietal;
PAap, anterior parietal processes;
PApf, parietal fontanelle;
PApp, postparietal process;
par, posterior ampullar recess;
PF, prefrontal;
PFplp, Prefrontal palatine process;
PL, palatine;
plf, perilymphatic foramen;
PLicg, internal choanal groove;
PLmp, palatine maxillary process;
PLpp, palatine pterygoid process;
PLvp, palatine vomerine process;
PM, premaxilla;
PMnp, premaxilla nasal process
PMvp, premaxilla vomerine process
PO, postorbital;
POjp, postorbital jugal process;
pp, parasphenoid process;
PR, prootic;
PRacr, acoustic recess;
PRan, acoustic nerve foramen;
PRap, alar process;
PRcp, crista prootica;
PRtp, superior trabecular process;
PT, pterygoid;
PTbf, Pterygoid: basipterygoid fossa;
PTecp, Pterygoid: ectopterygoid process;
PTfc, Pterygoid: fossa columellae;
PTpp, pterygoid palatine process;
PTqp, quadrate process;
pvsc, posterior vertical semicircular canal
QU, quadrate;

QUcc, quadrate cephalic condyle;
QUmac, quadrate mandibular condyle;
QUmc, quadrate medial conch;
QUtc, tympanic conch of quadrate;
S, stapes;
sanc, superior alveolar nerve canal;
SC, scleral ossicles; (add to figure)
SD, sphenoid;
SDbp, basipterygoid process;
SDds, dorsum sella;
SDpf, pituitary fossa;
SDvca, Vidian canal anterior opening;
SDvcp, Vidian canal posterior opening;
sm, statolithic mass;
SO, supraoccipital;
SOed, endolymphatic duct;
SOocc, osseous common crus;
SOpa, processus ascendens;
sof, suborbital fenestra;
SP, splenial;
SQ, squamosal;
sr, scleral ring;
ST, supratemporal;
SU, surangular;
SUasf, anterior surangular foramen;
SUpsf, posterior surangular foramen;
SX, septomaxilla;
v, vestibule;
vc, vomeronasal chamber;
VII, facial nerve foramen;
VO, vomer;
VOpp, vomer palatine process;
X, vagus nerve foramen;
XII, hypoglossal nerve foramen.

Supplementary Info 1. Excel Data File with Consistency and Correlation Coefficient analyses.

References

Ananjeva, N. B., Orlov, N.L., & Truong, N. Q. (2007). Agamid lizards (Agamidae, Acrodonta, Sauria, Reptilia) of Vietnam. *Zoosystematics and Evolution*, *83*, 13-21.

Ananjeva, N. B., Xianguang, G., & Yuezhao, W. (2011). Taxonomic diversity of agamid lizards (Reptilia, Sauria, Acrodonta, Agamidae) from China: A comparative analysis. *Asian Herpetological Research*, *2*, 117-128.

Atlas of Living Australia. (11 February 2015). http://biocache.ala.org.au/occurrences/79fbc4d5-1167-4052-bec6-4696afd26bec.

Averianov, A., & Danilov, I. (1996). Agamid lizards (Reptilia, Sauria, Agamidae) from the Early Eocene of Kyrgyzstan. *Neues Jahrbuch Für Geologie Und Paläontologie, 12*, 739-750.

Badham, J. A. (1976). The *Amphibolurus barbatus* species group (Lacertilia: Agamidae). *Australian Journal of Zoology*, *24*, 423-443.

Banzato, T., Selleri, P., Veladiano, I. A., Martin, A., Zanetti, E., & Zotti, A. (2012). Comparative evaluation of the cadaveric, radiographic and computed tomographic anatomy of the heads of green iguana (*Iguana iguana*), common tegu (*Tupinambis merianae*) and bearded dragon (*Pogona vitticeps*). *BMC Veterinary Research*, *8*, 53.

Beddard, F. E. (1905). Some notes on the Cranial Osteology of the Mastigure Lizard, *Uromastix*. *Proceedings of the Zoological Society of London*, *75*(1), 2-9.

Bell, C. J., Mead, J. I., & Swift, S. L. (2009). Cranial osteology of *Moloch horridus* (Reptilia: Squamata: Agamidae). *Records of the Western Australian Museum*, *25*, 201-237.

Bell, C. J., & Mead, J. I. (2014). Not enough skeletons in the closet: collections-based anatomical research in an age of conservation conscience. *The Anatomical Record*, *297*, 344-348.

Bellairs, A. A. (1970). The Life of Reptiles. Vol. 1. New York: Universe Books.

Blain, H., Bailon, S., Agustí, J., Piñero-García, P., Lozano-Fernández, I., Sevilla, P., López-García, J. M., Romero, G., & Mancheño, M. A. (2013). Youngest agamid lizards from Western Europe (Sierra de Quibas, Spain, Late Early Pleistocene). *Acta Palaeontologica Polonica*, 59, 873-878.

Borsuk- Białynicka, M., & Moody, S. M. (1984). Priscagaminae, a new subfamily of the Agamidae (Sauria) from the Late Cretaceous of the Gobi Desert. *Palaeontologica*, *29*, 51-81, pls.14-19.

Brůna, J. Jr. (1996). Australian agamid genenera *Caimanops*, *Chelosania* and *Cryptagama* (Jaroslav, K. & Kocurek, G., Trans.). *Chamaeleo*, *6*, 13-15.

Byrne, M., Yeates, D. K., Joseph, L., Kearney, M., Bowler, J., Williams, M. A. J., Cooper, S., Donnellan, S. C., Keogh, S., Leys, R., Melville, J., Murphy, D. J., Porch, N, & Wyrwoll, K. (2008). Birth of a biome: insights into the assembly and maintenance of the Australian arid zone biota. *Molecular Ecology,* 17, 4398-4417.

Caldwell, M. W. (1999). Squamate phylogeny and the relationships of snakes and mosasauroids. *Zoological Journal of the Linnean Society*, *125*, 115-147.

Camp, C. L. (1923). Classification of the lizards. *Bulletin of the American Museum of Natural History*, *48*, 289-481.

Chen, I., Stuart-Fox, D., Hugall, A. F., & Symonds, M. R. (2012). Sexual selection and the evolution of complex color patterns in dragon lizards. *Evolution*, *66*, 3605-3614.

Clemente, C. J., Withers, P. C., Thompson, G., & Lloyd, D. (2008). Why go bipedal? Locomotion and morphology in Australian agamid lizards. *Journal of Experimental Biology*, *211*, 2058-2065.

Cogger, H. G. (1983). *Reptiles and Amphibians of Australia, 3rd ed*. Sanibel Island, Florida: Ralph Curtis Publishing.

Cogger, H. G. (1992). *Reptiles and Amphibians of Australia, 4th ed*. Ithaca, New York: Cornell University Press

Cogger, H. G. (1996). *Reptiles and Amphibians of Australia, 5th ed*. San Diego, California: Academic Press.

Cogger, H. G. (2000). *Reptiles and Amphibians of Australia, 6th ed*. Sanibel Island, Florida: Ralph Curtis Publishing.

Cogger, H. (2014). *Reptiles and amphibians of Australia, 7th ed*. Victoria, Australia: CSIRO Publishing.

Cogger, H. G., Cameron, E. E., & Cogger, H. M. (1983). *Amphibia and Reptilia* (Vol. 1). Canberra, Australia: The Australian Government Publishing Service.

Collar, D. C., Schulte, J. A., O'Meara, B. C., & Losos, J.B. (2010). Habitat use affects morphological diversification in dragon lizards. *Journal of Evolutionary Biology*, *23*, 1033-1049.

Conrad, J. L. (2008). Phylogeny and systematics of Squamata (Reptilia) based on morphology. *Bulletin of the American Museum of Natural History*, *310*, 1-182.

Cooper, J. S., & Poole, D. F. G. (1973). The dentition and dental tissues of the agamid lizard, *Uromastyx*. *Journal of Zoology*, *169*, 85-100.

Doughty, P., Maryan, B., Melville, J., & Austin, J. (2007). A new species of *Ctenophorus* (Lacertilia: Agamidae) from Lake Disappointment, Western Australia. *Herpetologica*, *63*, 72-86.

Doughty, P., Kealley, L., Shoo, L. P., & Melville, J. (2014). Revision of the Western Australian pebble-mimic dragon species-group (Tympanocryptis cephalus: Reptilia: Agamidae). *Zootaxa*, *4039*, 85-117.

El-Toubi, M. R. (1945). Notes on the cranial osteology of *Uromastix aegyptia* (Forskal). *Bulletin of the Faculty of Science, Cairo University*, *25*, 1-10.

Edwards, D. L., Melville, J., Joseph, L., & Keogh, J. S. (2015). Ecological Divergence, Adaptive Diversification, and the Evolution of Social Signaling Traits: An Empirical Study in Arid Australian Lizards. *The American Naturalist, 186,* E144-E161.

El-Toubi, M. R. (1947). Some observations on the osteology of the lizard, *Agama stellio* (Linn.). *Journal of Morphology*, *81*,135-149.

Estes, R., Pregill, G., de Queiroz, K., & Gauthier, J. (1988). Phylogenetic relationships within Squamata. in Estes, R. & Camp, C.L. (eds.), *Phylogenetic Relationships of the Lizard Families*. Pp. 119-281. Stanford, California: Stanford University Press.

Evans, S. E., Prasad, G. V. R., & Manhas, B. K. (2002). Fossil lizards from the Jurassic Kota formation of India. *Journal of Vertebrate Paleontology*, *22*, 299-312.

Evans, S. E. (2008). The skull of lizards and tuatara. In Gans, C, Gaunt, A. S., & Adler, K. (eds.), *Biology of the Reptilia Volume 20, Morphology H: The Skull of Lepidosauria*. Pp. 1-347. Ithaca, New York: Society for the Study of Amphibians and Reptiles.

Fathinia, B., Rastegar-Pouyani, N., Bahrami, A. M., & Abdali, G. (2011). Comparative skull anatomy and dentition of *Trapelus lessonae* and *T. ruderatus* (Sauria: Agamidae) from Ilam Province, Iran. *Russian Journal of Herpetology*, *18*, 83-92.

Fischer, J. G. (1881). Beschreibung neuer Reptilien. *Archiv für Naturgeschichte*, *47*(1), 225-238.

Frost, D. R., & Etheridge, R. (1989). A phylogenetic analysis and taxonomy of iguanian lizards (Reptilia: Squamata). *Miscellaneous Publication, Museums of Natural History, University of Kansas, 81*, 1–65.

Gauthier, J. A., Estes, R., & de Queiroz, K. (1988). A phylogenetic analysis of Lepidosauromorpha. In R. Estes and G. Pregill (eds.), *Phylogenetic Relationships of the Lizard Families*. Pp. 15-98. Stanford, California: Stanford University Press.

Gauthier, J. A., Kearney, M., Maisano, J. A., Rieppel, O., & Behlke, A. D. (2012). Assembling the squamate tree of life: perspectives from the phenotype and the fossil record. *Bulletin of the Peabody Museum of Natural History*, *53*, 3-308.

Gray, J. E. (1845). *Catalogue of the specimens of lizards in the collection of the British Museum*. London, England: Trustees of the British Museum.

Greer, A. E. (1987). Observations on the osteology and natural history of the agamid lizard *Ctenophorus clayi*. *The Western Australian Naturalist, 17*, 5-7.

Greer, A.E. (1989a). The Biology and Evolution of Australian Lizards. *Surrey Beatty and Songs*, Chipping Norton.

Greer, A. E. (1989a). Observations on the osteology and natural history of the agamid lizard *Ctenophorus femoralis*. *Western Australian Naturalist*, *18*, 21-23.

Günther, A. (1875). A list of the saurians of Australia and New Zealand. In: Richardson, J., & Gray, J. E. (eds.), *The zoology of the voyage of H.M.S. Erebus and Terror, during the years 1839 to 1843. By authority of the Lords Commissioners of the Admiralty.Vol. 2*. Pp. 9-19. England: E. W. Jansen.

Harris, V. A. P. (1963). *Anatomy of the Rainbow Lizard Agama agama, L.* London: Hutchinson.

Herrel, A., & De Vree, F. (2009). Jaw and hyolingual muscle activity patterns and bite forces in the herbivorous lizard *Uromastyx acanthinurus*. *Archives of Oral Biology*, *54*, 772-782.

Heying 2003 – present in previous version

Hocknull, S. A. (2000). *The phylogeny and fossil record of Australopapuan dragon lizards (Squamata: Agamidae)* (Unpublished B.S. Honours Thesis). University of Queensland, Brisbane, Australia.

Hocknull, S. A. (2002). Comparative maxillary and dentary morphology of the Australian dragons (Agamidae: Squamata): a framework for fossil identification. *Memoirs of the Queensland Museum, 48*, 125-146.

Hocknull, S. A. (2005). Ecological succession during the late Cenozoic of central eastern Queensland: extinction of a diverse rainforest community. *Memoirs of the Queensland Museum*, *51*, 39-122.

Honda, M., Ota, H., Kobayashi, M., Nabhitabhata, J., Yong, H. S., Sengoku, S., & Hikida, T. (2000). Phylogenetic relationships of the family Agamidae (Reptilia: Iguania) inferred from mitochondrial DNA sequences. *Zoological Science*, *17*, 527-537.

Hugall, A. F. & Lee, M.S. (2004). Molecular claims of Gondwanan age for Australian agamid lizards are untenable. *Molecular Biology and Evolution*, *21*, 2102-2110.

Hugall, A. F., Foster, R., Hutchinson, M., & Lee, M. S. (2008). Phylogeny of Australasian agamid lizards based on nuclear and mitochondrial genes: implications for morphological evolution and biogeography. *Biological Journal of the Linnean Society*, *93*, 343-358.

Iordansky, N. N. (1966) Cranial kinesis in lizards: functional significance. *Zoologicheskii zhurnal, 45*, 1398–1410.

Jollie, M. T. (1960). The head skeleton of the lizard. *Acta Zoologica*, *41*, 1-64.

Lee, M. S. (2005). Squamate phylogeny, taxon sampling, and data congruence. *Organisms Diversity & Evolution*, *5*, 25-45.

Lemmrich, W. (1931). Der Skleralring der Vögel*, Jenaische Zeitschrift für Naturwissenschaft*, *65*, 513-586.

Levy, E., Kennington, W. J., Tomkins, J. L., & LeBas, N. R. (2012). Phylogeography and population genetic structure of the ornate dragon lizard, *Ctenophorus ornatus*. *PloS One*, *7*, e46351.

Macey, J. R., Schulte, J. A., & Larson, A. (2000). Evolution and phylogenetic information content of mitochondrial genomic structural characters illustrated with acrodont lizards. *Systematic Biology*, *49*, 257-277.

Manthey, U., & Schuster, N. (1996). *Agamid lizards*. Neptune City, New Jersey: TFH Publications.

McLean, C. A., Moussalli, A., Sass, S., & Stuart-Fox, D. (2013). Taxonomic assessment of the *Ctenophorus decresii* complex (Reptilia: Agamidae) reveals a new species of dragon lizard from Western New South Wales. *Records of the Australian Museum*, *65*, 51-63.

Melville, J., Schulte, J. A., & Larson, A. (2001). A molecular phylogenetic study of ecological diversification in the Australian lizard genus *Ctenophorus*. *Journal of Experimental Zoology*, *291*, 339-353.

Melville, J., Harmon, L. J., & Losos, J. B. (2006). Intercontinental community convergence of ecology and morphology in desert lizards. *Proceedings of the Royal Society Series B: Biological Sciences*, *273*, 557-563.

Melville, J., Smith, K., Hobson, R., Hunjan, S., & Shoo, L. (2014). The role of integrative taxonomy in the conservation management of cryptic species: the taxonomic status of endangered earless dragons (Agamidae: Tympanocryptis) in the grasslands of Queensland, Australia. *PloS one*, *9*, e101847.

Moazen, M., Curtis, N., Evans, S. E., O'Higgins, P., & Fagan, M. J. (2008). Rigid-body analysis of a lizard skull: modelling the skull of *Uromastyx hardwickii*. *Journal of Biomechanics*, *41*, 1274-1280.

Molnar E. M. (1991). Fossil reptiles in Australia. In Vickers-Rich, P., Monaghan, J.M., Baird, R.F. & Rich, T.H. (eds.), *Vertebrate Palaeontology of Australasia* (605-702). Melbourne, Australia: Pioneer Design Studio.

Moody, S. M. (1980). *Phylogenetic and Historical Biogeographical Relationships of the Genera in the Family Agamidae (Reptilia: Laceratilia)* (Unpublished Masters thesis). University of Michigan, Ann Arbor, Michigan.

O'Leary, M. A., & Kaufman, S. G. (2012). MorphoBank 3.0: Web application for morphological phylogenetics and taxonomy. http://www.morphobank.org .

Oelrich, T. M. (1956). The anatomy of the head of *Ctenosaura pectinata* (Iguanidae), *University of Michigan Museum of Zoology, Miscellaneous Publicatons*, *94,* 1-122.

Ord, T. J. & Stuart-Fox, D. (2006). Ornament evolution in dragon lizards: multiple gains and widespread losses reveal a complex history of evolutionary change. *Journal of Evolutionary Biology*, *19*, 797-808.

Östman, Ö. & Stuart-Fox, D. (2011). Sexual selection is positively associated with ecological generalism among agamid lizards. *Journal of Evolutionary Biology, 24*, 733-740.

Porro, L. B., Ross, C. F., Iriarte-Diaz, J., O'Reilly, J. C., Evans, S. E., & Fagan, M. J. (2014). *In vivo* cranial bone strain and bite force in the agamid lizard *Uromastyx geyri*. *Journal of Experimental Biology*, *217*, 1983-1992.

Pyron, R. A., Burbrink, F. T., & Wiens, J. J. (2013). A phylogeny and revised classification of Squamata, including 4161 species of lizards and snakes. *BMC Evolutionary Biology*, *13*, 93.

Rabosky, D. L., Cowan, M. A., Talaba, A. L., & Lovette, I. J. (2011). Species interactions mediate phylogenetic community structure in a hyperdiverse lizard assemblage from arid Australia. *The American Naturalist*, *178*, 579-595.

Rasband, W.S. (1997-2014). ImageJ, U. S. National Institutes of Health, Bethesda, Maryland, USA, http://imagej.nih.gov/ij/.

Schulte, J. A., Melville, J., & Larson, A. (2003). Molecular phylogenetic evidence for ancient divergence of lizard taxa on either side of Wallace's Line. *Proceedings of the Royal Society of London Series B: Biological Sciences*, *270*, 597-603.

Siebenrock, F. (1895). Das skelet der Agamidae. *Sitzungsberichte der Mathematisch-Naturwissenschaftlichen Classe der Kaiserlichen Akademie der Wissenschaften*, *104*, 1089-1196, platten 1-6.

Smirina, E. M., & Ananjeva, N. B. (2007). Growth layers in bones and acrodont teeth of the agamid lizard *Laudakia stoliczkana* (Blanford, 1875) (Agamidae, Sauria). *Amphibia-Reptilia*, *28*, 193-204.

Smith, K. L., Harmon, L. J., Shoo, L. P., & Melville, J. (2011). Evidence of constrained phenotypic evolution in a cryptic species complex of agamid lizards. *Evolution*, *65*, 976-992.

Smith, K. T. (2011). On the phylogenetic affinity of the extinct acrodontan lizard *Tinosaurus* In: Shuchmann K-L, (Ed.). *Tropical Vertebrates in a Changing World*. Pp. 9-27. Bonn, Switzerland: Zoologisches Forshungsmuseum Alexander Koenig.

Storr, G. M. (1966). The *Amphibolurus reticulatus* species-group (Lacertilia: Agamidae) in Western Australia. *Journal of the Royal Society of Western Australia,* Herausgeber: Zoologisches Forschungsmuseum Alexander Koenig, Bonn. *49*, 17-25.

Storr, G. M. (1981). Three new agamid lizards from Western Australia. *Records of the Western Australian Museum*, *8*, 599-607.

Stuart-Fox, D., &. Owens, I. P. (2003). Species richness in agamid lizards: chance, body size, sexual selection or ecology? *Journal of Evolutionary Biology*, *16*, 659-669.

Thompson, G. G., & Withers, P. C. (2005). The relationship between size-free body shape and choice of retreat for Western Australian *Ctenophorus* (Agamidae) dragon lizards. *Amphibia-Reptilia*, *26*, 65-72.

Townsend, T. M., Larson, A., Louis, E., & Macey, J. R. (2004). Molecular phylogenetics of Squamata: The position of snakes, amphisbaenians, and dibamids, and the root of the squamate tree. *Systematic Biology*, *53*, 735-757.

Underwood, G. (1970). The eye. In Gans and T. S. Parsons (eds.) *Biology of the Reptilia. Volume 2*: *Morphology* B. C. Pp. 1–97. Academic Press, London.

Uetz, P. (ed). 2016. The Reptile Database, http://www.reptile-database.org, accessed March 21, 2016.

Vitt, L. J., & Caldwell, J. P. (2013). *Herpetology: An introductory biology of amphibians and reptiles*. Cambridge, Massachusetts: Academic Press.

Wagner, P., Melville, J., Wilms, T. M. & Schmitz, A. (2011). Opening a box of cryptic taxa – the first review of the North African desert lizards *Trapelus mutabilis* Merrem, 1820 complex (Squamata: Agamidae) with descriptions of new taxa. *Zoological Journal of the Linnean Society*, *163*, 884–912.

Waite, E. R. (1993). Reptiles and Amphibians of South Australia (Civil War Series) (Facsimile reprints in herpetology). Adler, K. (ed.). Ithaca, New York: *Society for the Study of Amphibians & Reptiles*. (Original work published 1929).

Wever, E.G. (1978). The Reptile Ear. Princeton, NJ: Princeton University Press.

Wiens, J. J., Hutter, C. R., Mulcahy, D. G., Noonan, B. P., Townsend, T. M., Sites, J. W., & Reeder, T. W. (2012). Resolving the phylogeny of lizards and snakes (Squamata) with extensive sampling of genes and species. *Biology Letters*, *8*, 1043-1046.

Wilson, S. K. (2012). Australian lizards: a natural history. Collingwood, Australia: Csiro Publishing.

Wilson, S., & Swan, G. (2013). Complete guide to reptiles of Australia. Chatswood, Australia: New Holland.

Witten, G. J. (1982). *Comparative morphology and karyology of the Australian members of the family Agamidae and their phylogenetic implications* (Doctoral dissertation). The University of Sydney. Sydney, Australia. http://hdl.handle.net/2123/2228

Witten, G. J. (1984). Relationships of *Tympanocryptis aurita* Storr, 1981. *Records of the Western Australian Museum*, *11*, 399-401.

Witten, G. J. (1993). Family Agamidae. In: Glasby, C. J., Ross, G. J. B., Beesley, P. L. (eds.) *Fauna of Australia, Vol. 2A*. (240-252). Canberra, Australia: Australian Government Publishing Service.

Zar, J. H. (2010). Biostatistical analysis 5th edition. Upper Saddle River, New Jersey: Prentice Hall.